

NASA-CR-168066
19830023615

NASA CR-168,066

20 July 1983

FINAL REPORT
LOX/HYDROCARBON FUEL CARBON FORMATION
AND MIXING DATA ANALYSIS

CONTRACT NAS 3-22823

BY

J. FANG
PROJECT ENGINEER

AEROJET LIQUID ROCKET COMPANY
P. O. BOX 13222
SACRAMENTO, CALIFORNIA 95813

PREPARED FOR
NATIONAL AERONAUTICS & SPACE ADMINISTRATION
LEWIS RESEARCH CENTER
CLEVELAND, OHIO 44135

J. P. WANHAINEN, PROJECT MANAGER

LIBRARY COPY

JUL 11 1983

LANGLEY RESEARCH CENTER
LIBRARY, NASA
HAMPTON, VIRGINIA



NF01891

1 Report No CP-168	2 Government Accession No 066	3 Recipient's Catalog No	
4 Title and Subtitle LOX/Hydrocarbon Fuel Carbon Formation and Mixing Data Analysis		5 Report Date November 1983	
7 Author(s) J. Fang		6 Performing Organization Code	
9 Performing Organization Name and Address Aerojet Liquid Rocket Company Post Office Box 13222 Sacramento, CA 95813		8 Performing Organization Report No	
12 Sponsoring Agency Name and Address National Aeronautics and Space Administration NASA/Lewis Research Center 21000 Brookpark Road Cleveland, Ohio 44135		10 Work Unit No	
15 Supplementary Notes Project Manager - John Wanhainen NASA/Lewis Research Center 21000 Brookpark Road Cleveland, Ohio 44135		11 Contract or Grant No NAS 3-22823	
		13 Type of Report and Period Covered Contractor Report, Final	
		14 Sponsoring Agency Code	
16 Abstract The results of a previous high-speed single-element photographic study of LOX/Hydrocarbon propellant combustion have shown regions of dark clouds emanating from the propellant spray. The prevalence of these dark clouds was found to be dependent on chamber pressure, fuel temperature, propellant mixture ratio, and injector element design; and they have been interpreted as areas of fuel vaporization-dependent carbon formation. The present study is an attempt to verify the hypothesis of fuel-vaporization limited carbon formation through analytical effort.			
By applying the Priem-Heidmann Generalized-Length vaporization correlation, the computer model developed by the present study predicts the spatial variation of propellant vaporization rate using the injector cold-flow results to define the streamtubes. The calculations show that the overall and local propellant vaporization rate and mixture ratio change drastically as the injection element type or the injector operating condition is changed. These results are compared with the regions of carbon formation observed in the photographic combustion testing. The correlation shows that the fuel vaporization rate and the local mixture ratio produced by the injector element have first order effects on the degree of carbon formation. Low fuel vaporization rates significantly increase the degree of carbon formation. Also, fuel rich zones containing vaporizing liquid fuel, are sources of carbon formation. For similar injector operating conditions, propane produces less carbon formation than RP-1 because of its higher vaporization rate. Chamber pressure also appears to have an effect on carbon formation which is observed to decrease with increasing pressure.			
As a result, the degree of carbon formation can be controlled by controlling the fuel vaporization rate and the local combustor mixture ratio distribution. These parameters, on the other hand, are a function of the injector element design and the propellant properties and operating condition.			
17 Key Words (Suggested by Author(s))	18 Distribution Statement Unclassified - Unlimited		
19 Security Classif (of this report) Unclassified	20 Security Classif (of this page) Unclassified	21 No of Pages 182	22 Price*

* For sale by the National Technical Information Service, Springfield, Virginia 22161

FOREWORD

This final report is submitted for the LOX/Hydrocarbon Fuel Carbon Formation and Mixing Data Analysis Program per the requirements of Contract NAS 3-22823. The work was performed by the Aerojet Liquid Rocket Company (ALRC) for the National Aeronautics and Space Administration-Lewis Research Center (NASA-LeRC). The objective of the program was to correlate the combustion phenomena observed under NASA/JSC Contract NAS 9-15724 with the calculated propellant combustion parameters through the use of injector cold-flow testing and analytical evaluation of propellant vaporization and mixing characteristics.

The NASA-LeRC project manager was Mr. J. P. Wanhanen. The ALRC program manager was Mr. R. W. Michel, and the project engineer was Dr. J. Fang. The following individuals also contributed to the success of the program:

Arnold R. Keller	Cold-Flow Testing
Sharon L. Munger	Word Processing
Jerry L. Pieper	Reviewing

TABLE OF CONTENTS

	<u>Page</u>
I INTRODUCTION	1
A. Background	1
B. Objective	2
C. Scope	2
D. Approach	2
II SUMMARY	4
III HOT-FIRE DATA	7
A. Test Results Summary	7
B. Data Selection	10
IV INJECTOR COLD-FLOW TESTING	20
A. Objective	20
B. Method and Apparatus	20
C. Results	23
V VAPORIZATION ANALYSIS	38
A. Generalized-Length Model Summary	38
B. Atomization Process Considerations	41
C. Application of Generalized-Length Model	46
D. Vaporization Model	46
E. Input and Results	51

TABLE OF CONTENTS (CONT.)

	<u>Page</u>
VI DATA CORRELATION	53
A. Fuel Vaporization Rate Effect	53
B. Chamber Pressure Effect	53
C. Mixing Effect	58
VII CONCLUSIONS AND RECOMMENDATIONS	71
A. Conclusions	71
B. Recommendations	72
REFERENCES	73
DISTRIBUTION LIST	75
APPENDICES	
A. Hot-Fire Data Summary	A-1
B. Injector Cold-Flow Data Summary	B-1
C. Vaporization Computation Flowchart and Computer Program Listing	C-1
D. Vaporization Analysis Input Data	D-1
E. Predicted Fuel Vaporization and Liquid Phase Mixture Ratio	E-1
F. Nomenclature	F-1

LIST OF TABLES

<u>Table No.</u>	<u>Title</u>	<u>Page</u>
I	Hot-Fire Tests Selected for Analysis	11
II	Injector Hot-Fire and Cold-Flow Nominal Operating Conditions	24
III	Survey of Exponent of Velocity Dependency of Drop Size	43

LIST OF FIGURES

<u>Figure No.</u>	<u>Title</u>	<u>Page</u>
1	Test Chamber Assembly	8
2	High-Speed Photographs of Carbon Formation Phenomena, EDM-LOL Injector	9
3	Operating Condition Dependency of OFO Triplet Carbon Formation	13
4	Operating Condition Dependency of TLOL Carbon Formation	14
5	Operating Condition Dependency of EDM-LOL Carbon Formation	15
6	Operating Condition Dependency of PAT Carbon Formation	16
7	OFO Triplet Injector Configuration	18
8	Transverse Like-On-Like (TLOL) Injector Configuration	18
9	Electrode Discharge Machined Like-on-Like (EDM-LOL) Injector Configuration	19
10	Pre-Atomized Triplet (PAT) Injector Configuration	19
11	Injector Cold-Flow Setup	32
12	Physical Properties of Freon TF Solvent	22
13	OFO Triplet Injector	25
14	EDM-LOL Injector	26
15	PAT and TLOL Injectors Cold Flow Mixture Ratio and Mass Distributions, Axial Distance at 1.5 Inches	27
16	PAT Injector	28
17	OFO Triplet Injectfor Cold-Flow Spray Pattern	29
18	OFO Injector Cold-Flow Mixing Pattern	31

FIGURE LIST (cont.)

<u>Figure No.</u>		<u>Page</u>
19	EDM-LOL Injector Cold-Flow Spray Pattern	29
20	EDM-LOL Injector Cold-Flow Mixing Pattern	32
21	TLOL Injector Cold-Flow Spray Pattern	33
22	TLOL Injector Cold-Flow Mixing Pattern	34
23	PAT Injector Cold-Flow Spray Pattern	33
24	PAT Injector Cold-Flow Mixing Pattern	36
25	Zoning of the Window View of the Combustion Field	37
26	Generalized Length Correlation with Mass Vaporized (Reference 3)	39
27	Drop Size Determined from Experimental LOX/Heptane Engine Performance (Reference 3)	40
28	Impinging Jet Fan Angle Predicted by Simplified Spray Model	44
29	Mass Fraction Contained in the Fan Angle Predicted by the Simplified Spray Model For Impinging Jets	45
30	Triplet Fan Angle Predicted by Simplified Spray Model	47
31	Zoning of the Cross-Sectional View of the Combustion Field	49
32	OFO Triplet Carbon Formation Correlation with Fuel Vaporization Rate	54
33	TLOL Carbon Formation Correlation with Fuel Vaporization Rate	55
34	EDM-LOL Carbon Formation Correlation with Fuel Vaporization Rate	56
35	PAT Carbon Formation Correlation with Fuel Vaporization Rate	57
36	OFO Triplet Carbon Formation Correlation with Chamber Pressure and Fuel Vaporization Rate	59

FIGURE LIST (cont.)

<u>FIGURE NO.</u>	<u>TITLE</u>	<u>PAGE</u>
37	TLOL Carbon Formation Correlation with Chamber Pressure and Fuel Vaporization Rate	60
38	EDM-LOL Carbon Formation Correlation with Chamber Pressure and Fuel Vaporization Rate	61
39	PAT Carbon Formation Correlation with Chamber Pressure and Fuel Vaporization Rate	62
40	OFO Triplet Liquid Mixture Ratio Distribution on Plane No. 3	64
41	TLOL Liquid Mixture Ratio Distribution on Plane No. 3 (2 pages)	65
42	EDM-LOL Liquid Mixture Ratio Distribution on Plane No. 3	67
43	PAT Liquid Mixture Ratio Distribution on Plane No. 3	68
44	High-Speed Photograph of OFO Triplet Carbon Formation Phenomena, Test 116	69
45	High-Speed Photograph of TLOL Carbon Formation Phenomena, Test 129	69
46	High-Speed Photograph of EDM-LOL Carbon Formation Phenomena, Test 161	69
47	High-Speed Photograph of PAT Carbon Formation Phenomena, Test 178	69

I INTRODUCTION

A. Background

Two key areas for limiting the cost of future space transportation systems are economical engine development and operation and optimal utilization of low-cost propellants, such as the liquid oxygen/hydrocarbons (LOX/HC). As a result, it is imperative to characterize LOX/HC combustion through the analysis and test of various injector element designs to provide a data base to rationally select the most promising propellant combination(s) and injector elements for future technology efforts and engine development programs.

High-speed single-element photography has been proven to be an economical and effective method for characterizing and evaluating hypergolic propellant combustion (Reference 1). The results have been successfully applied to several engine development programs at Aerojet Liquid Rocket Company (ALRC). Recently, the same technique was successfully used to characterize LOX/HC propellant combustion under a study contract sponsored by NASA/JSC (Reference 2) in which high-speed photographs were taken of the impingement spray field and adjacent combustion zone. A total of 127 tests were conducted using four different fuels (RP-1, propane, liquid and gaseous methane, and ammonia) and seven different injector element types (Oxidizer-Fuel-Oxidizer (OFO) Triplet, Rectangular Unlike Doublet (RUD), Platelet Transverse Like-on-Like (TLOL) Doublet, Unlike Doublet (UD), Electrode-Discharge-Machined Like-on-Like (EDM-LOL) Doublet, Pre-Atomized Triplet (PAT), and Slit Triplet). These photographs show regions of dark clouds emanating from the propellant spray. The prevalence of these dark clouds was found to be dependent on chamber pressure, fuel temperature,

propellant mixture ratio, and injector element design; and they have been interpreted as areas of fuel vaporization-dependent carbon formation. However, the interpretation has not been substantiated through experimental measurement or analytical evaluation. Since this observation is key to understanding carbon formation and hence, performance and compatibility within LOX/HC engines, it is imperative that substantiation be provided.

B. Objective

The objective of this effort is to improve the understanding and the prediction techniques of LOX/HC carbon formation and combustion performance. Analytical combustion models and supporting cold flow data were used to estimate propellant mass distributions under hot-fire conditions for correlation of carbon formation regions observed in existing photographic combustion to verify the hypothesis of fuel-vaporization limited carbon formation.

C. Scope

The analytical models which were used are limited to those with successful previous experiences or those justifiable by experimental evidences. The propellant mass distribution in the combustion chamber was assumed identical to that determined by the injector cold-flow testing. The carbon formation data was limited to those reported in Reference 2 and no additional hot-fire tests were conducted.

D. Approach

The basic approach for this study consisted of the determination of the propellant droplet spray cold-flow mass distribution and calculation of the vaporization rates of individual streamtubes to provide the basis for the prediction of spatial variation of liquid and vapor phase mixing. These predictions were subsequently used to correlate with regions of suspected

carbon formation within the spray and recirculation gas zones. The program consists of the following three technical tasks:

Task I, Selection of Data for Analysis, resulted in the selection of 40 tests from the 127 tests conducted under contract NAS 9-15724 (Reference 2) for further analytical evaluation. The selected tests included data obtained from four injector element types (EDM-LOL, TLOL, OFO Triplet and PAT) and two fuels (RP-1 and propane).

Task II, Data Analysis, consisted of two subtasks: (1) injector cold-flow testing to measure the liquid-phase mass distributions; and (2) vaporization analysis to predict the gas temperature, and liquid/vapor propellant mass distributions in various locations in the chamber.

During Task III, Data Correlation and Analysis Update, the calculated combustion parameters were correlated with the observed combustion phenomena to define the carbon formation mechanism.

II SUMMARY

The photographic carbon formation data of Reference 2 were reviewed. From the 127 hot-fire tests conducted, forty tests were selected for further analytical evaluation of the propellant vaporization and mixing characteristics. These tests included two hydrocarbon fuels (RP-1 and propane) and four injectors (OFO Triplet, TLOL, EDM-LOL, and PAT). Each injector exhibited its unique carbon formation characteristics and the tests selected covered wide range of injector/propellant operating conditions showing large variations of carbon formation.

All four injectors were cold-flow tested using a collection device to characterize the propellant mixing pattern. The sprays issuing from the injector or formed by the impinging jets were picked up by a 4.83 cm x 4.83 cm (1.49" x 1.49") collector head, which was evenly divided into 100 (10 x 10) flow passages. The fluids through each passage were collected by a glass tube. Since the propellant simulants (Freon for the oxidizer and water for the fuel) were immiscible, the volume of each of the two simulants collected by any given location was determined readily. This measurement was repeated for various distances between the injector and the collector head, to establish the mass and mixture ratio distributions of the two propellants at various chamber axial locations.

A vaporization computer model was written to predict spatial variation of propellant vaporization rate using the injector cold flow results to define local zones (streamtubes). This model applied the Priem-Heidmann Generalized-Length vaporization correlation to the individual streamtubes determined from the cold flow measurements. Consideration was also made to

include the off-nominal gas temperature effect on the vaporization rate caused by mixture ratio variation.

Results of this analysis show that the fuel vaporization rate and the local mixture ratio produced by the injector element have first order effects on the degree of carbon formation. Low fuel vaporization rates significantly increase the degree of carbon formation. Also, fuel rich zones containing liquid (vaporizing) fuel are sources of carbon formation. For similar injector operating conditions, propane produces less carbon formation than RP-1 because of its higher vaporization rate. Chamber pressure also appears to have an effect on carbon formation which is observed to decrease with increasing pressure.

As a result, the degree of carbon formation can be controlled by controlling the fuel vaporization rate and the local combustor mixture ratio distribution. These parameters, on the other hand, are a function of the injector element design and the propellant properties and operating condition.

The present study was limited to uni-element injectors, which inherently possess large amount of hot gases recirculating in the combustion chamber. In order to have a closer simulation of full scale engine combustion environment, further investigations using multi-element injectors are recommended.

The vaporization analysis of the present study included the effect of propellant mixing, which was characterized by injector cold-flow. This approach of integrating the mixing data into the propellant vaporization analysis was found to be practical in usage and realistic in modeling; yet, the computation was simple and straight forward. Hence, an engine combustion performance model can be readily developed using the present

model as a frame work. Such a model is useful and convenient for engine design or data analysis.

III HOT-FIRE DATA

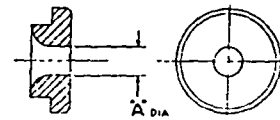
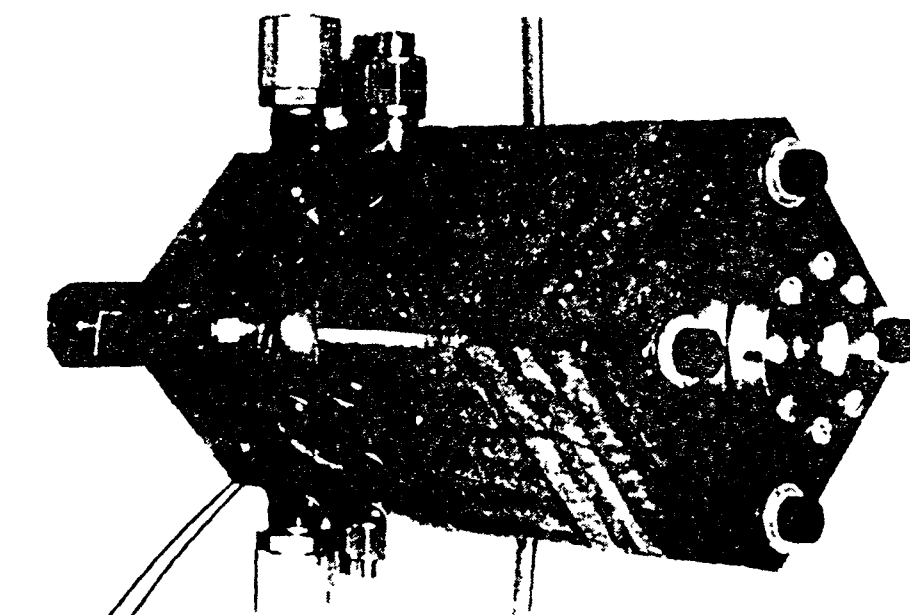
A. Test Results Summary

The work undertaken by Reference 2 resulted in the design and testing of seven single element injectors and four fuels with the aim of photographically characterizing combustion phenomena of LOX/HC propellant combinations. The seven injectors tested were the OFO Triplet, the Platelet Transverse Like-on-Like Doublet (TLOL), the Rectangular Unlike Doublet (RUD), the Unlike Doublet (UD), the Electrode Discharge Machined Like-on-Like Doublet (EDM-LOL), the Platelet Pre-Atomized Triplet (PAT), and the EDM Slit Triplet. The fuels tested were RP-1, Propane, Methane and Ammonia. The hot firings were conducted in a specifically constructed square chamber fitted with quartz windows for photographically viewing the impingement spray field. Removable copper inserts were used for varying the nozzle configuration to provide the desired operating chamber pressures.

Figure 1 shows the test chamber assembly and the nozzle insert.

Test photographic results showed that the appearance of LOX/HC combustion is markedly different from previously observed storable propellant combustion (Reference 1). In the fuel rich zone, the flame was usually yellow-brownish. However, some times the flame became reddish with visible black smoke streaks which in extreme cases filled the entire combustion chamber. Figure 2 displays two photographic results. In the top photograph, black clouds are clearly visible downstream of the impingement zone. The occurrence of these clouds was assumed to indicate the formation of free carbon during the combustion process. Under different conditions, no black clouds were observed in the flame produced by the same injector and propellants as shown in the bottom photograph.

1 1 1 1 1 1 1 1 1 1 1 1 1 1 1 1



Copper Nozzle

"A" Diameter	
089	257
1	269"
113	281
125	297
129	328
140	332
150	370
166	413
173	435
189	465
196	500
213	567
234	600
250	75 "

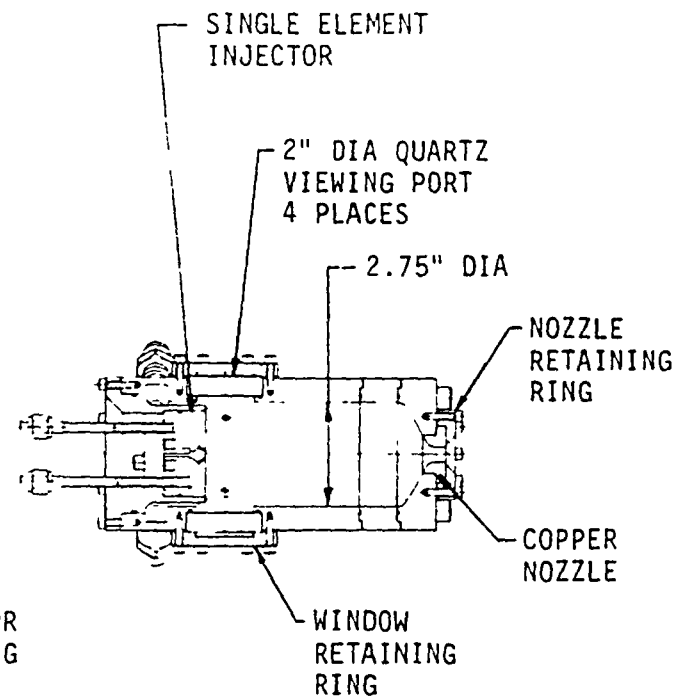
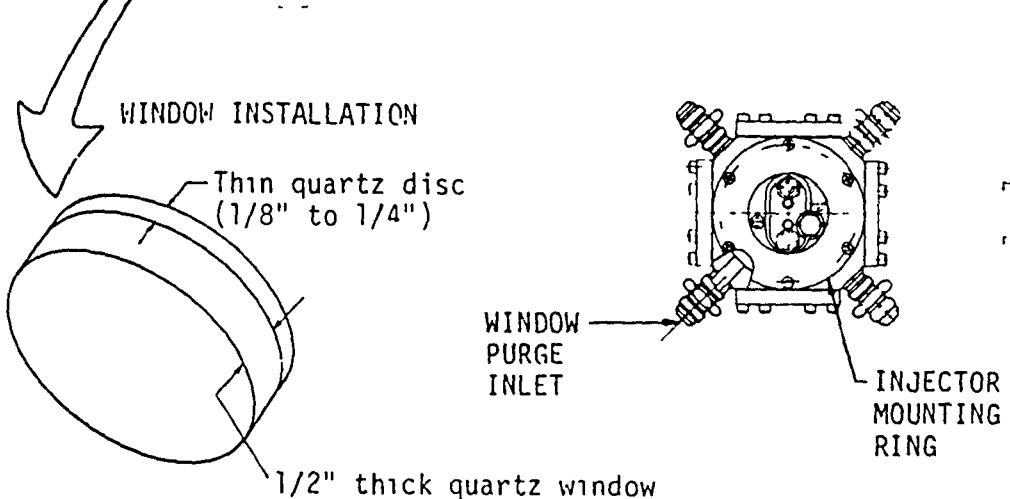
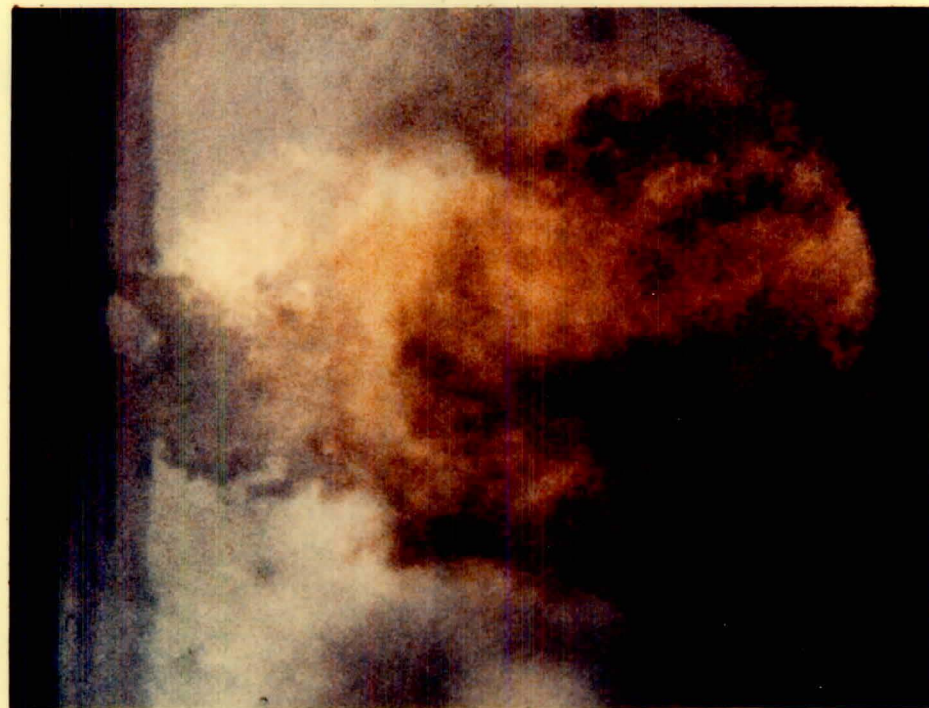


FIGURE 1. TEST CHAMBER ASSEMBLY



$P_c = 4205 \text{ kPa}$

Test No. = 172

$MR = 2.95$

Propellants = LOX/Propane

$T_f = 54^\circ\text{C}$



$P_c = 2205 \text{ kPa}$

Test No. = 169

$MR = 3.10$

Propellants = LOX/Propane

$T_f = 70^\circ\text{C}$

FIGURE 2. HIGH-SPEED PHOTOGRAPHS OF CARBON FORMATION PHENOMENA
EDM-LOL INJECTOR

Appendix A summarizes the test data accumulated by Reference 2. One hundred and twenty-seven (127) tests were conducted over a chamber pressure range of 860-10340 kPa (125-1500 psia), a fuel temperature range of -154 to 70 °C (-245 to 158°F), and a fuel velocity range of 15 to 213 m/sec (50-700 ft/sec). As noted in Reference 2, the data show the following carbon formation trends:

"As the fuel vaporization rate increases in the injector face near-zone, carbon formation decreases. This suggests that oxidizer/fuel mixing in liquid phase promotes carbon formation. Small drop size, high fuel temperature, and late oxidizer/fuel mixing relative to the point of atomization reduce carbon formation."

B. Data Selection

Among the 127 hot-fire tests, 40 tests were selected for further analysis during this effort. As shown in Table I, these tests include four injectors (OFO Tdriplet, TLOL, EDM-LOL, and PAT) and two fuels (RP-1 and propane).

Major considerations in the selection process, listed in order of priority, were (1) quality of existing photographic data, (2) tests comprising a wide range of operating variables, (3) previous analytical characterization of the injector element (e.g., drop size and distribution analyses), and (4) potential application to future engine systems.

The Unlike Doublet injector was tested only with ammonia, which naturally does not yield carbon formation data. The Slit Triplet injector was tested with gaseous methane, resulting in poor mixing without evidence of carbon deposits. The tests with the RUD injector did not yield good quality data for analysis. For that injector, the RP-1 tests were unsuccessful, and

TABLE I HOT-FIRE TESTS SELECTED FOR ANALYSIS

<u>TEST NO.</u>	<u>INJECTOR</u>	<u>FUEL</u>	<u>PC (kPa)</u>	<u>MR</u>	<u>T_f (°C)</u>	<u>MODE</u>
101	OFO Triplet	RP-1	3170	2.40	10	S (Slightly Clouded)
105	OFO Triplet	RP-1	3310	2.80	10	S
106	OFO Triplet	RP-1	3345	2.75	10	S
109	OFO Triplet	RP-1	3275	2.40	13	S
110	OFO Triplet	RP-1	3310	2.70	19	S
111	OFO Triplet	RP-1	3310	2.70	19	S
116	OFO Triplet	RP-1	10340	2.60	10	C (Clear)
120	TLOL	RP-1	930	2.35	5	O (Obscure)
121	TLOL	RP-1	2135	2.80	3	M (Moderately Clouded)
122	TLOL	RP-1	5380	2.75	7	C
123	TLOL	RP-1	3275	2.65	2	S
124	TLOL	RP-1	3275	2.65	2	S
127	TLOL	RP-1	1725	2.85	1	M
128	TLOL	RP-1	2760	3.10	4	S
129	TLOL	RP-1	5515	2.80	7	C
130	TLOL	Propane	930	2.50	7	S
131	TLOL	Propane	2000	2.65	6	C
132	TLOL	Propane	3725	3.00	6	C
133	TLOL	Propane	5445	2.80	7	C
157	EDM-LOL	Propane	5515	2.80	8	M
158	EDM-LOL	Propane	3860	2.85	-2	O
159	EDM-LOL	Propane	2035	2.90	4	O
160	EDM-LOL	Propane	1035	2.80	-1	O
161	EDM-LOL	Propane	5515	2.90	16	M
162	EDM-LOL	Propane	3790	2.95	16	O
164	EDM-LOL	Propane	2000	2.90	27	O
165	EDM-LOL	Propane	5515	2.85	64	C
168	EDM-LOL	Propane	3790	2.90	68	M
169	EDM-LOL	Propane	2205	3.10	70	C
171	EDM-LOL	Propane	4415	2.80	51	S
178	PAT	Propane	3860	2.75	21	S
179	PAT	Propane	2070	2.85	19	S
182	PAT	Propane	1035	2.90	18	M
184	PAT	Propane	2070	2.85	19	S
187	PAT	Propane	5515	2.90	19	C
189	PAT	Propane	1070	2.80	17	M
190	PAT	Propane	1140	2.75	17	S
193	PAT	Propane	3860	2.80	49	S
194	PAT	Propane	2345	3.00	46	S
197	PAT	Propane	3480	3.00	6	S

the propane tests had poor visibility due to either heavy carbon formation or poor external lighting. Consequently, the remaining four injectors were considered for analysis. The reasons justifying their selection are outlined below.

The EDM-LOL injector is considered as a candidate because of its historical use with LOX/HC propellants and because of the variety of carbon formation modes it displayed at different hot-fire operating conditions.

The TLOL injector is also an interesting candidate because it is a platelet version of the EDM-LOL, having a smaller unlike impingement angle and a longer unlike impingement height. These differences between the EDM-LOL and the TLOL were found to result in entirely different mixing patterns and quantities of carbon formation.

The PAT injector, tested extensively on Contract NAS 9-15724, displayed a tendency to avoid carbon formation until lower chamber pressures were reached. The propellant streams are preatomized before impingement and have long free-stream lengths.

The OFO Triplet injector was selected because historically, it is a very high-performing element. Also, it provides an excellent design contrast to the PAT injector since it utilizes oxidizer external impingement on an internal fuel jet whereas the PAT element has the oxidizer fan contained within fuel fans.

Figures 3 through 6 show the carbon formation dependency on chamber pressure, mixture ratios and fuel temperature for the tests conducted with the OFO Triplet, TLOL, EDM-LOL, and PAT injectors. The tests selected for further analysis are identified by underlining. For each injector, the tests selected were limited to those having mixture ratios close to a specific value because the propellant mixing is affected by mixture

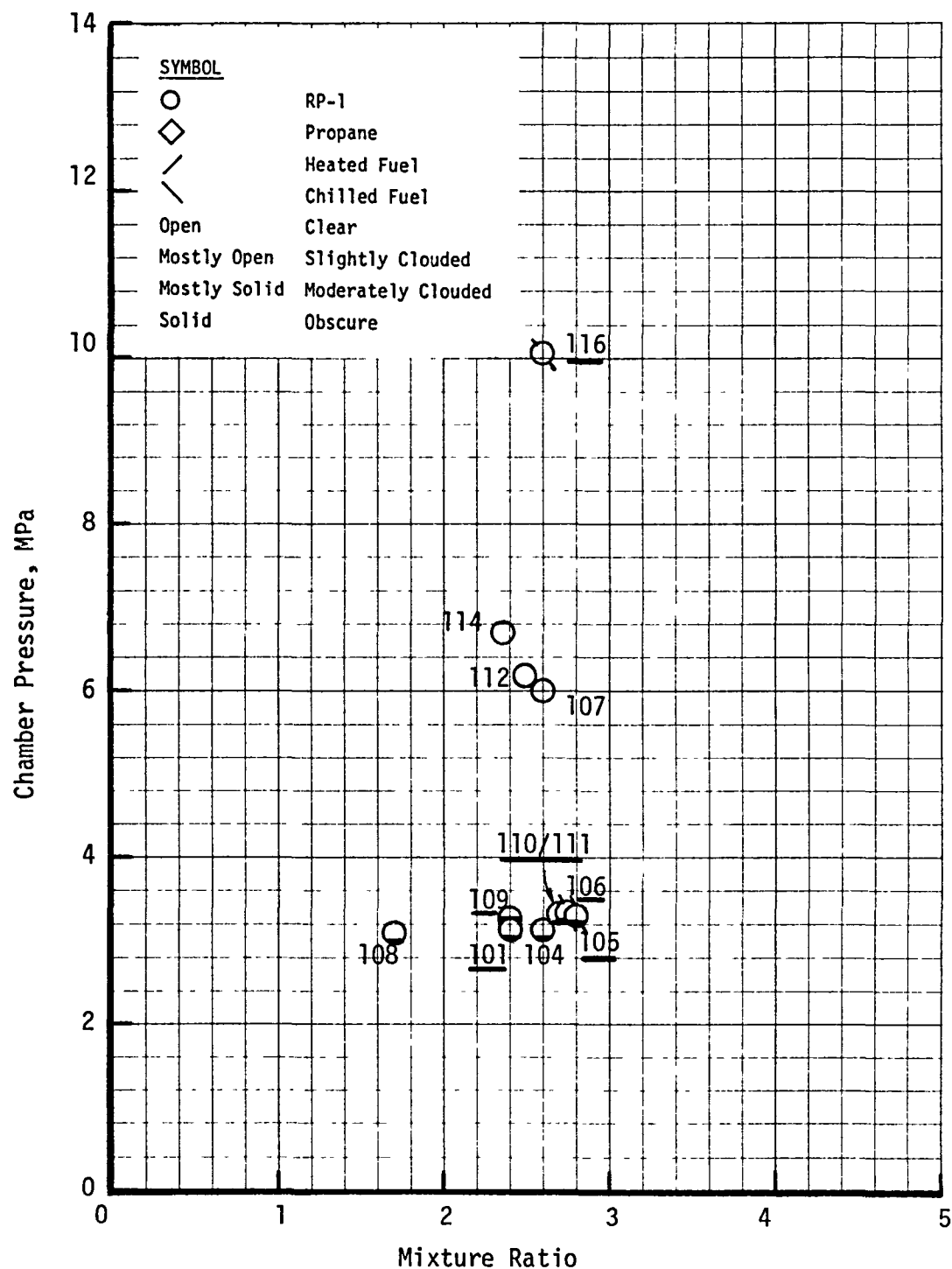


FIGURE 3. OPERATING CONDITION DEPENDENCY OF OFO TRIPLET CARBON FORMATION

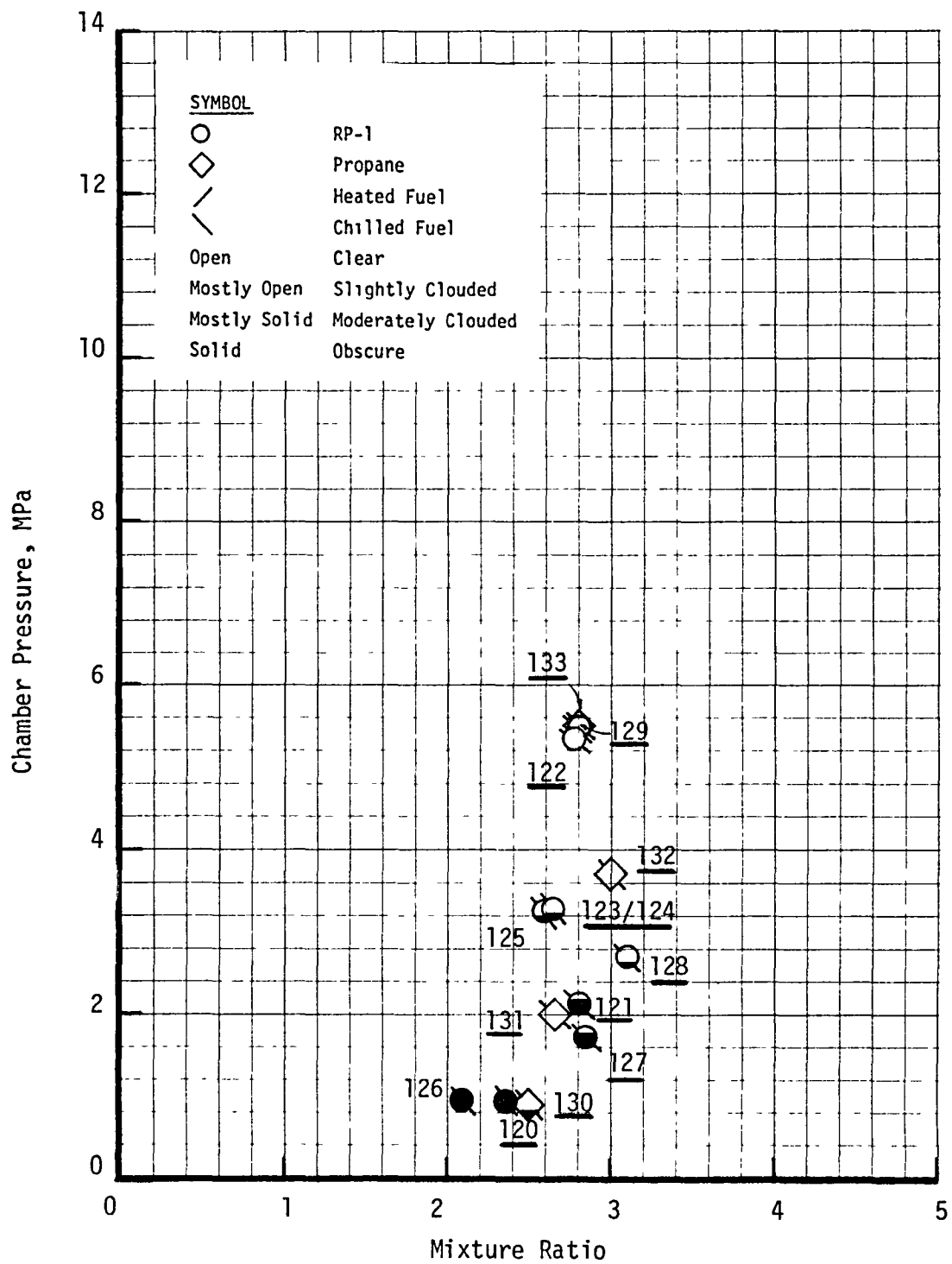


FIGURE 4. OPERATING CONDITION DEPENDENCY OF TLOL CARBON FORMATION

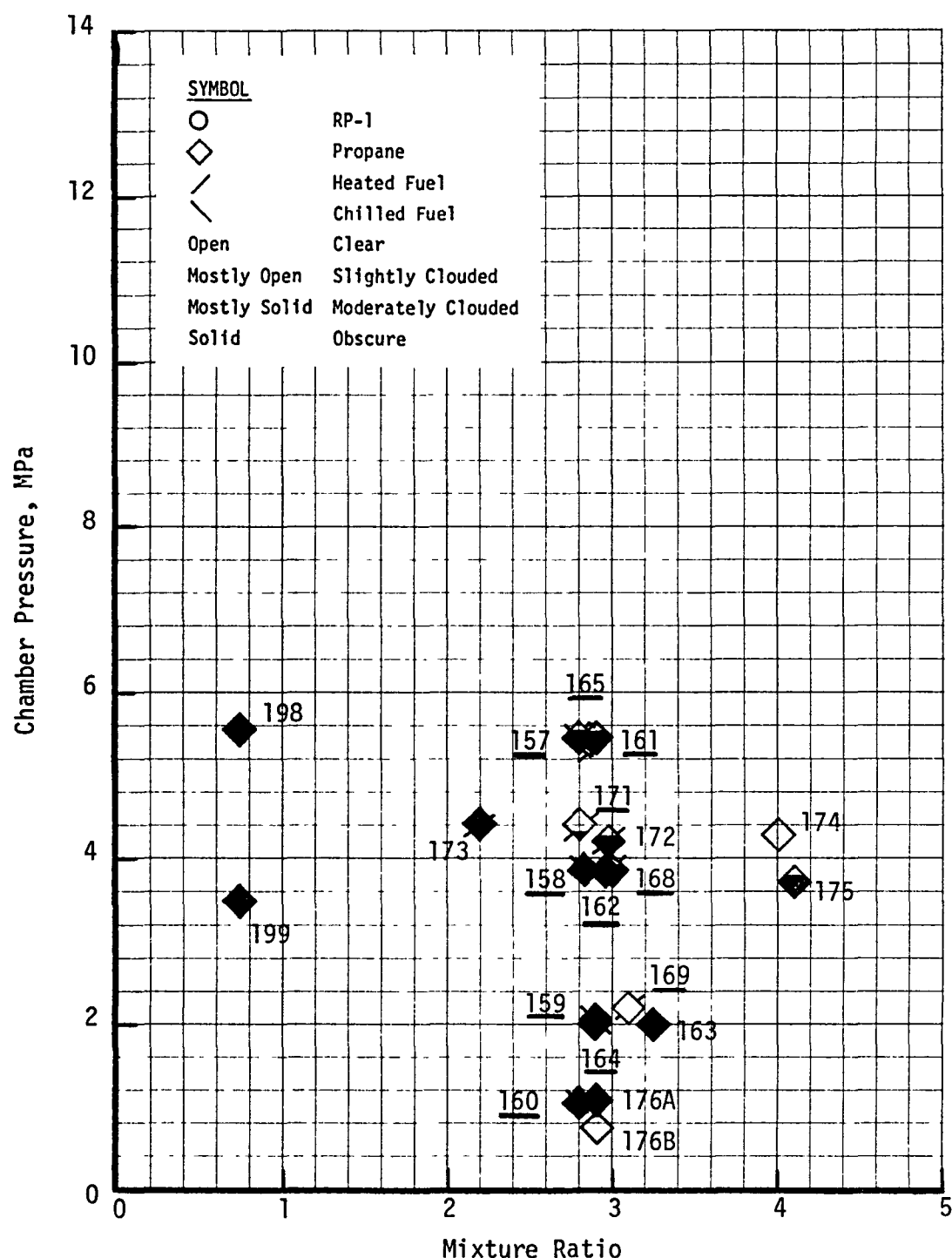


FIGURE 5. OPERATING CONDITION DEPENDENCY OF EDM-LOL CARBON FORMATION

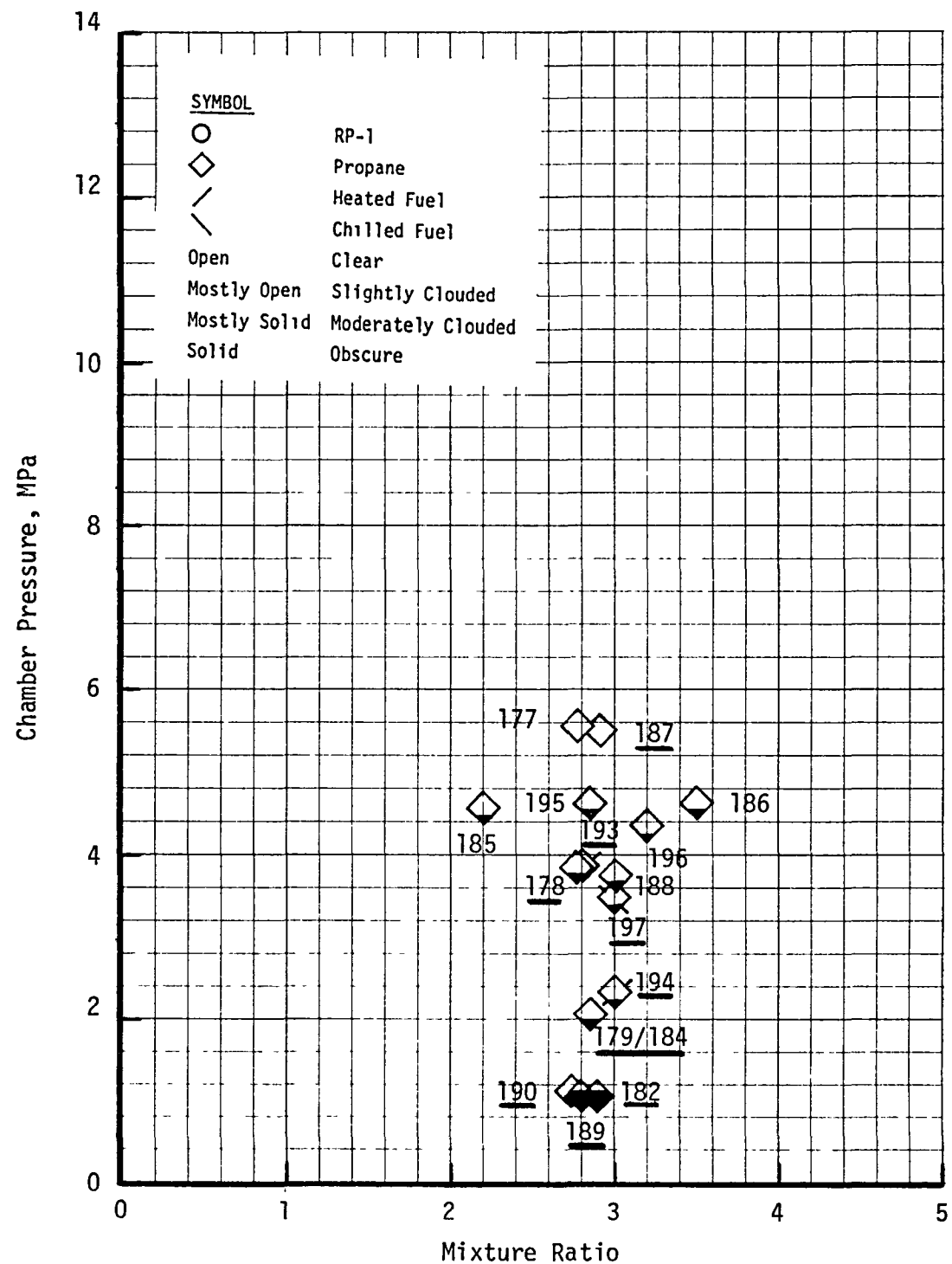


FIGURE 6. OPERATING CONDITION DEPENDENCY OF PAT CARBON FORMATION

ratio (or momentum ratio) and the cold-flow tests were limited to only one momentum ratio per injector. Figures 7 through 10 show the injection element configurations for the OFO Triplet, TLOL, EDM-LOL, and PAT injectors, respectively. The propellant atomization and mixing of the OFO Triplet injector are brought about by the unlike coherent jet streams impingement. For the TLOL and EDM-LOL injectors, the propellant atomization results from like-on-like impingement and the mixing is accomplished by canting both spray fans toward each other resulting in edge-on-edge unlike impingement. The atomization prior to the unlike impingement for the PAT injector is carried out by splashing the jet against an internal plate for the fuel or by internal jets impingement for the oxidizer. The mixing is achieved by the simultaneous broad-side impingement of the spray fans.

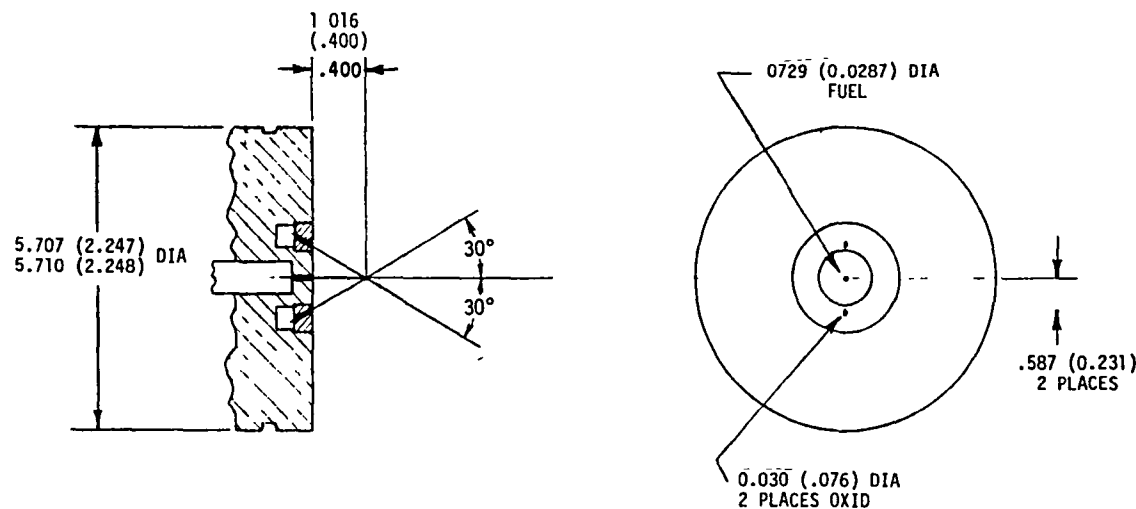


FIGURE 7. OFO TRIPLET INJECTOR CONFIGURATION

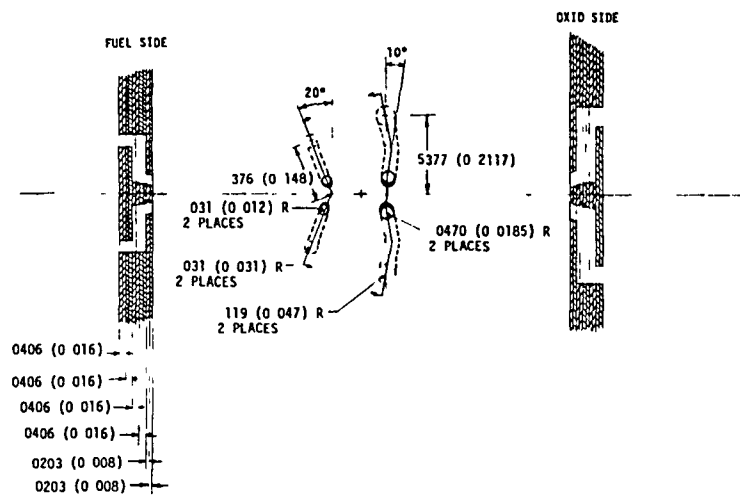


FIGURE 8. TRANSVERSE LIKE-ON-LIKE (TLOL) INJECTOR CONFIGURATION

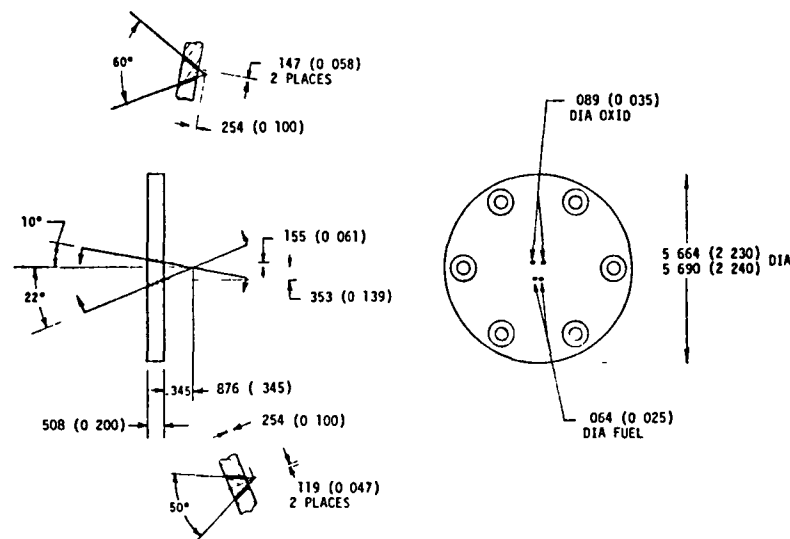


FIGURE 9. ELECTRODE DISCHARGE MACHINED LIKE-ON-LIKE (EDM-LOL) INJECTOR CONFIGURATION

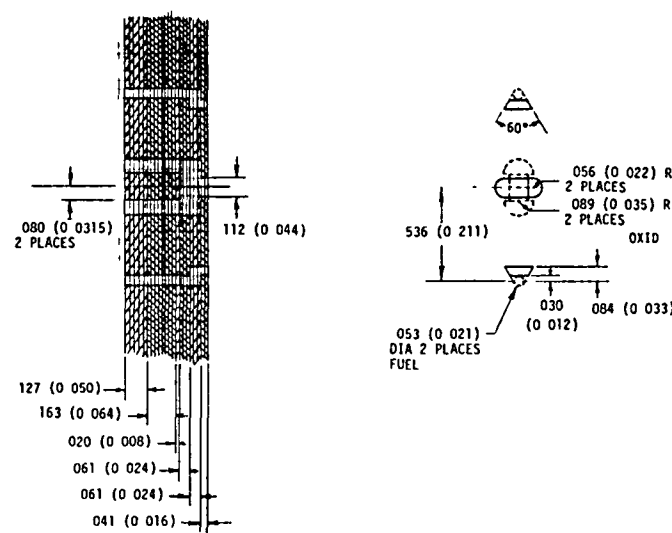


FIGURE 10. PRE-ATOMIZED TRIPLET (PAT) INJECTOR CONFIGURATION

IV INJECTOR COLD-FLOW TESTING

A. Objective

The propellant mixing of a uni-element injector is determined only by the intra-element mixing mechanism as opposed to the combination of intra- and inter-element mixing for a multi-element injector. Thus, a multi-element injector results in more uniform mixing than a uni-element injector across the entire chamber cross-section. In order to apply the vaporization correlation of Reference 3, which was based on multi-element injector data, to the present case of uni-element injector, the effect of mixing characteristics on spray combustion must be included. Moreover, the photographs of Reference 2 show localized carbon formation for some cases, indicating the strong mixing effect on carbon formation. The objective of the injector cold-flow testing was to experimentally determine the mass distributions of the oxidizer and fuel at various cross-sections of the chamber for use in the combustion analysis.

B. Method and Apparatus

The same injector bodies previously hot-fire tested in Reference 2 were used for the cold-flow testing. This experiment was conducted at the ALRC Physics Research Lab (A-Area) using the test setup shown in Figure 11. Tap water and Freon TF solvent were used as fuel and oxidizer simulants, respectively. The simulant bottles were pressurized with gaseous nitrogen. In order to maintain the injector manifold pressures at desired values, the nitrogen flows were controlled by pressure regulators. The physical properties of the Freon used are given in Figure 12.

The sprays formed by the injected liquids were intercepted by a spray collector consisting of a 10×10 grid of flow passages. The fluids were then collected by the glass tubes, with one tube for each grid. Since

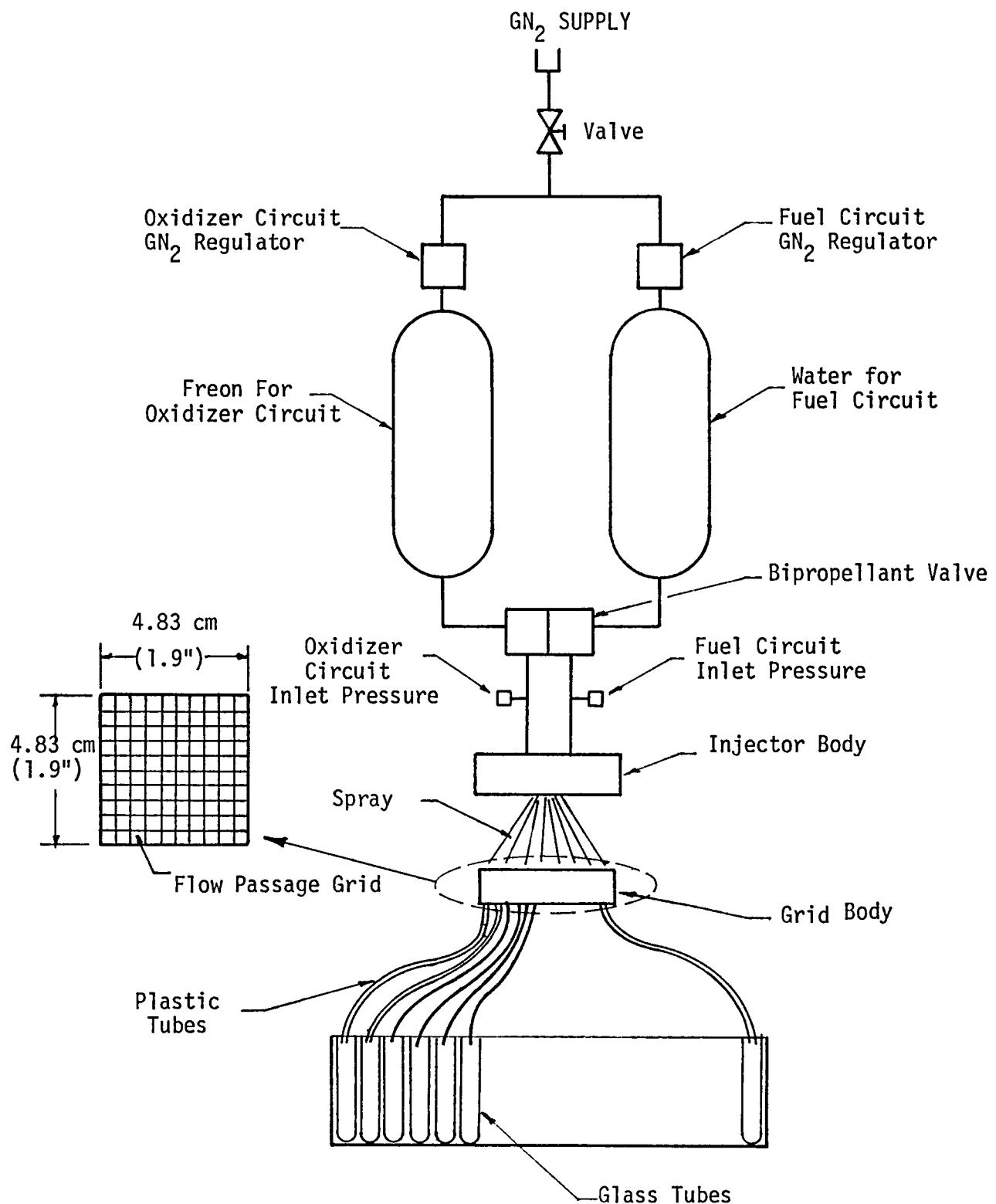
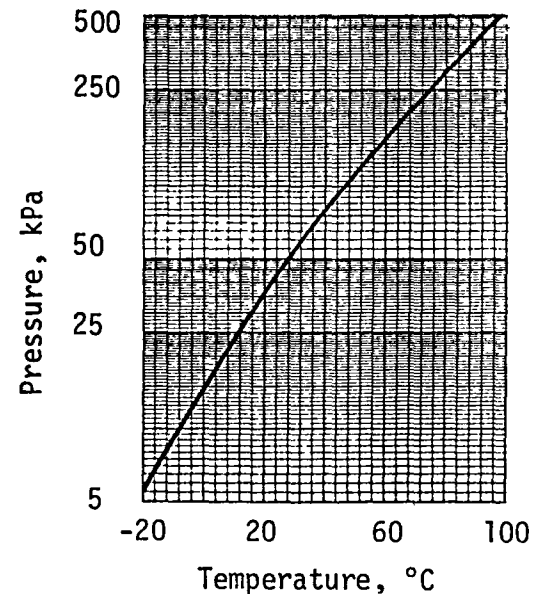
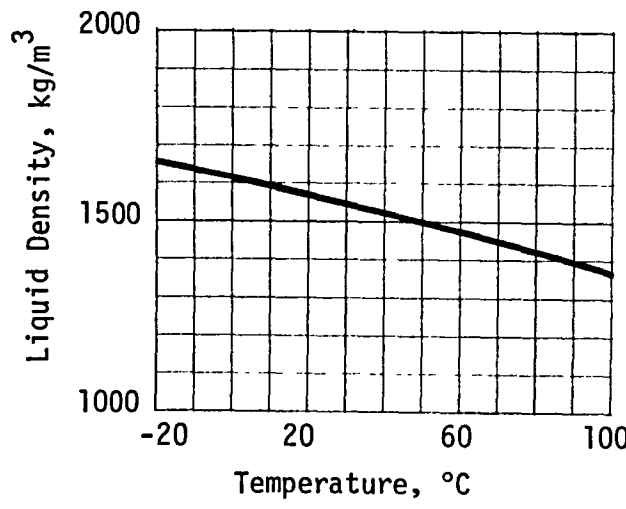


FIGURE 11. INJECTOR COLD-FLOW SETUP



Chemical Formula	$\text{CCl}_2\text{F} - \text{CClF}_2$
Molecular Weight	187.4
N.B.P.	47 °C
Freezing Point	-35 °C
Critical Temperature	214 °C
Critical Pressure	3413 kPa
Heat of Vaporization at NBP	146.82 kJ/kg
Liquid Specific Heat at 21 °C	0.892 kJ/kg °C
Liquid Viscosity at 21 °C	6.940×10^{-5} kg/m-s
Surface Tension at 25 °C	19.0 dynes/cm
Solubility of Water at 21 °C, % by Wt.	0.009

FIGURE 12. PHYSICAL PROPERTIES OF FREON TF SOLVENT

the simulants are immiscible, the mass distributions of both simulants for a given injector and test condition were readily determined from the collected fluids.

C. Results

For each injector, experiments were run at four different distances between the injector face and the grid face: 1.27 cm (0.5"), 2.54 cm (1.0"), 3.81 cm (1.5"), and 5.08 cm (2.0"), except for the OFO Triplet injector. For that injector, the spray exceeded the collector face area at the 5.08 cm (2.0") distance and therefore the measurements were made only at the shorter distances.

All experiments were made at oxidizer-to-fuel momentum ratios corresponding to the nominal mixture ratios of hot-fire tests. Table II summarizes the nominal injector operating conditions of both hot-fire tests and cold-flow experiments for the four injectors.

The data obtained from such cold-flow tests are summarized in Appendix B. Each grid of the collector head is represented by a block coordinate, (I, J), which contains, in order, oxidizer-to-fuel mixture ratio, oxidizer mass fraction, and fuel mass fraction. The approximate locations of the injection orifice projections on the collector head are also shown. For the case where the collector head is 3.81 cm (1.5 inches) below the injector face, the mixture ratios, oxidizer mass fractions and fuel mass fractions are shown in 3-dimensional representation in Figures 13 through 16.

The OFO Triplet injector was found to have misimpingement in a manner such that part of one oxidizer jet stream passes by the other two jets without mixing, as shown in Figure 17. This same jet stream also impinges on the fuel jet before the other oxidizer jet does. These two

TABLE II - INJECTOR HOT-FIRE AND COLD-FLOW NOMINAL OPERATING CONDITIONS

INJECTOR	EDM-LOL	OFO-TRIPLET	T-LOL	PAT
HOT-FIRE				
Oxidizer	LOX	LOX	LOX	LOX
Fuel	Propane	RP-1	RP-1	Propane
ρ_0 , kg/m ³	1156	1156	1156	1156
ρ_f , kg/m ³	498	803	803	498
Nominal MR	2.9	2.6	2.8	2.9
Momentum Ratio	1.82	2.14	2.43	1.46
COLD-FLOW				
Oxidizer	Freon	Freon	Freon	Freon
Fuel	Water	Water	Water	Water
ρ_0 , kg/m ³	1589	1589	1589	1589
ρ_f , kg/m ³	1002	1002	1002	1002
Momentum Ratio Sought	1.82	2.14	2.43	1.46
Reqd $\Delta P_o / \Delta P_f$	0.915	0.977	1.082	0.590
Tested ΔP_o , N/m ²	316	309	370	274
Tested ΔP_f , N/m ²	343	309	343	480

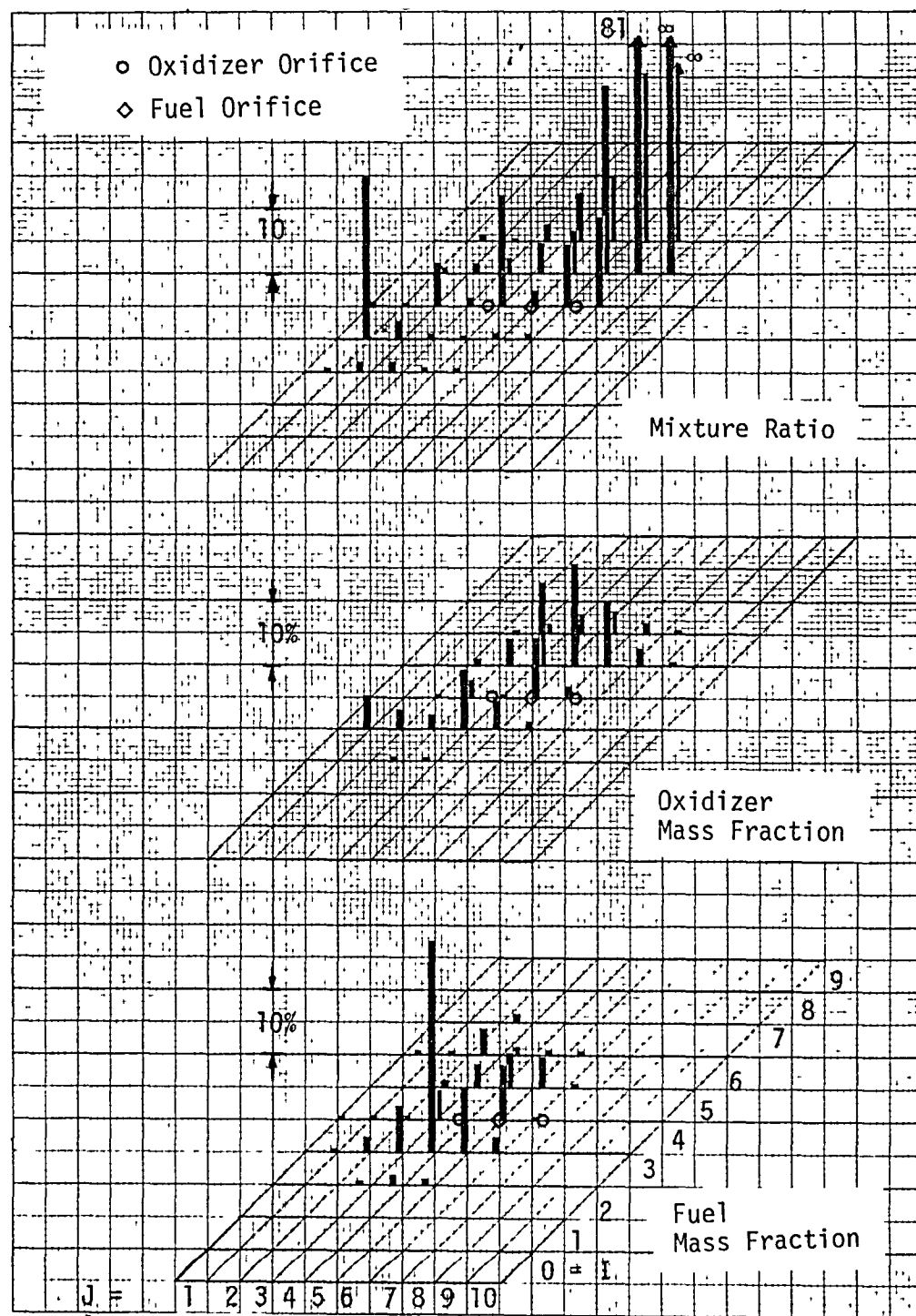


FIGURE 13. OFO TRIPLET COLD-FLOW MIXING PATTERN AT 3.81 CM AXIAL LOCATION

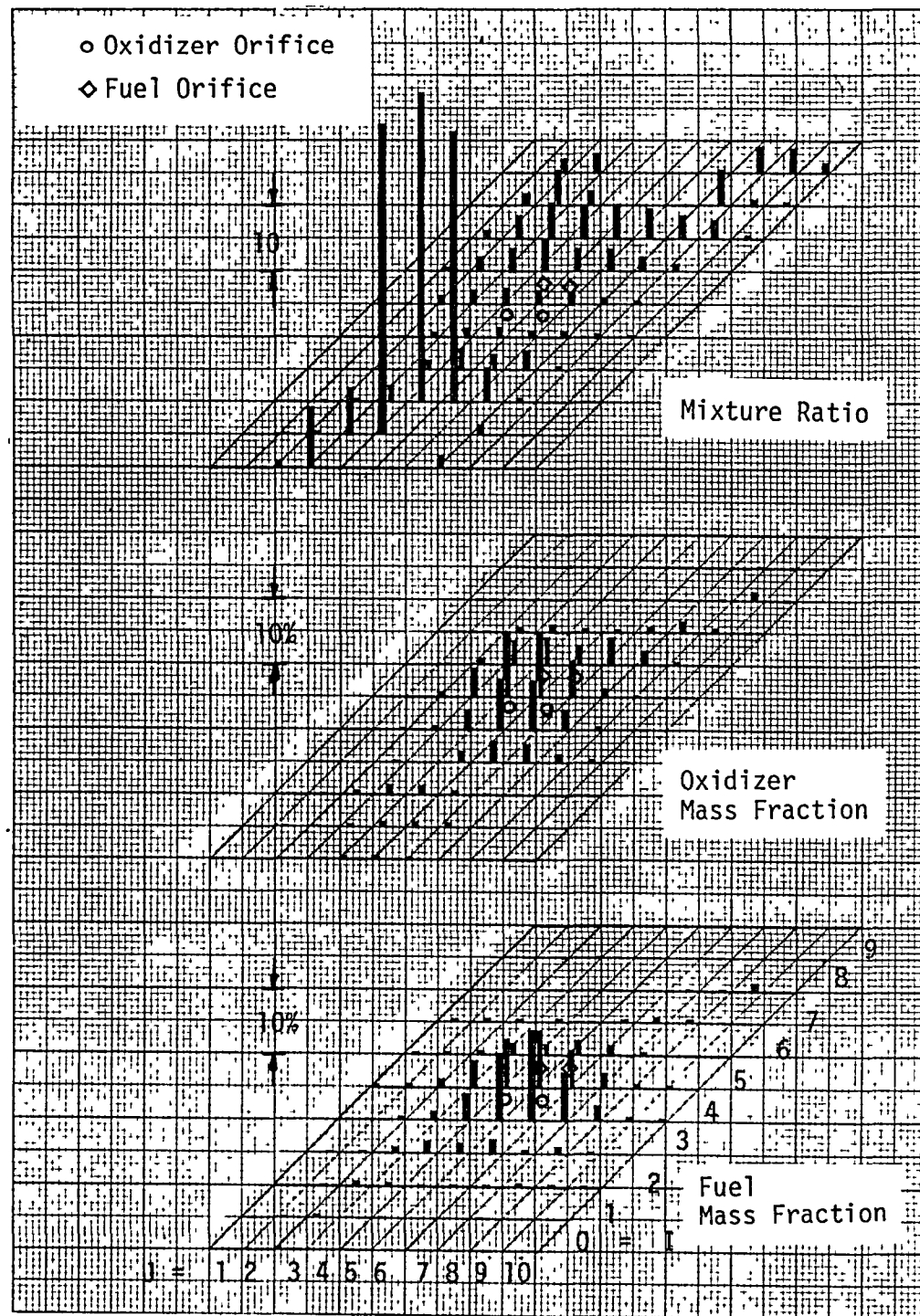


FIGURE 14. EDM-LOL INJECTOR COLD-FLOW MIXING PATTERN AT 3.81 CM AXIAL LOCATION

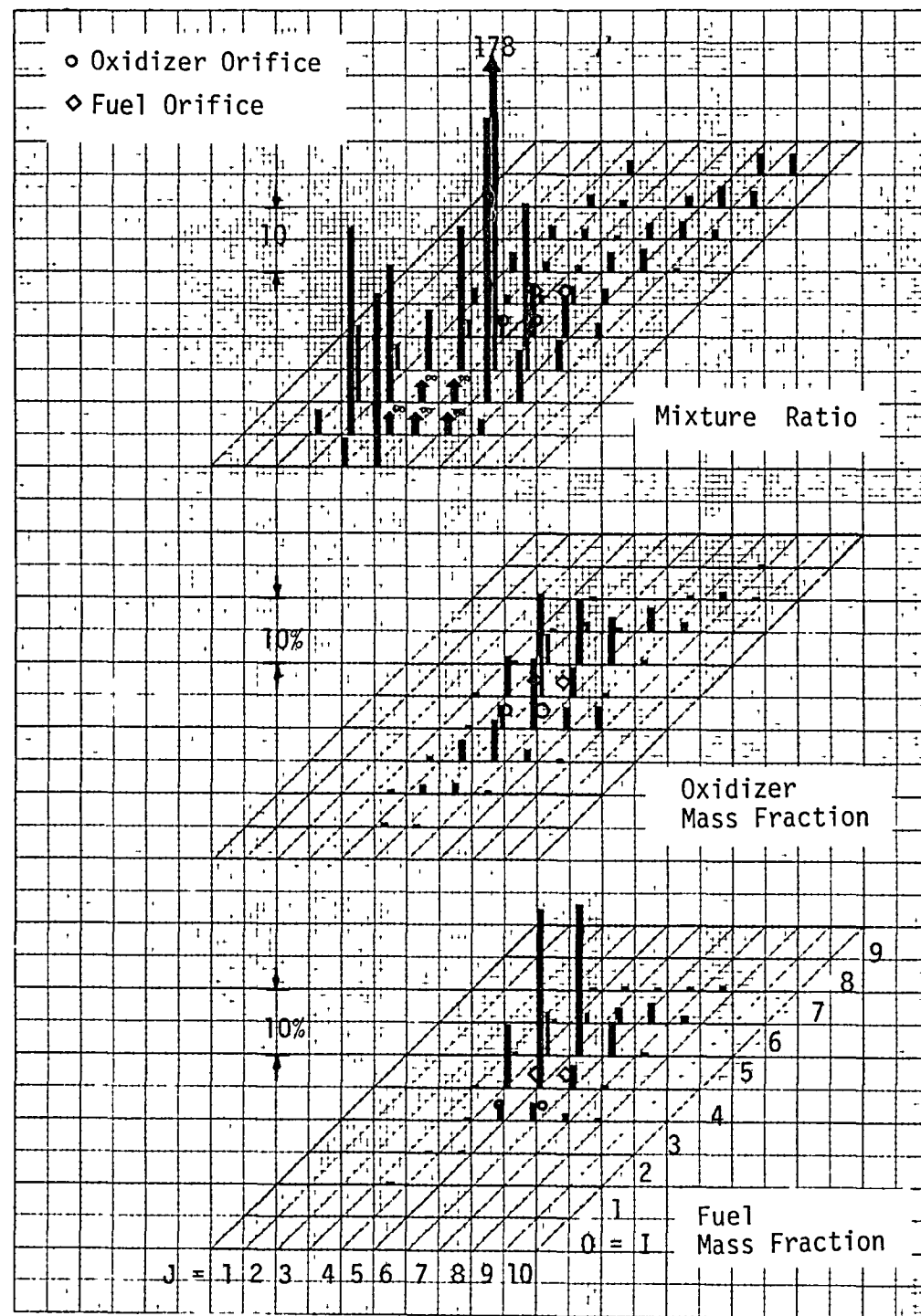


FIGURE 15. TLOL INJECTOR COLD-FLOW MIXING PATTERN AT 3.81 CM AXIAL LOCATION

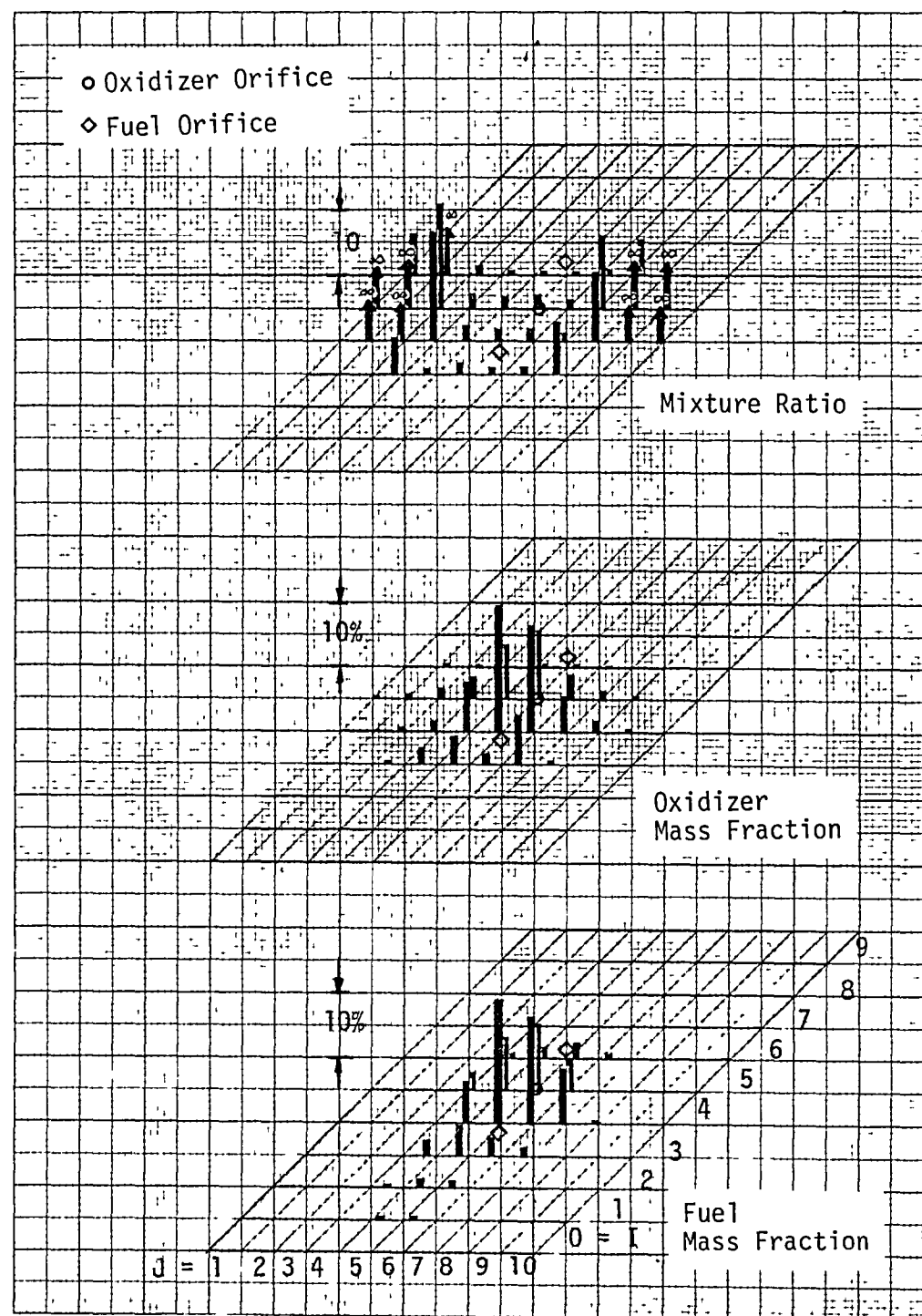


FIGURE 16. PAT INJECTOR COLD-FLOW MIXING PATTERN AT 3.81 CM AXIAL LOCATION

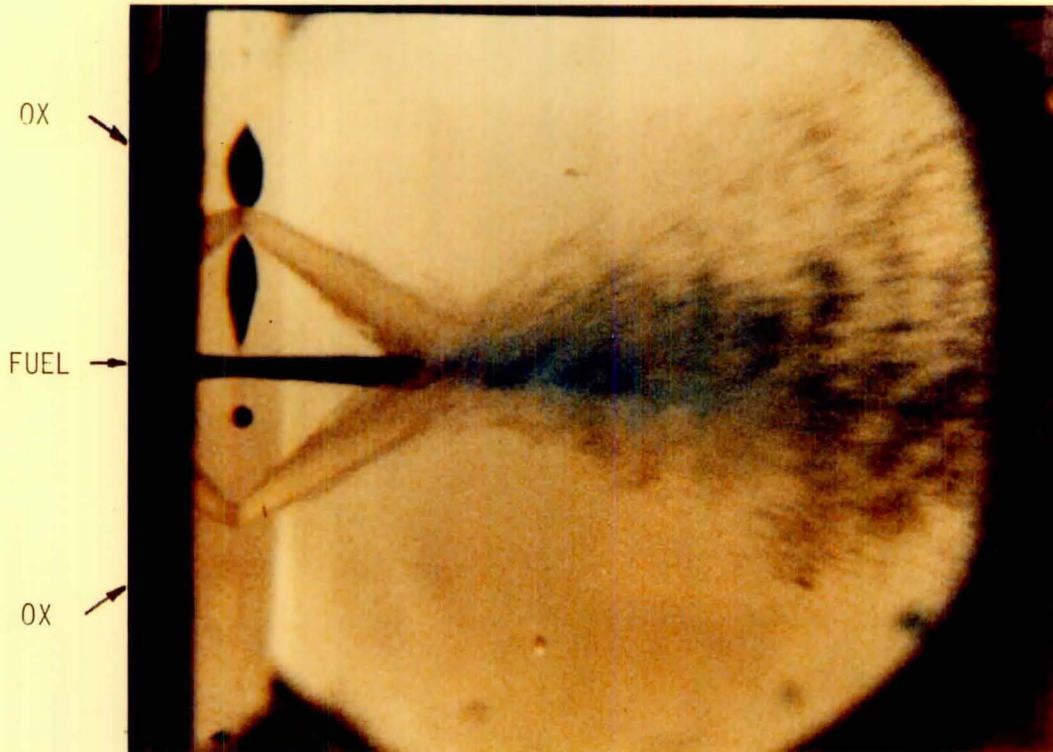


FIGURE 17. OFO TRIPLET INJECTOR COLD-FLOW SPRAY PATTERN



FIGURE 19. EDM-LOL INJECTOR COLD-FLOW SPRAY PATTERN

anomalies result in the uncommon cold-flow mixing pattern indicated by Figure 13. Figure 18 describes this mixing pattern and its causes.

The spray fans of the EDM-LOL element are shown in Figure 19. The unlike cant angles of the spray centerlines are 10° for the oxidizer and 22° for the fuel resulting in an unlike impingement height of 0.88 cm (.35 in.). Figure 14 shows that the fluids of both circuits are mostly concentrated in the center of the spray field so that the mass fraction decreases as it moves away from the center. Figure 20 schematically shows the mixing distribution pattern observed from Figure 14. A fuel-rich zone is sandwiched between two oxidizer-rich zones. Nominal mixture ratios appear along the oxidizer-rich and fuel-rich interfaces.

The spray fans of the TLOL element are shown in Figure 21. This element is a platelet version of the conventional LOL (EDM-LOL) element. The total included angle between the centerlines of the impinging unlike fans is 15° instead of 32° as used in EDM-LOL. This yields a long unlike impingement height approximately equal to 1.42 cm (.56 in.). Figure 15 shows that although the oxidizer spray of the TLOL element spreads much like the oxidizer spray of the EDM-LOL element due to high oxidizer momentum, the fuel is confined to a narrow area and hardly spreads and penetrates into the oxidizer-dominated zone. Figure 22 is a sketch of the mixing pattern observed from the data. This poor mixing is caused by the small unlike impingement angle.

The spray fans of the PAT element are shown in Figure 23. This element has a spray pattern different from the OFO Triplet in two ways. First, the PAT injector consists of two fuel orifices (Splash Plate elements) on the opposite sides of a single oxidizer orifice (X-Doublet element). This arrangement is just opposite to the OFO Triplet arrangement. Second, each

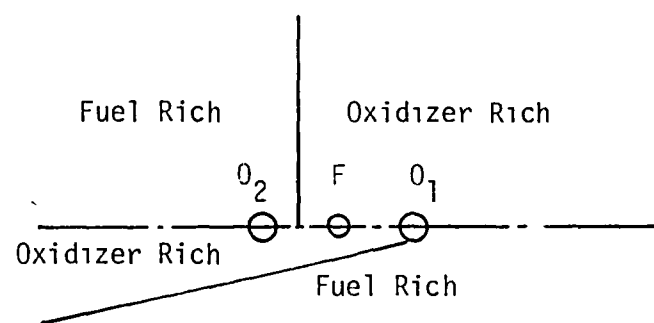
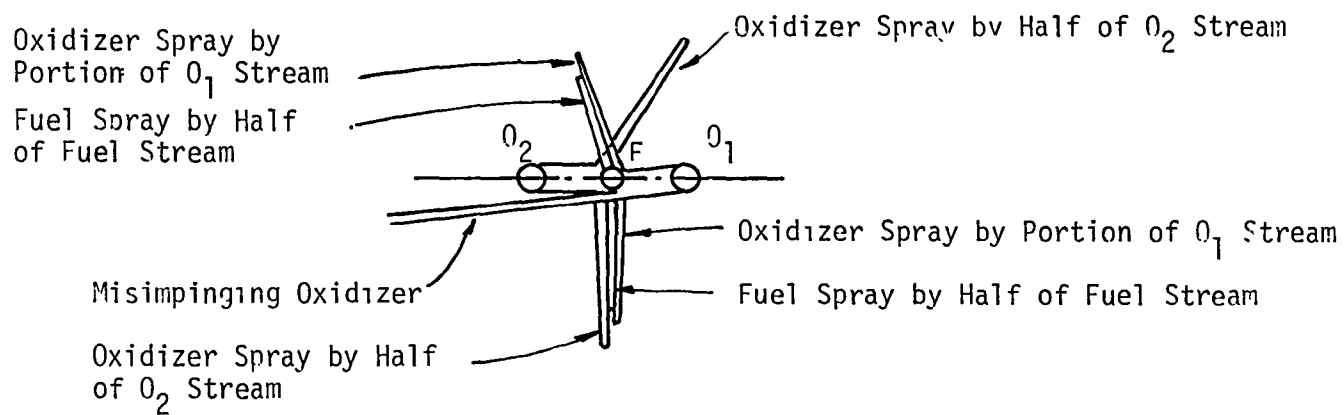
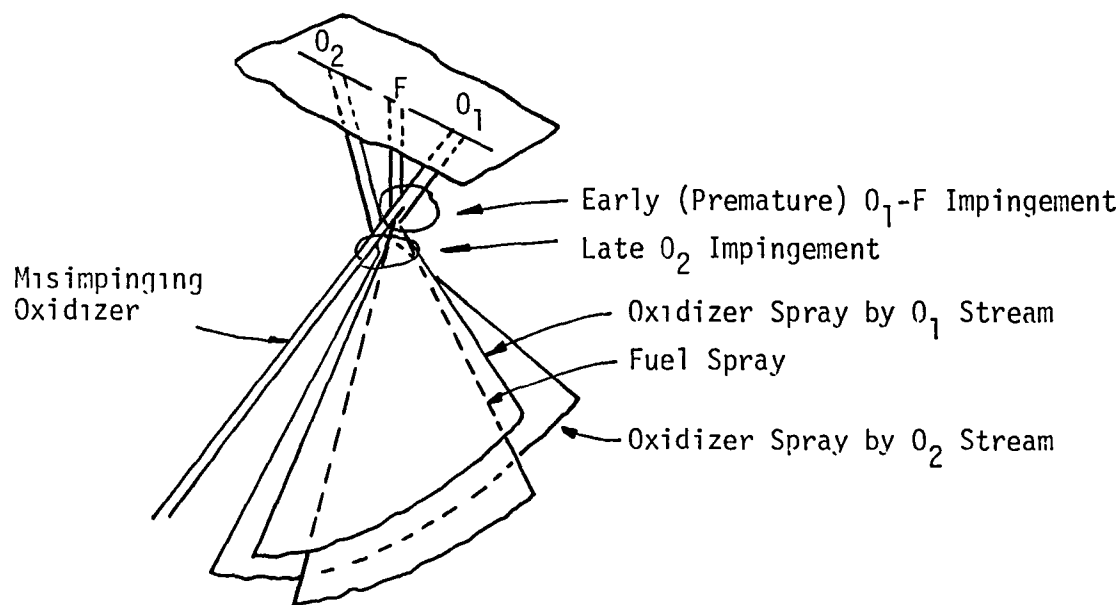


FIGURE 18. OFO INJECTOR COLD-FLOW MIXING PATTERN

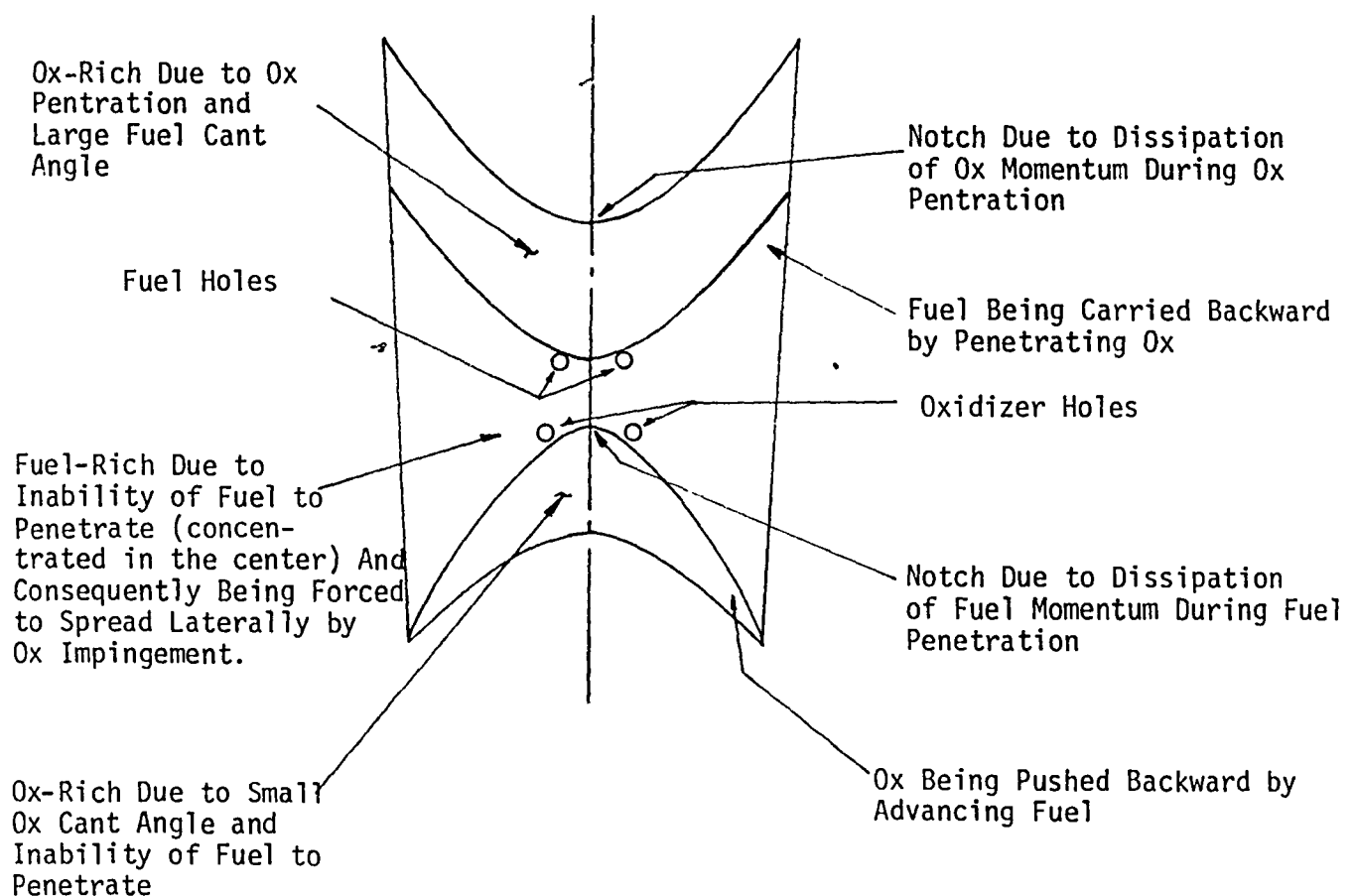
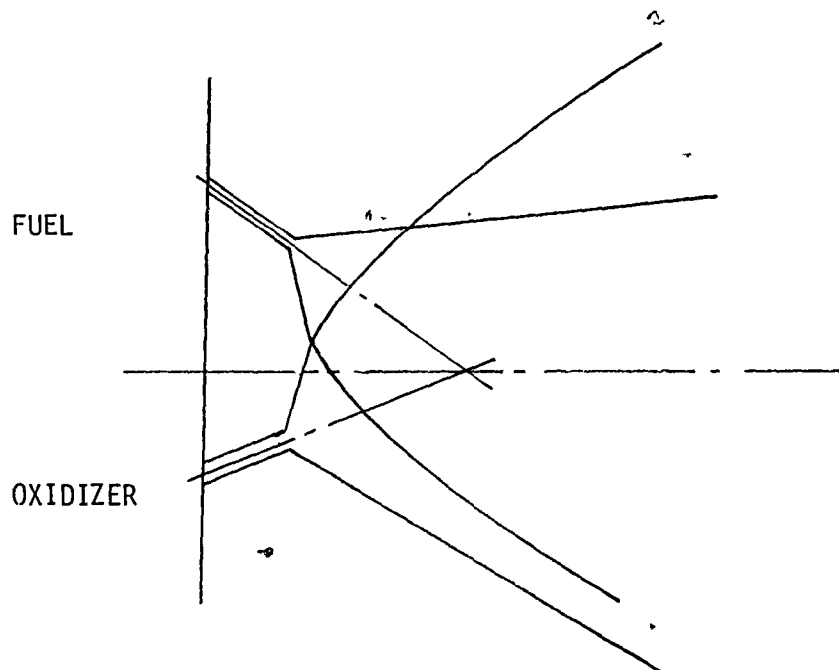


FIGURE 20. EDM-LOL INJECTOR COLD-FLOW MIXING PATTERN



FIGURE 21. TLOL INJECTOR COLD-FLOW SPRAY PATTERN

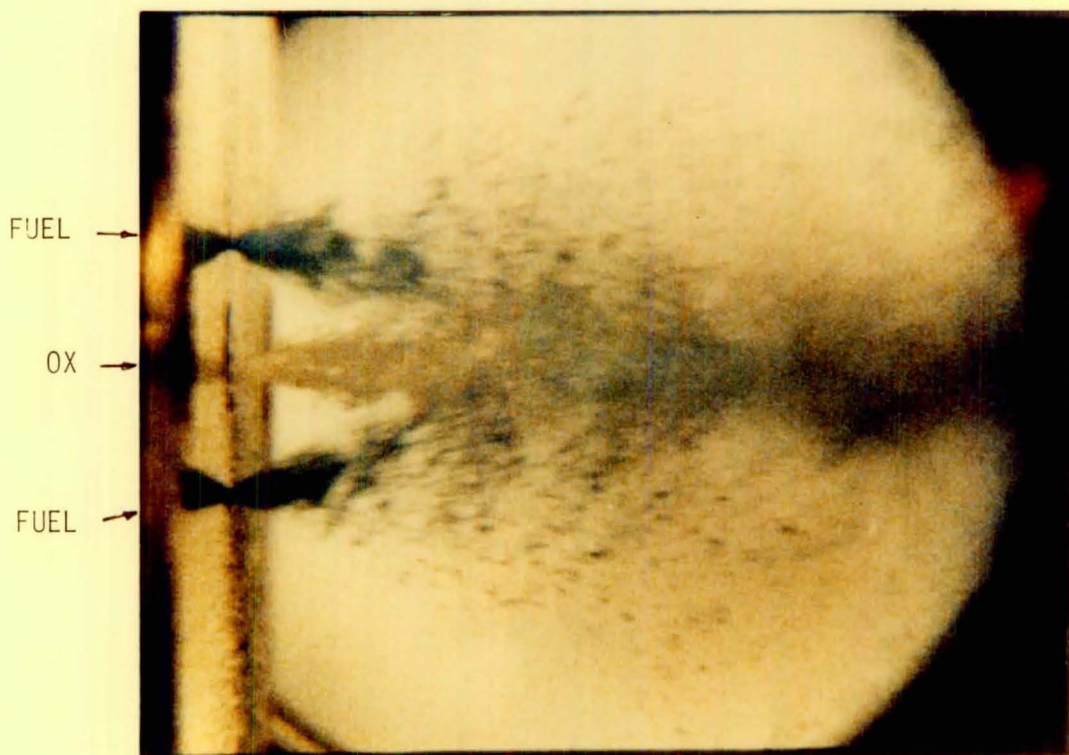


FIGURE 23. PAT INJECTOR COLD-FLOW SPRAY PATTERN

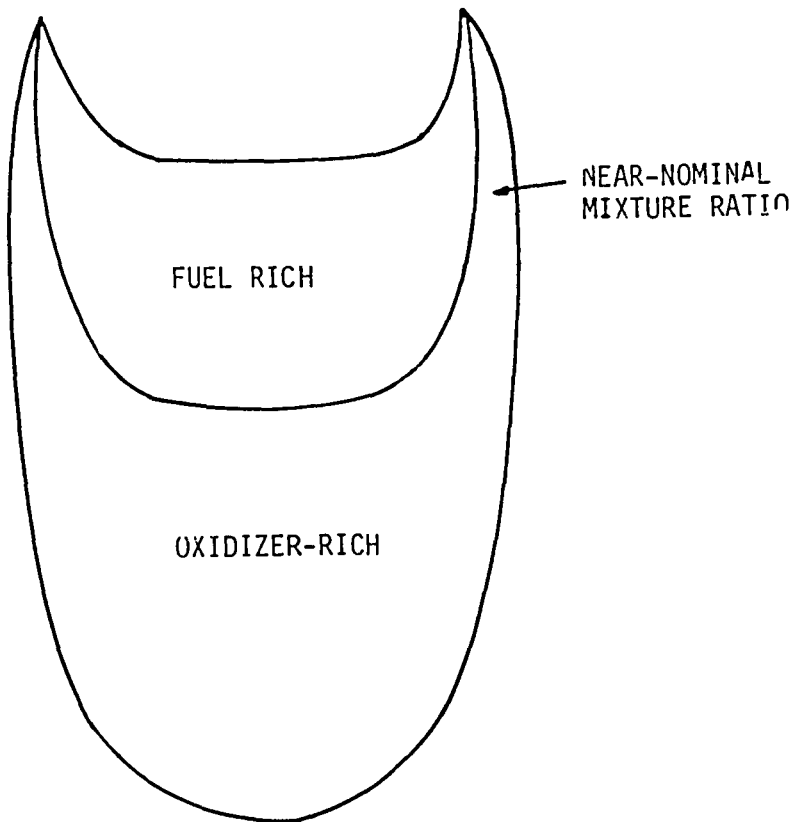
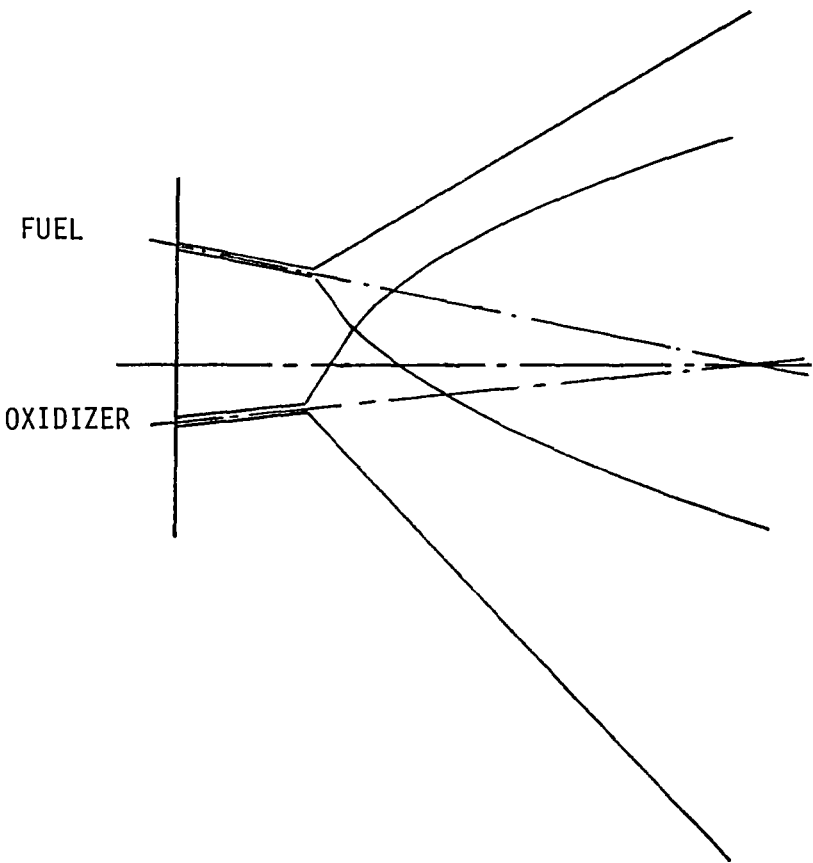


FIGURE 22. TLOL INJECTOR COLD-FLOW MIXING PATTERN

orifice of the PAT injector produces a spray fan, resulting in sheet-on-sheet impingement instead of coherent jet impingement as in the OFO Triplet. Figure 16 shows a bell-shape type of fan-span mass distribution for both the oxidizer and fuel fans. The fuel has a much smaller fan angle than the oxidizer which results in a mixing pattern consisting of a slightly fuel-rich zone along the element centerline and two oxidizer-rich zones, carrying small total mass fraction, on each side of the fuel-rich zone. The small fuel cant angle results in long unlike impingement height approximately equal to 3.38 cm (1.33 in). This causes a poor mixing pattern similar to that observed for the TLOL injector. Figure 24 qualitatively outlines the contour of the mixing pattern.

Figure 25 is a sketch of the hot-fire view window, through which the photographs of spray combustion fields were taken as described in Reference 2. Corresponding to the cold-flow testing, the entire view scope can be divided into three planes perpendicular to the chamber axis and located at 1.27 cm (0.5"), 2.54 cm (1.0"), and 3.81 cm (1.5"), respectively, downstream from the injector face. On each plane, there are as many as 100 (10 x 10) square cross-sections with dimensions at 0.48 cm x 0.48 cm (0.19" x 0.19"). Each cross-section represents a grid of cold-flow collector head and has propellant mass fractions determined by cold-flow tests. This arrangement allows a direct comparison of the vaporization analysis results with the hot-fire photographs.

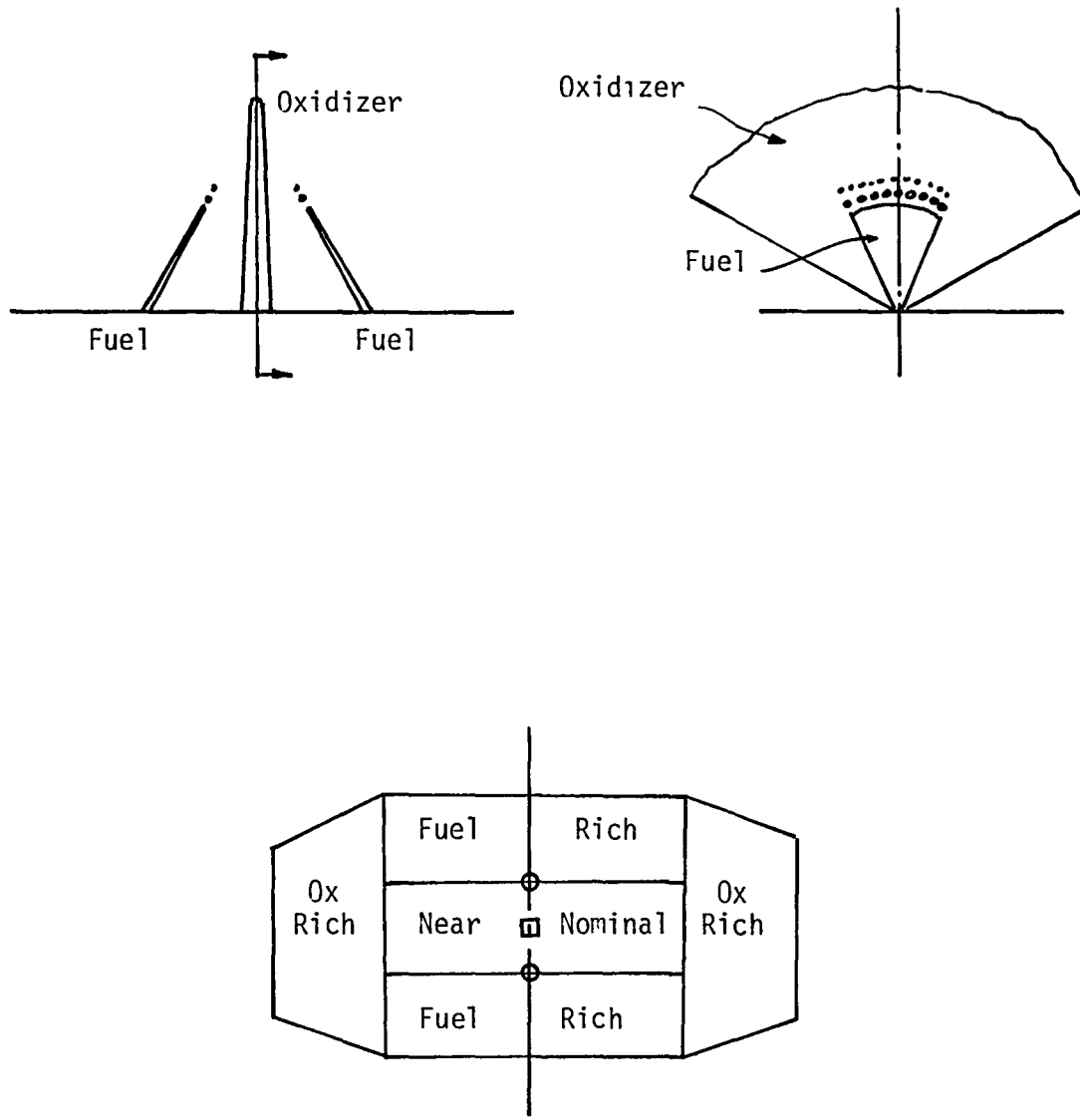


FIGURE 24. PAT INJECTOR COLD-FLOW MIXING PATTERN

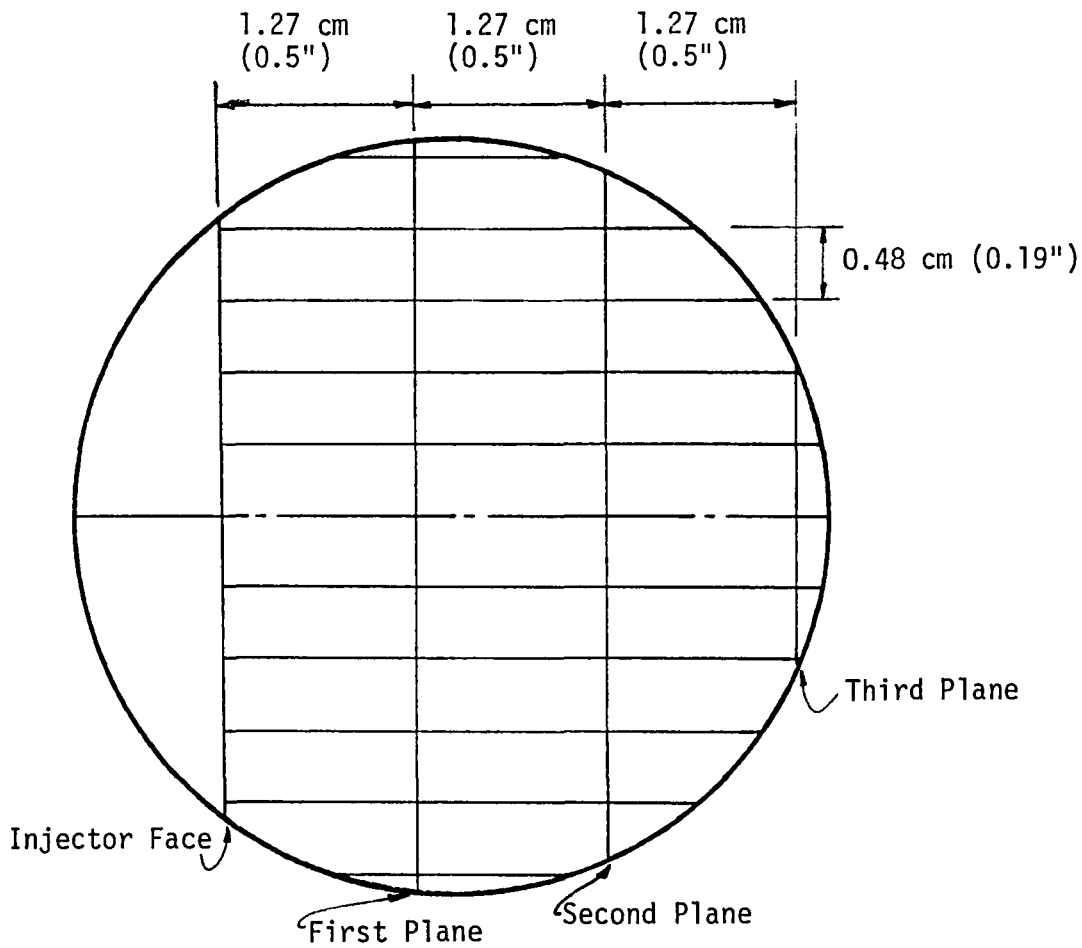


FIGURE 25. ZONING OF THE WINDOW VIEW OF THE COMBUSTION FIELD

V VAPORIZATION ANALYSIS

A. Generalized-Length Model Summary

The present vaporization analysis is based on the Priem-Heidmann Generalized-Length model reported in Reference 3. This model, correlates the propellant mass vaporized with an effective chamber length (generalized length, L_{gen}), defined by the following equation:

$$L_{gen} = (L_c/C_R)^{0.44} + 0.833 L_N/(C_R^{0.22} S^{0.33}) \quad (Pc/2068)^{0.66} K_P K_J \quad (1)$$

where

$$K_P = (1 - T_r)^{0.4} (H_v/325.64)^{0.8} (M/100)^{0.35}$$

$$K_J = (r_m/76.20)^{1.45} (V/328)^{0.75}$$

Nomenclature is defined in Appendix F. Figure 26 shows the average value of propellant mass vaporized as a function of L_{gen} , with extrapolations from the correlation of Reference 3 for vaporization less than 1% or greater than 99%.

The correlations of the mass-median droplet radius, r_m , shown in Figure 27 were determined by Reference 3 from LOX/Heptane hot-fire performance data by assuming equal drop size for both propellants. The injection velocity is at 19.8 m/sec (65 ft/sec). The impinging jets (like-on-like) and triplet types of injector have an impingement half angles equal to 45°. In order to apply this drop size correlation to other engine operating conditions, the effects of propellant properties, injection velocity, and injector element configuration must be included.

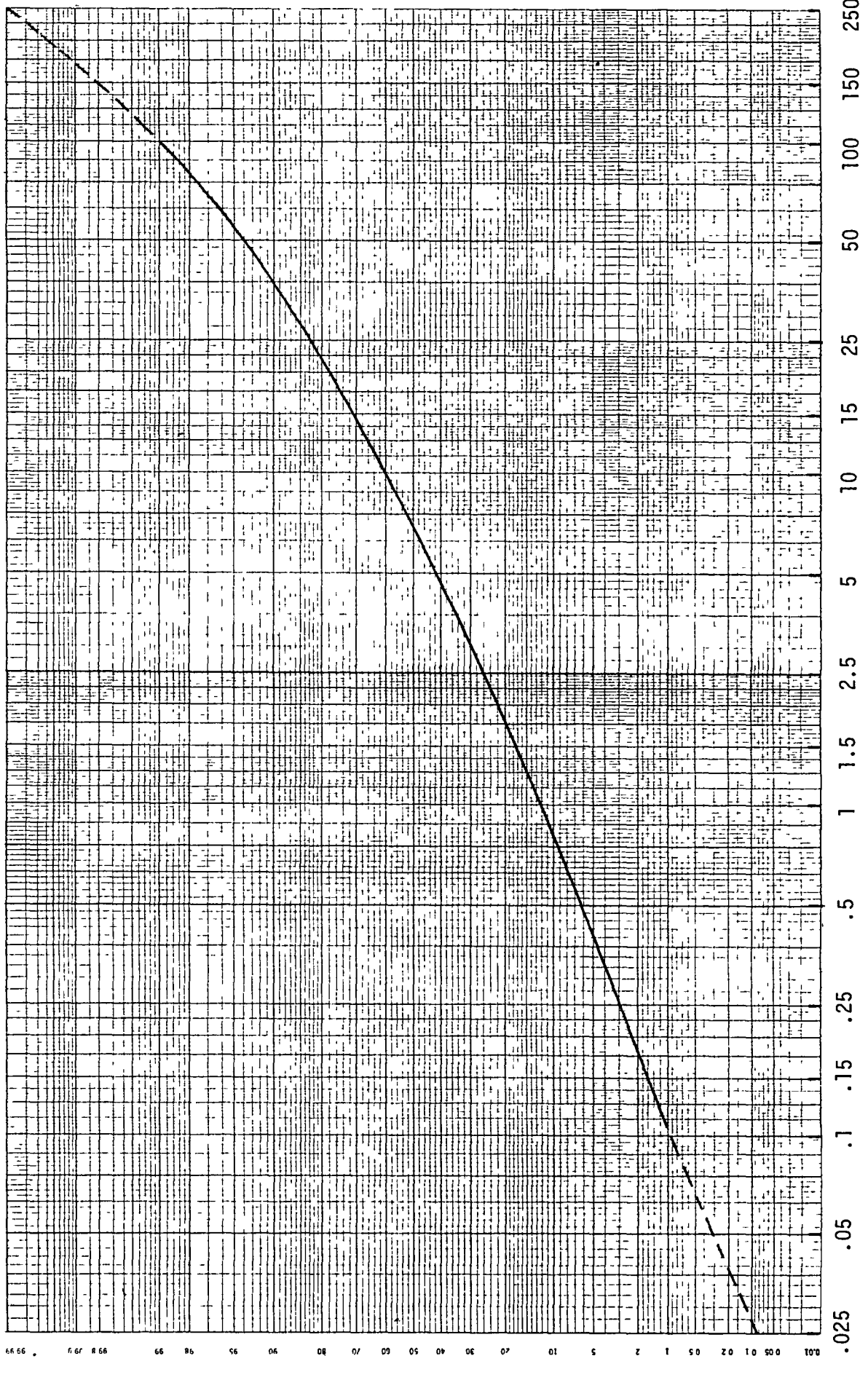


FIGURE 26. GENERALIZED LENGTH CORRELATION WITH MASS VAPORIZED (REFERENCE 3)

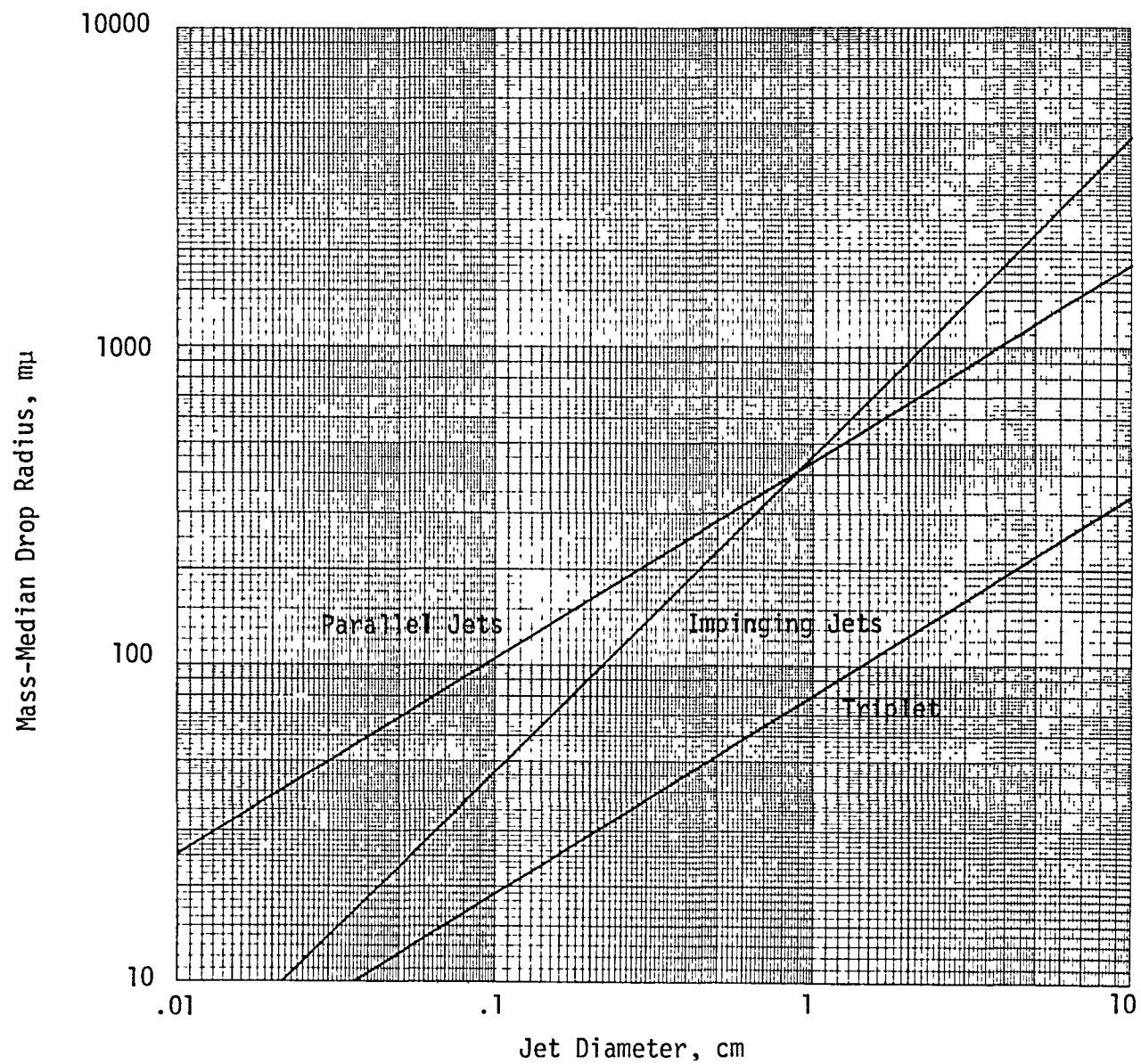


FIGURE 27. DROP SIZE DETERMINED FROM EXPERIMENTAL LOX/HEPTANE ENGINE PERFORMANCE (REFERENCE 3)

For the effects of propellant surface tension (σ), viscosity (μ), and density (ρ) on the mass median drop size (r_m), Reference 3 recommended the following relationship based on the result of Reference 4:

$$r_m = 99.29 r_{m, \text{uncor}} (\sigma\mu/\rho)^{0.25} \quad (2)$$

The effects of the injection velocity and injector configuration which are not included in Reference 3 are accounted for by the present investigation as discussed in the following subsection.

B. Atomization Process Considerations

Liquid droplets are formed through the disintegration of jets or sheets. All four injectors considered in the present study produce droplets by sheet disintegration. With this type of injector, a propellant sheet is either issued directly from the injection orifice such as Splash-Plate and X-Doublet, or formed by impinging jets such as OFO Triplet and Like-On-Like doublet. The self-formed sheet and the majority of the liquid mass of the impinging-jet-formed sheet exist as a forward diverging fan with attenuating fan thickness. The lateral edges of the fan break up and form drops when the declining surface tension becomes less than the propellant momentum. Due to aerodynamic instability, the leading edge of the fan breaks up into ligaments, which subsequently form droplets. This droplet formation process is affected by injector configuration, propellant physical and hydraulic properties, and the surrounding gas physical properties.

A survey of the values reported in the open literature for the exponent of the injection velocity dependency of drop size is shown in Table

III. The most reasonable value seems to be 0.66 since it was reported by most investigators and by both experimental and theoretical results. As a result, this exponent has been used to account for the injection velocity effect on drop size.

The injector configuration affects the drop size by its orifice size and the fan angle it yields. The orifice size effect has been provided by the correlation shown in Figure 27. The fan angle model and the effect of fan angle on drop size are discussed herein.

Both experimental (References 15, 16, and 17) and theoretical (Reference 18) investigations have shown that the liquid sheets formed by two like impinging jets are disk-like in shape with the thickness varying circumferentially. The sheet thickness is uniform when the total impingement angle is 180° . However, as the impingement angle decreases the mass of the liquid becomes more and more concentrated along the forward symmetrical axis and the thinner portions of the sheet break up earlier so that the sheet appears like a forward diverging fan instead of a disk-like sheet. One can use an iterative solution to arrive at the fan angle as a function of impingement angle, as shown in Figure 28. The fan angle predicted by this simplified model is shown in Figure 29 to contain no less than 88% of the mass predicted by Hasson model (Reference 18).

The sheets formed by the two outer jets of a triplet injector are identical to that formed by the like-on-like impinging jets except the fan thickness is reduced by half. The sheet formed by the middle jet stream is controlled by the impingement angle and the momentum ratio of the unlike fluids. Figure 30 shows the fan angles for a 30° half-impingement-angle

TABLE III
SURVEY OF EXPONENT OF VELOCITY DEPENDENCY OF DROP SIZE

<u>DROP SIZE CORRELATED EXPERIMENTAL</u>	<u>AUTHOR</u>	<u>REF.</u>	<u>EXPONENT</u>	<u>INJECTION DEVICE</u>
d_{max}	Mugele	5	-0.66	Pressure nozzle & Impinging Jet
d_{32}	Mugele	5	-0.55	Pressure nozzle & Impinging Jet
d_{32}	Dombrowski & Hooper	6	-0.79	Impinging Jet
d_{32}	Jasuja	7	-0.86	Pressure nozzle
d_{50} ($=d_m$)	Longwell	8,9	-0.66	Pressure nozzle
d_{32}	Fraser	10	-0.706	Pressure nozzle
<u>Theoretical</u>				
d	Hagerty & Shea	11	-1	Plane sheet
d	Fraser, et. al.	12	-2/3	Spray fan
d	Dombrowski & Hooper	13	-2/3	Spray fan, long wave length
d	Dombrowski & Hooper	13	-0.72	Spray fan, medium wave length
d	Dombrowski & Hooper	13	0	Spray fan, short wave length
d	Dombrowski & Johns	14	-2/3	Spray fan

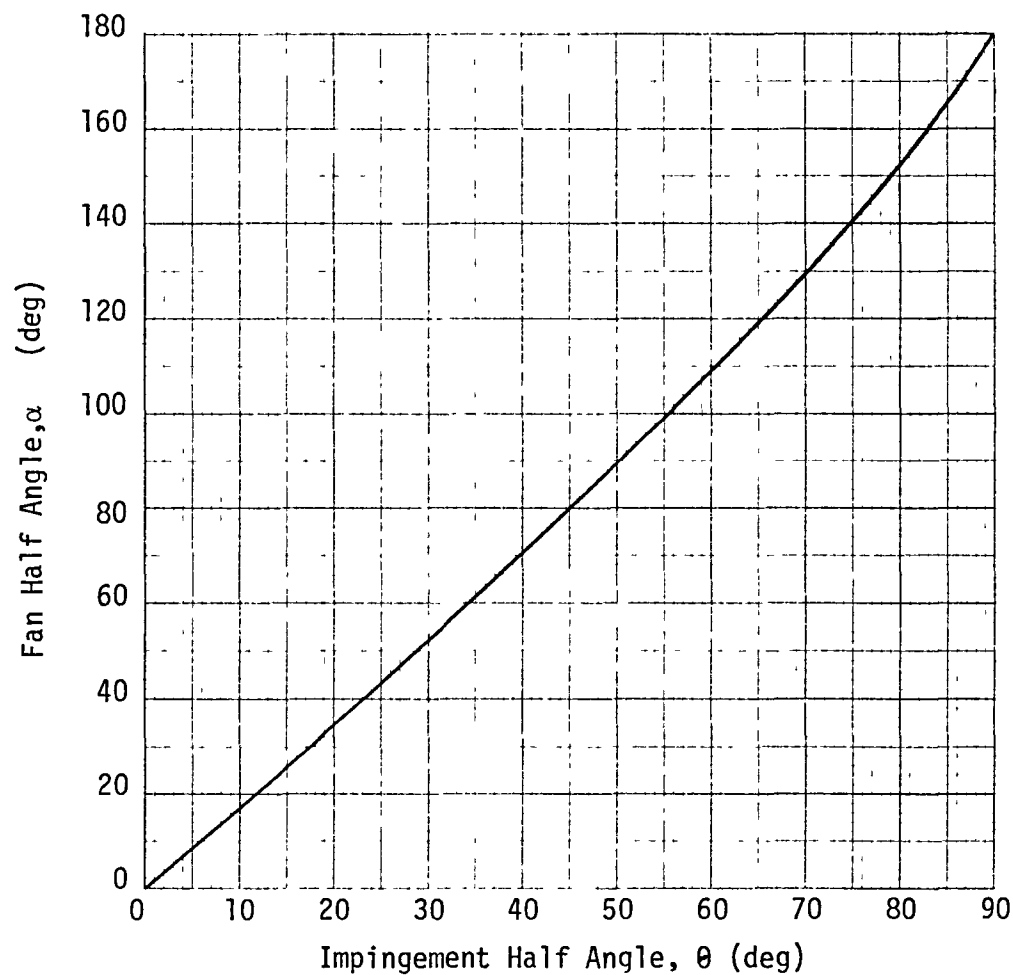


FIGURE 28. IMPINGING JET FAN ANGLE PREDICTED BY SIMPLIFIED SPRAY MODEL

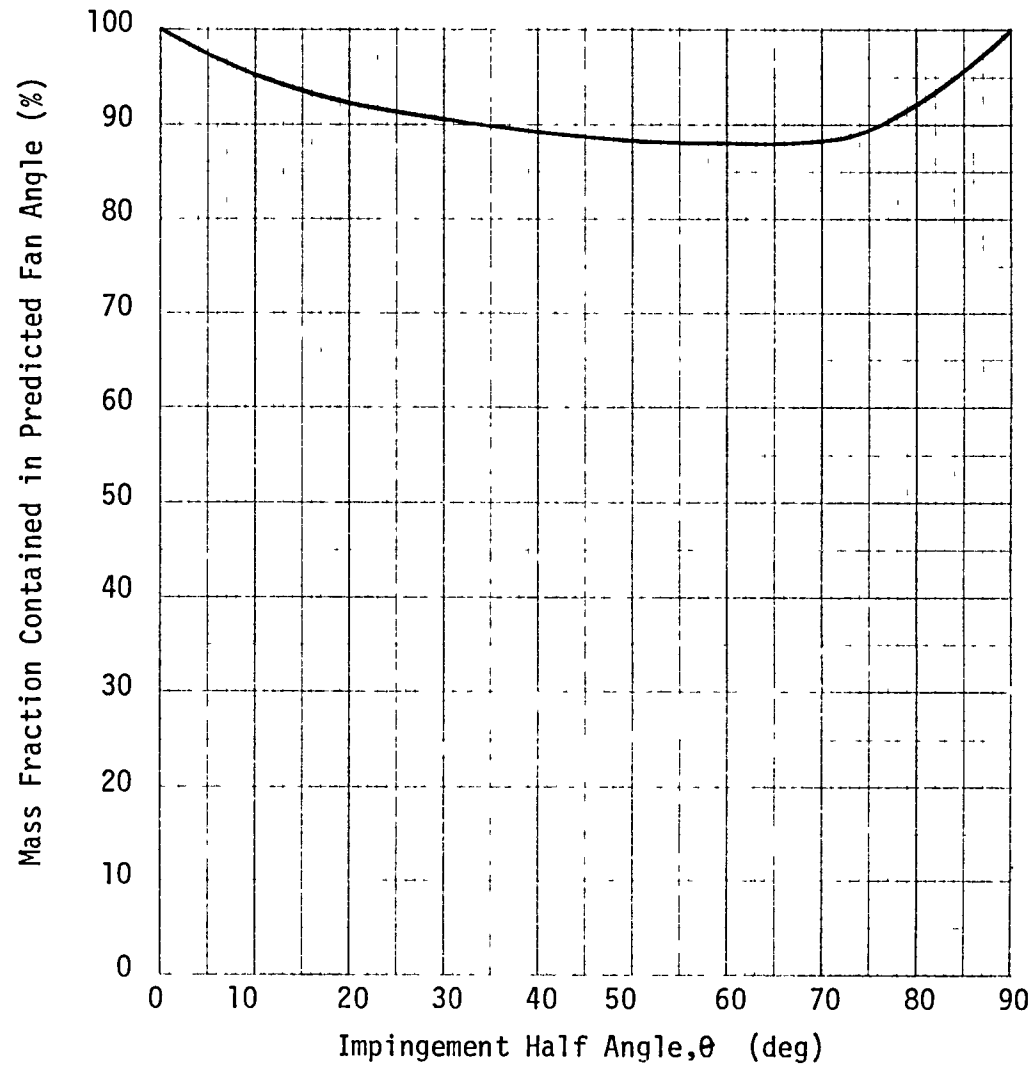


FIGURE 29. MASS FRACTION CONTAINED IN THE FAN ANGLE PREDICTED BY THE SIMPLIFIED SPRAY MODEL FOR IMPINGING JETS

triplet injector. If the maximum mixing efficiency occurs at equal fan angles, the uni-element cold-flow data of Reference 19 appear to validate the predicted middle jet fan angle.

Because of constant density and conservation of the mass, the fan angle controls the fan thickness, which in turn determines the drop size. Reference 14 implies that the exponent of the fan angle dependency of drop size is -1/3. As a result, the drop size increases or decreases as the fan angle decreases or increases.

C. Application of Generalized-Length Model

In applying the L_{gen} model to a general case, in which the propellant injection velocity and the injection element type or configuration are different from those of Reference 3, modifications to the original drop size correlation are necessary. The following calculation procedures were used by the present investigation for determining propellant vaporization efficiency.

1. Determine the uncorrected drop size from Figure 27 and the fan angle from Figure 28 or 30.
2. Calculate the corrected mass-median droplet radius using the following equation:

$$r_m = r_{m,uncor} \times 3.07 \times 10^3 \times \frac{\sigma\mu}{\rho}^{0.25} V^{-0.66} \alpha^{-1/3} \quad (3)$$

3. Use equation (1) to determine the value of generalized length.
4. Use Figure 26 to determine the percentage of propellant mass vaporized at a given chamber axial location.

D. Vaporization Model

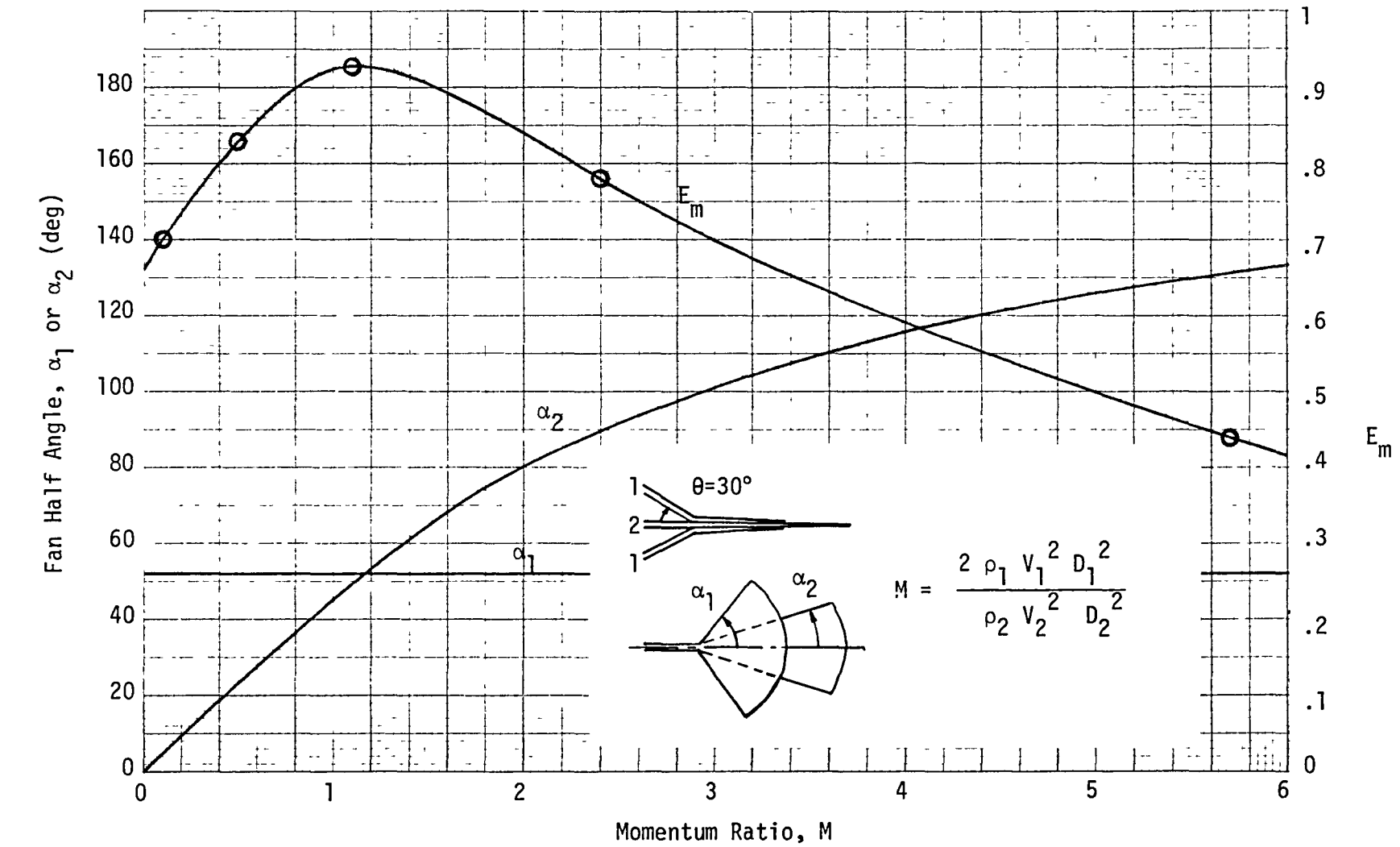


FIGURE 30. TRIPLET FAN ANGLE PREDICTED BY SIMPLIFIED SPRAY MODEL

The vaporization analysis performed by the present study is based on the L_{gen} model with the modifications described precedingly. The combustion chamber within the scope of the view window is divided axially into three equally spaced regions as shown in Figure 25. Each plane corresponds to a cold-flow collector-plane location, relative to the injector face. A three dimensional representation of the zoning is provided in Figure 31.

A vaporization computer model based on this spatial arrangement was formulated as described below.

1. Consider a chamber control volume encompassed by a right rectangular cylinder with $4.83\text{ cm} \times 4.83\text{ cm}$ ($1.9'' \times 1.9''$) cross-section and 3.81 cm ($1.5''$) in length from the injector face.

2. The cylinder is divided axially into three sections of equal length with 1.27 cm ($0.5''$) each. Therefore, the entire control volume contains three exit planes perpendicular to the axis.

3. Each plane is further divided into 100 (10×10) grids with equal dimensions at $0.48\text{ cm} \times 0.48\text{ cm}$ ($0.19'' \times 0.19''$).

4. The propellant present in a grid came solely from a specified grid in the preceding plane, thereby forming a section of a streamtube between the two grids. Oxidizer and fuel in a grid may come from different grids of the preceding plane.

5. The Priem-Heidmann Generalized-Length vaporization correlation is assumed to be applicable to individual streamtubes.

6. The off-nominal gas temperature effect on vaporization rate is accounted for by a factor of $(T - T_s)/(T_n - T_s)$, where T is the actual local gas temperature, T_n is the nominal gas temperature of 2778°K (5000°R), T_s is either the propellant saturation temperature or the critical temperature

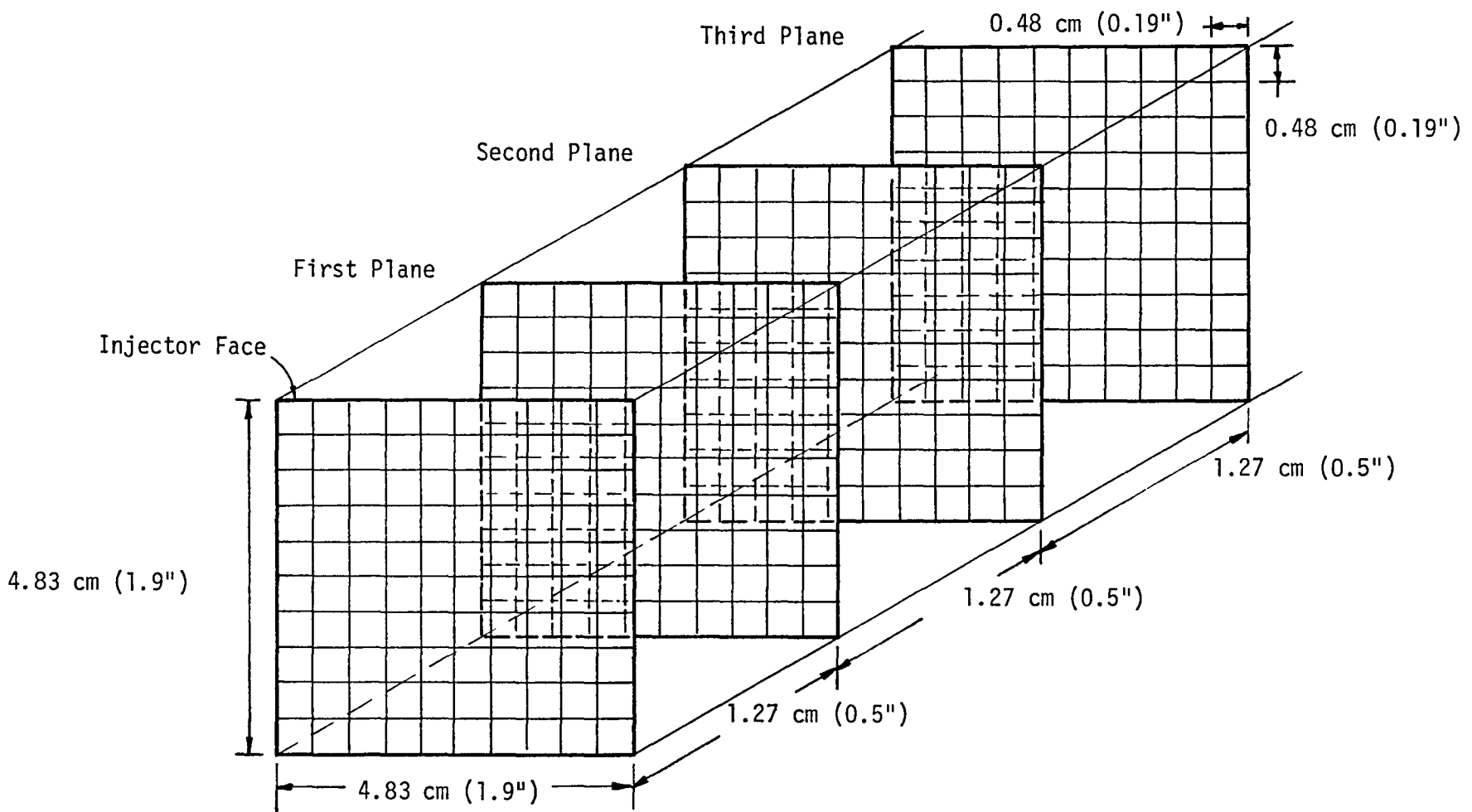


FIGURE 31. ZONING OF THE CROSS-SECTIONAL VIEW OF THE COMBUSTION FIELD

depending upon whether the chamber pressure is below or above the propellant critical pressure.

7. The vapors are assumed to travel together with the liquid droplets, from which they were evaporated.

8. The chemical reaction (propellant burning) does not take place between planes. The vapors produced in a streamtube section react instantaneously on arrival at their destined grid if the counterpart vapors are available at that location.

9. At a given propellant momentum ratio and axial location, the mass distribution of unburned propellant, including both vapor and liquid, is identical to that observed in cold flow tests.

10. The reaction of the oxidizer and fuel vapors produces equilibrium products from which the local temperature is determined. The equilibrium reaction computation is carried out by the ODE computer program of Reference 20.

11. No vaporization takes place in the preceding streamtube section, if the cold-flow mixture ratio in any grid is outside a specified range (extremely low or high).

12. The effect of the recirculating chamber gases is neglected.

The computation flowchart and program listing are provided in Appendix C. A sample run of the computer program including the input and output is also provided. The NAMELIST input includes chamber pressure (PC), operating mixture ratio (MRJ), chamber contraction ratio (CR), number of planes (NPLANE), propellant identification (IDO, IDF), propellant temperature (TO, TF), injection velocity (VO, VF), mass-median drop radius (RMO, RMF), and drop surface temperature (TSO, TSF). The propellant mass distribution is input through FORMAT input, which includes grid

number (J), mass fraction (CO, CF), and the corresponding grid number in the preceding plane (JO0, JF0). The output includes generalized length (LGO, LGF), gas temperature (TG), vaporization efficiency (EVO, EVF), vapor mixture ratio (MRV), and liquid mixture ratio (MRL).

E. Input and Results

The data input to the computer program for the 40 tests analyzed are summarized in Appendix D. The mixture ratios for the tests selected for a given injector are nearly constant and their equivalent momentum ratios are approximately equal to that of the cold-flow tests. For each injector, this results in only one mixing pattern identical to that characterized by the cold-flow tests. In preparing the mass distribution data tables, any grid containing less than 1% of the total propellant mass was neglected. This greatly reduces the size of mass distribution table and simplifies the computation without appreciable sacrifice of accuracy. The trajectories of propellants were empirically determined on the basis of measured mass distributions.

The propellant mass-median drop sizes were calculated using the method described in Section V.C. with the exception of the PAT fan angles. The fuel fan angle of the PAT injector is equal to 60° , the cup angle of the Splash Plate element. The oxidizer fan angle was determined to be 42° based on the cold-flow data. This oxidizer fan angle contains 80% of the total oxidizer flow.

Appendix E tabulates the fuel mass fraction vaporized and liquid mixture ratio at all three planes predicted by the computer program. It also provides two sets of mass average values. One is depth average, in which the mass average is taken from $I = 0$ to 9 at each J for the OFO Triplet injector, and from $J = 1$ to 10 at each I for the other three injectors. The

other is plane average, in which average is taken over the entire chamber cross section on each plane. The liquid mixture ratio represents the ratio of the liquid oxidizer to liquid fuel remaining for further vaporization and chemical reaction.

VI DATA CORRELATION

A. Fuel Vaporization Rate Effect

The photographically observed degrees of carbon formation shown in Figures 3 through 6 are compared to the average fuel vaporization efficiency at the 3.81 cm (1.5") plane in Figures 32 through 35. The degree of carbon formation is noted for each test by its location within one of four shaded bands for the four carbon formation classifications: clear, slightly clouded, moderately clouded, and obscure. The darker shading representing greater carbon formation and the lighter shading less carbon formation. The calculated vaporization rate is noted by a vertical line at the % vaporized shown on the horizontal scale. The correlations indicate that in general the carbon formation is intensified as the fuel vaporization is slowed down.

Figure 32 shows that, for the OFO Triplet injector, test 116 has the fastest RP-1 vaporization resulting in the clearest combustion flame. The TLOL injector was observed to yield much more carbon formation than the OFO Triplet injector when both injectors used RP-1 as fuel. Comparison between Figure 32 and Figure 33 indicates that this is due to the much slower RP-1 vaporization rate by the TLOL injector. Figure 33 also shows that the slower RP-1 vaporization due to its lower volatility is responsible for more carbon formation by RP-1 than by propane. Figures 34 and 35 further show the reduction in carbon formation by increasing the fuel vaporization rate for the EDM-LOL and PAT injectors.

B. Chamber Pressure Effect

In Figures 3 through 6, the chamber pressure appears to have an overwhelming effect on carbon formation. Therefore, a correlation was made to determine whether or not the pressure has direct control of the carbon

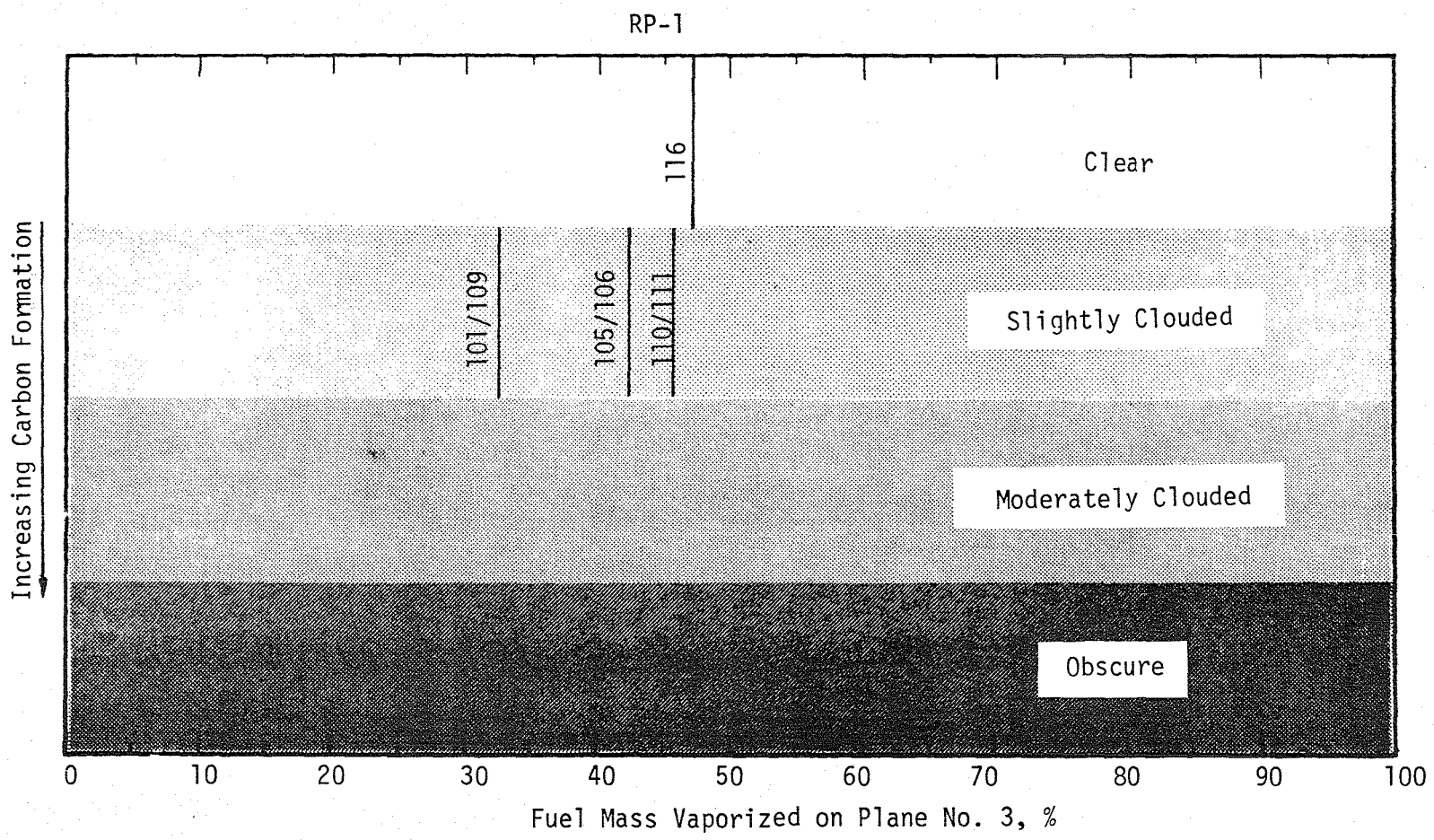


FIGURE 32. OFO TRIPLET CARBON FORMATION CORRELATION WITH FUEL VAPORIZATION RATE

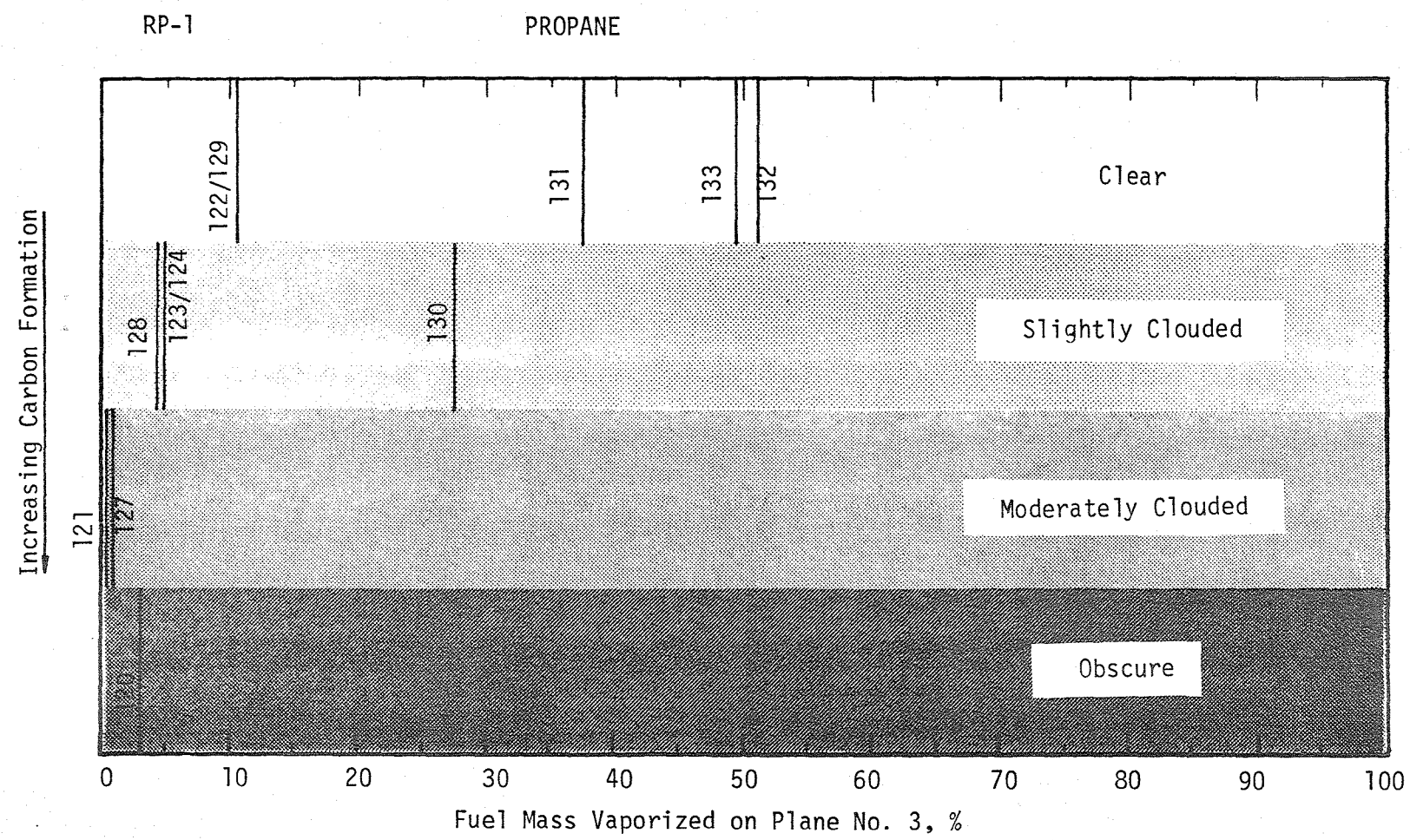


FIGURE 33. TLOL CARBON FORMATION CORRELATION WITH FUEL VAPORIZATION RATE

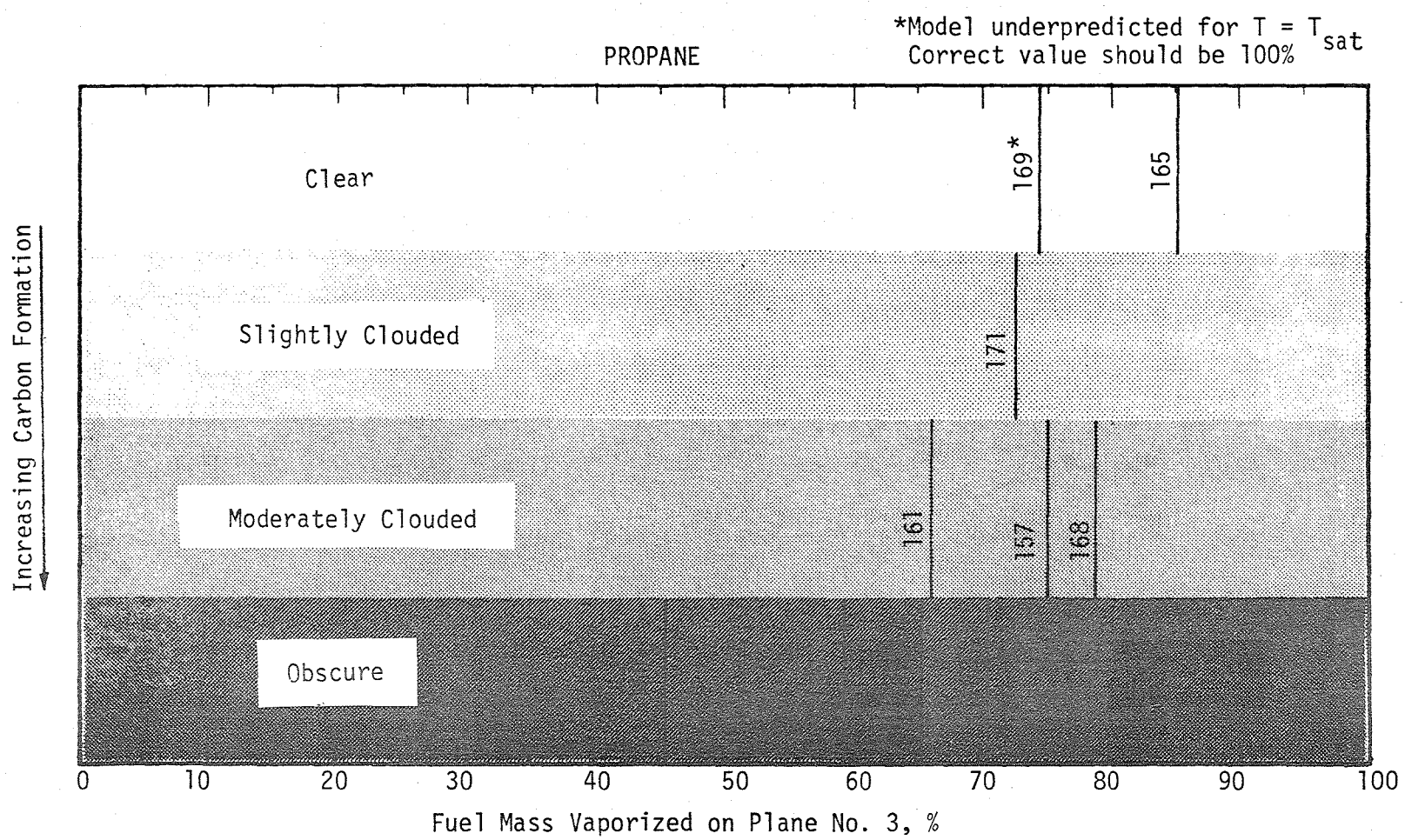


FIGURE 34. EDM-LOL CARBON FORMATION CORRELATION WITH FUEL VAPORIZATION RATE

LG
Increasing Carbon Formation

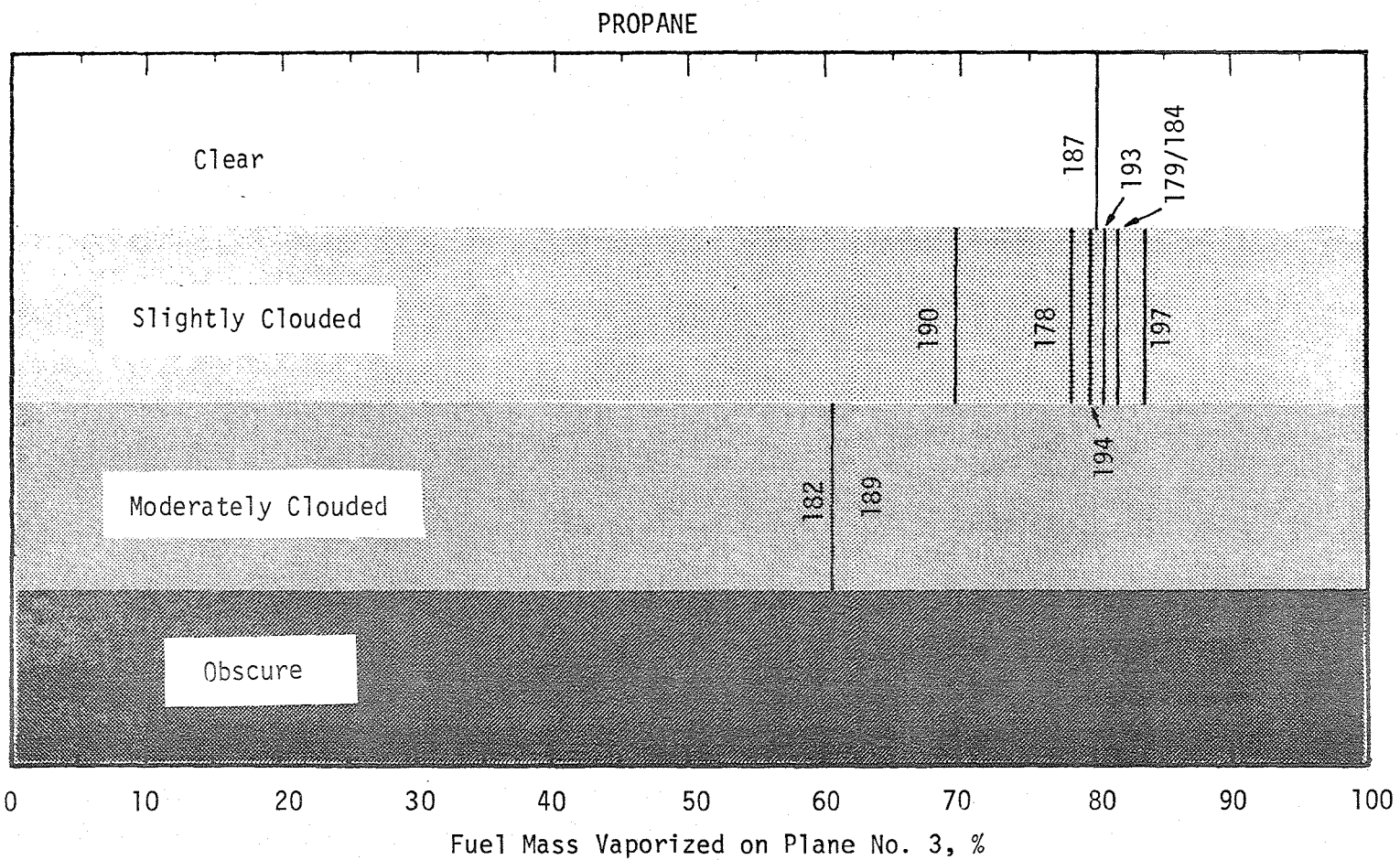


FIGURE 35. PAT CARBON FORMATION CORRELATION WITH FUEL VAPORIZATION RATE

formation in addition to its indirect effect through its influence on the vaporization rate. Figures 36 through 39 correlate the carbon formation with the chamber pressure as well as the fuel vaporization rate. The chamber pressure itself seemingly has a second order effect. High chamber pressure improves the clearness of the combustion flame at the same fuel vaporization for some cases. It explains why test 120 of the TLOL injector (Figure 37) was obscure and test 187 of the PAT injector (Figure 39) was clear. It also improves the EDM-LOL correlation (Figure 38), however, test 169 of the EDM-LOL injector does not agree well with the correlation trend because the propane was injected at the saturation temperature of the tested chamber pressure. Under that condition the propane undergoes flash vaporization upon entering the combustion chamber as shown by Figure 2. The Priem-Heidmann L_{gen} model is not valid for this case and underpredicts the vaporization rate for this case. Test 169 indeed is the most decisive evidence showing that fuel-vaporization rate controls carbon formation.

C. Mixing Effect

For the propane tests, the TLOL, EDM-LOL and PAT injectors exhibited different degrees of carbon formation even when they were operated at the same predicted fuel vaporization rate. This suggests that propellant mixing has a direct effect on carbon formation besides its influence on the vaporization rate.

In this study, the combustion zone of each injector was photographically viewed only from one fixed direction. Thus, the mixing characteristics discussed herein are limited to those exhibited in the plane perpendicular to that particular view. Figures 40 through 43 show the calculated depth-averaged liquid phase mixture ratios at the 3.81 cm (1.5")

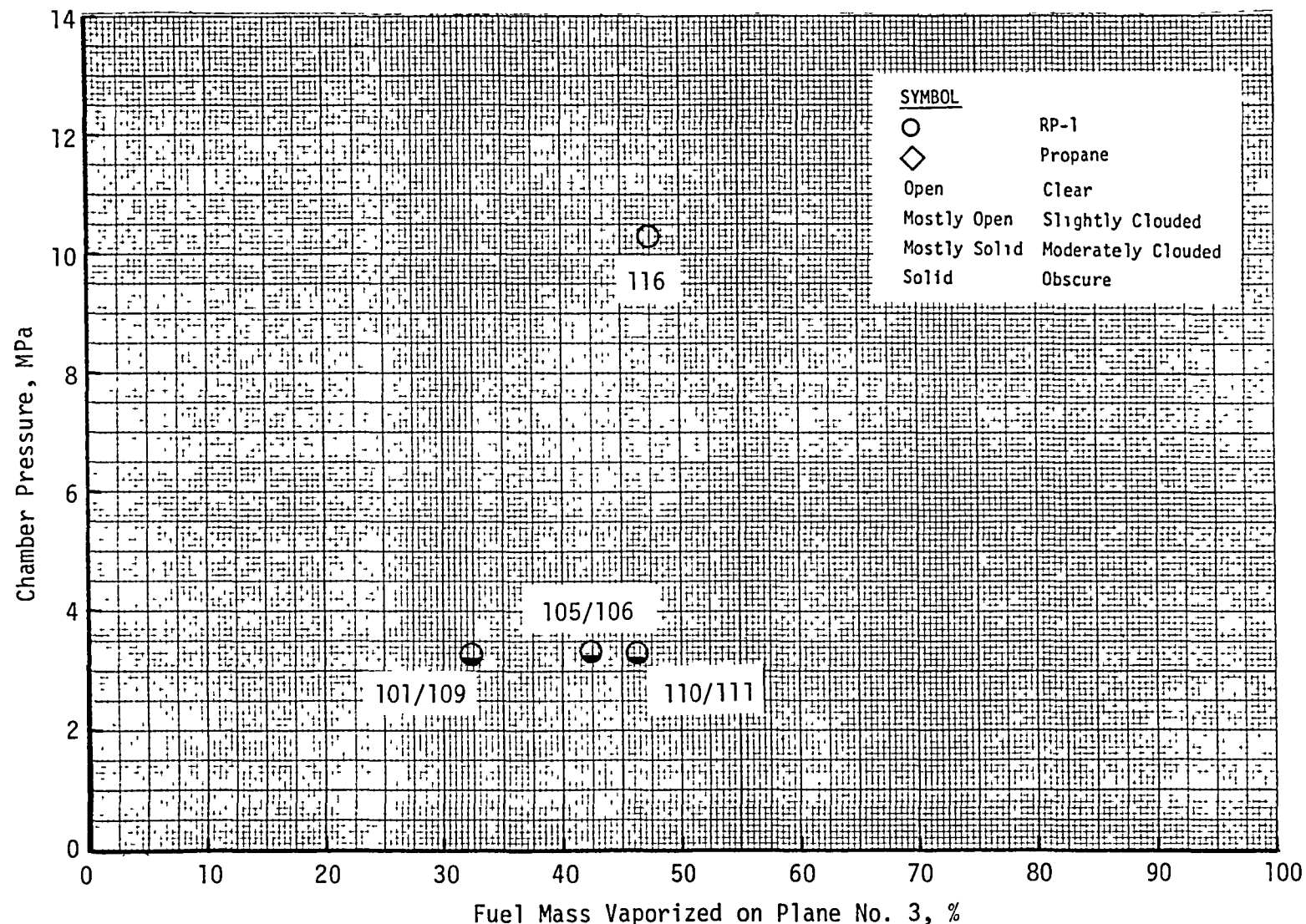


FIGURE 36. OFO TRIPLET CARBON FORMATION CORRELATION WITH CHAMBER PRESSURE AND FUEL VAPORIZATION RATE

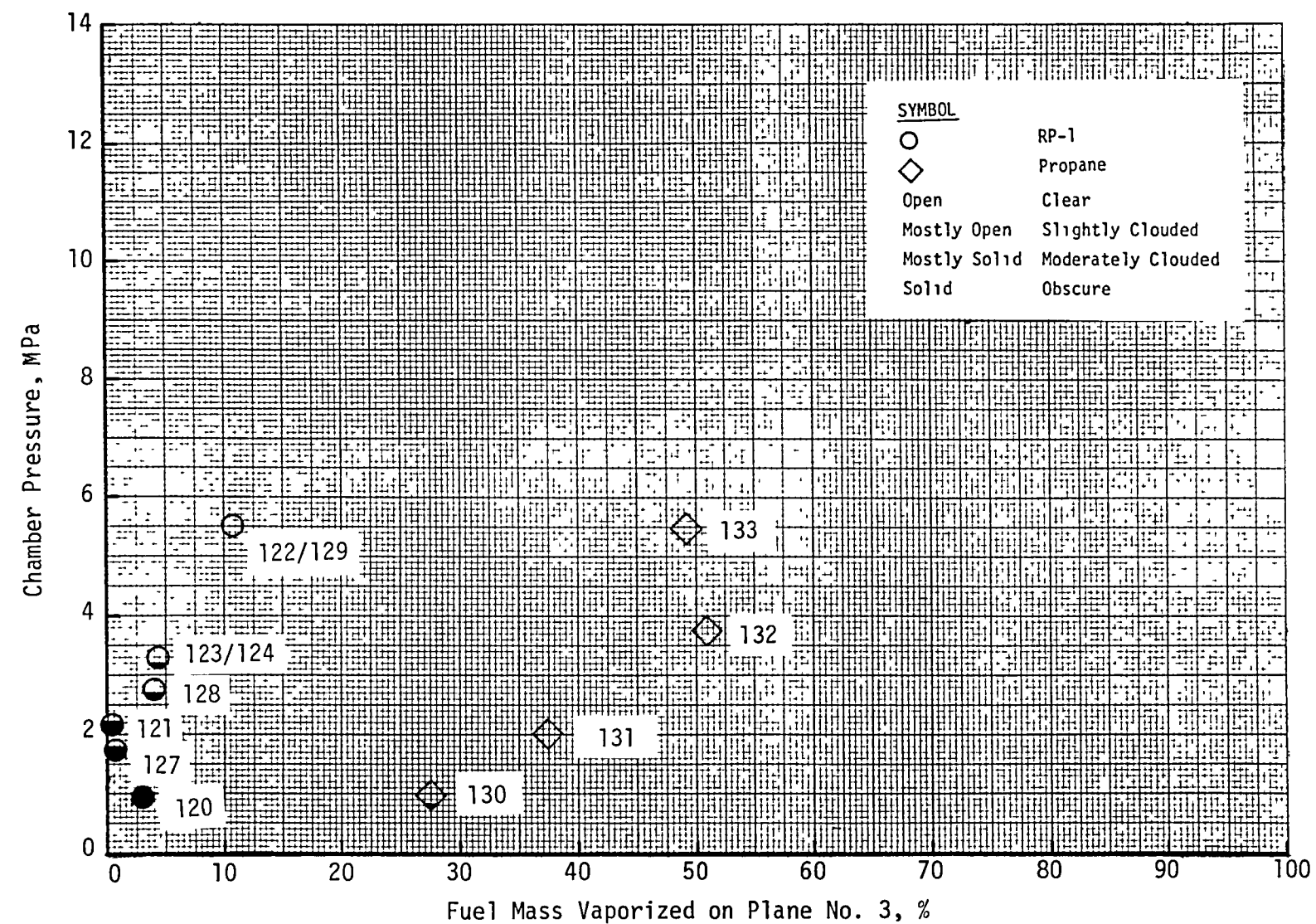


FIGURE 37. TLOL CARBON FORMATION CORRELATION WITH CHAMBER PRESSURE AND FUEL VAPORIZATION RATE

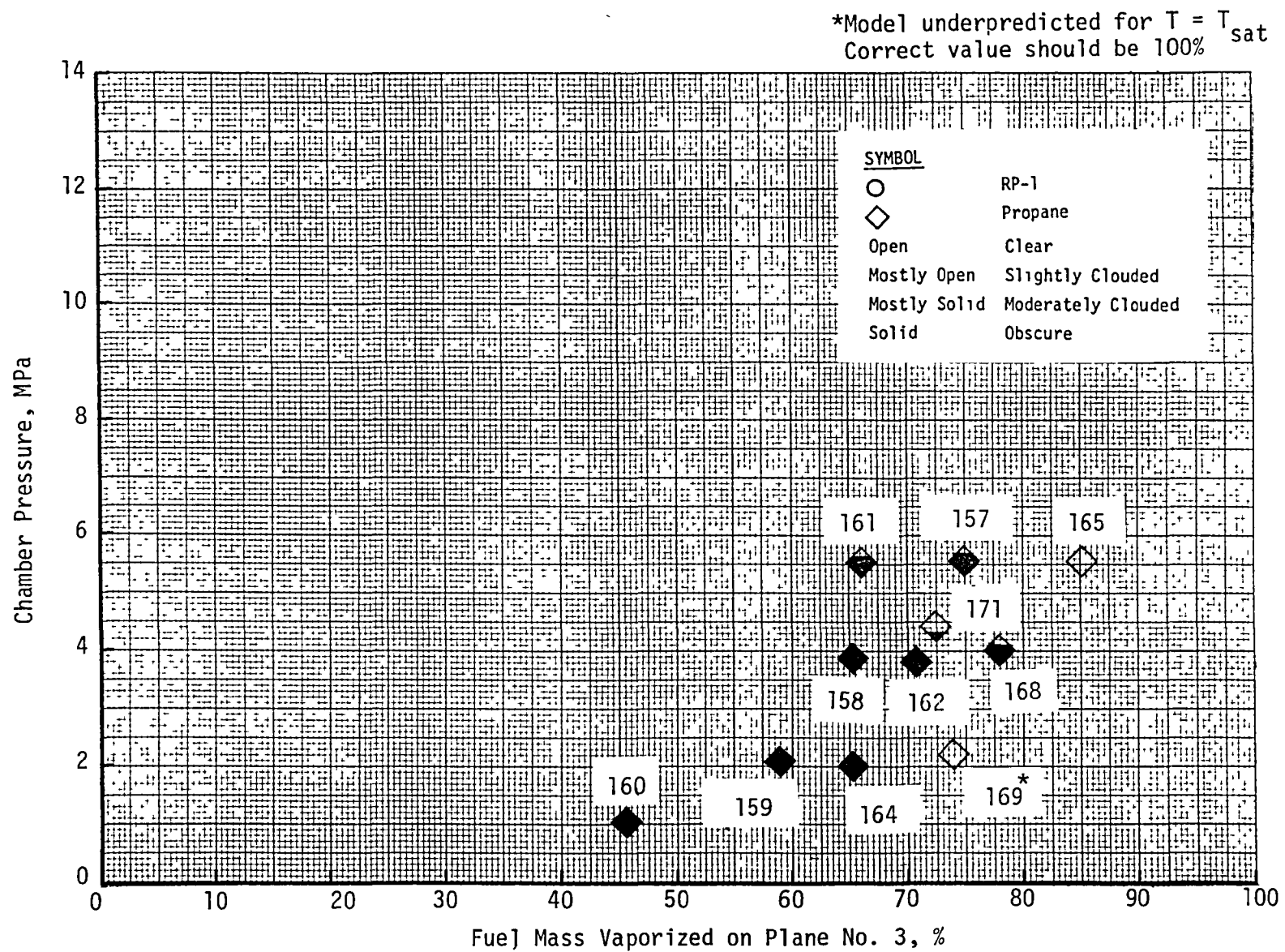


FIGURE 38. EDM-LOL CARBON FORMATION CORRELATION WITH CHAMBER PRESSURE AND FUEL VAPORIZATION RATE

62

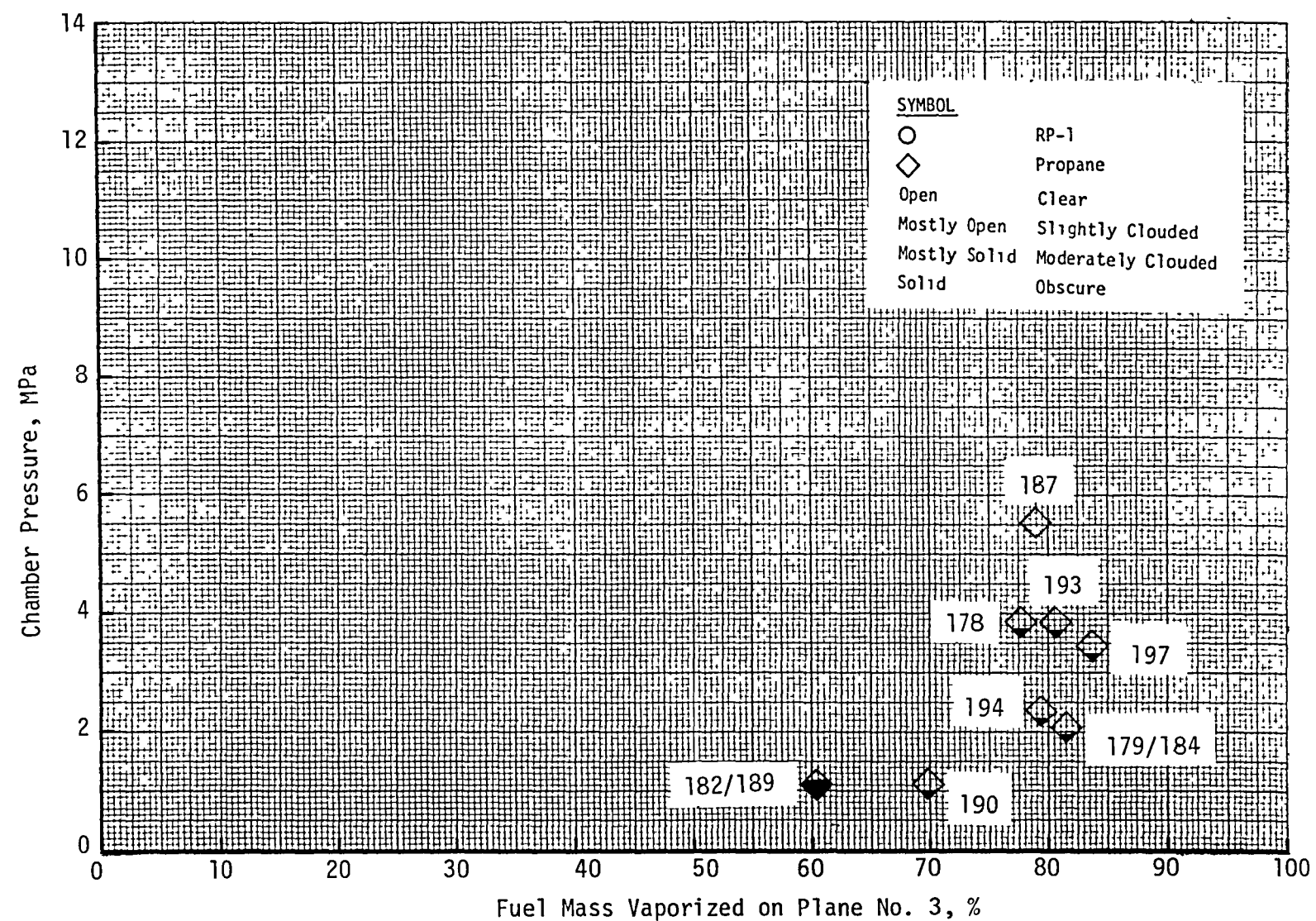


FIGURE 39. PAT CARBON FORMATION CORRELATION WITH CHAMBER PRESSURE AND FUEL VAPORIZATION RATE

plane. The distribution of this liquid mixture ratio across the chamber height is seen to vary significantly from one injector to another.

Figure 40 indicates the existence of a liquid phase fuel rich zone around the chamber center line, which is surrounded by two liquid phase oxidizer rich zones. A typical clear OFO flame is illustrated by Figure 44, which shows a small amount of dark clouds being emanated from and only existing around the center of the flame. Comparison of Figures 40 and 44 induces the direct association of the dark clouds to the unvaporized fuel. As they are migrating transversely through the oxidizer rich zone, the clouds are burned off in the oxidizer rich environment. Hence, it can be expected that the OFO Triplet element generates only a little amount of carbon that is confined at the center of the flame.

Figure 41 shows the predicted poor hot-fire liquid phase mixing for the TLOL injector. Oxidizer-rich zone exists on the oxidizer fan side, while the fuel-rich zone exists on the fuel fan side. A slightly oxidizer-rich zone appear on the back side of the fuel-rich zone but its effect on the overall flame characteristics is negligible because of its small mass fraction as shown in Figure 22. Figure 45 shows that the dark clouds of TLOL flame exists only on the fuel fan side, a liquid phase fuel rich zone.

Unlike the OFO Triplet and TLOL injectors, Figure 42 shows a much more uniform liquid phase mixture ratio distribution across the chamber for the EDM-LOL injector. Figure 46 shows that the dark clouds are emanated from everywhere throughout the entire mixed spray when they occur. This is another evidence of close relation between the carbon formation and the propellant mixing. For the EDM-LOL injector, once a carbon-laden cloud is formed, it will last indefinitely because of the lack of oxidizer-rich zone to burn it off due to the uniform mixing.

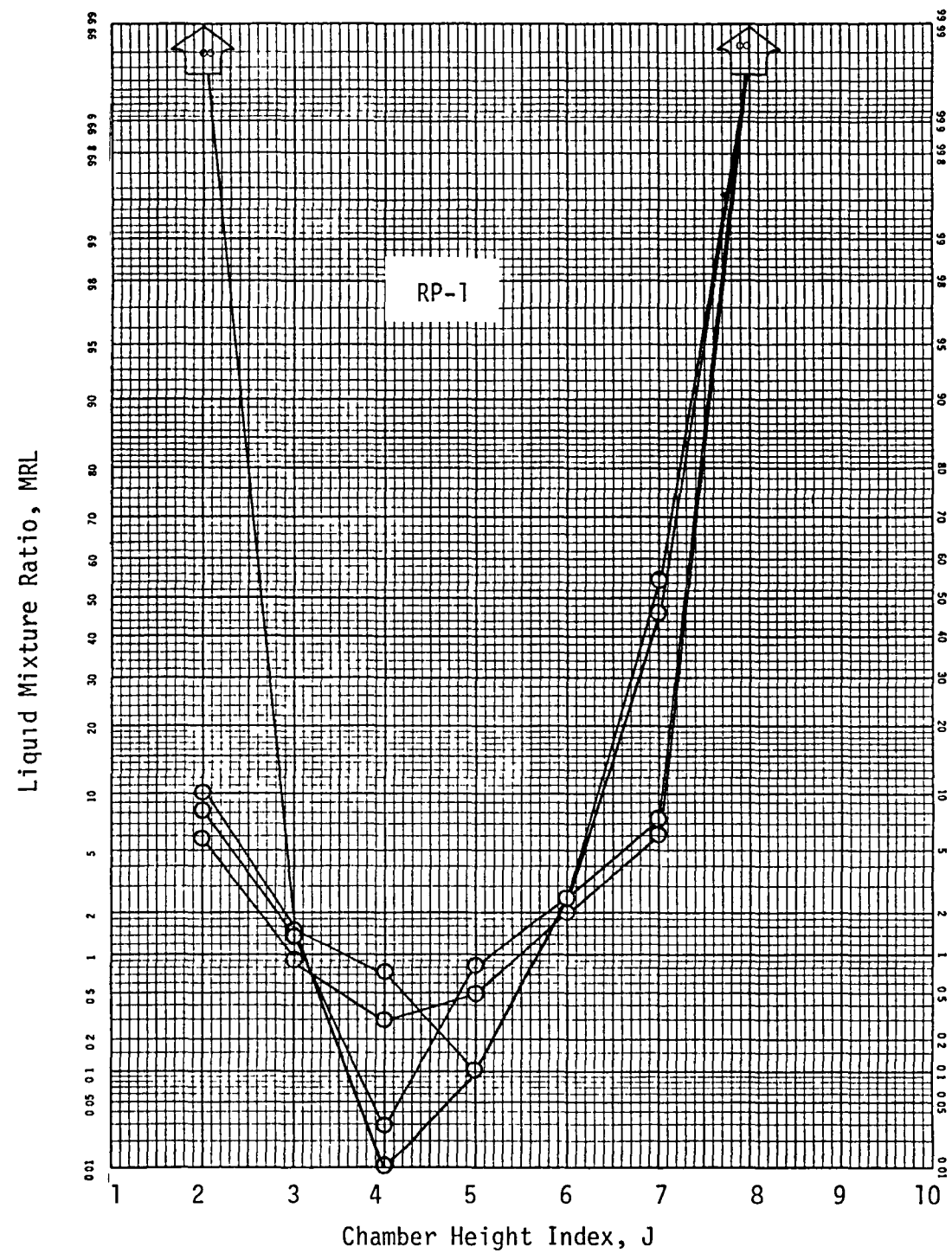


FIGURE 40. OFO TRIPLET LIQUID MIXTURE RATIO DISTRIBUTION ON PLANE NO. 3

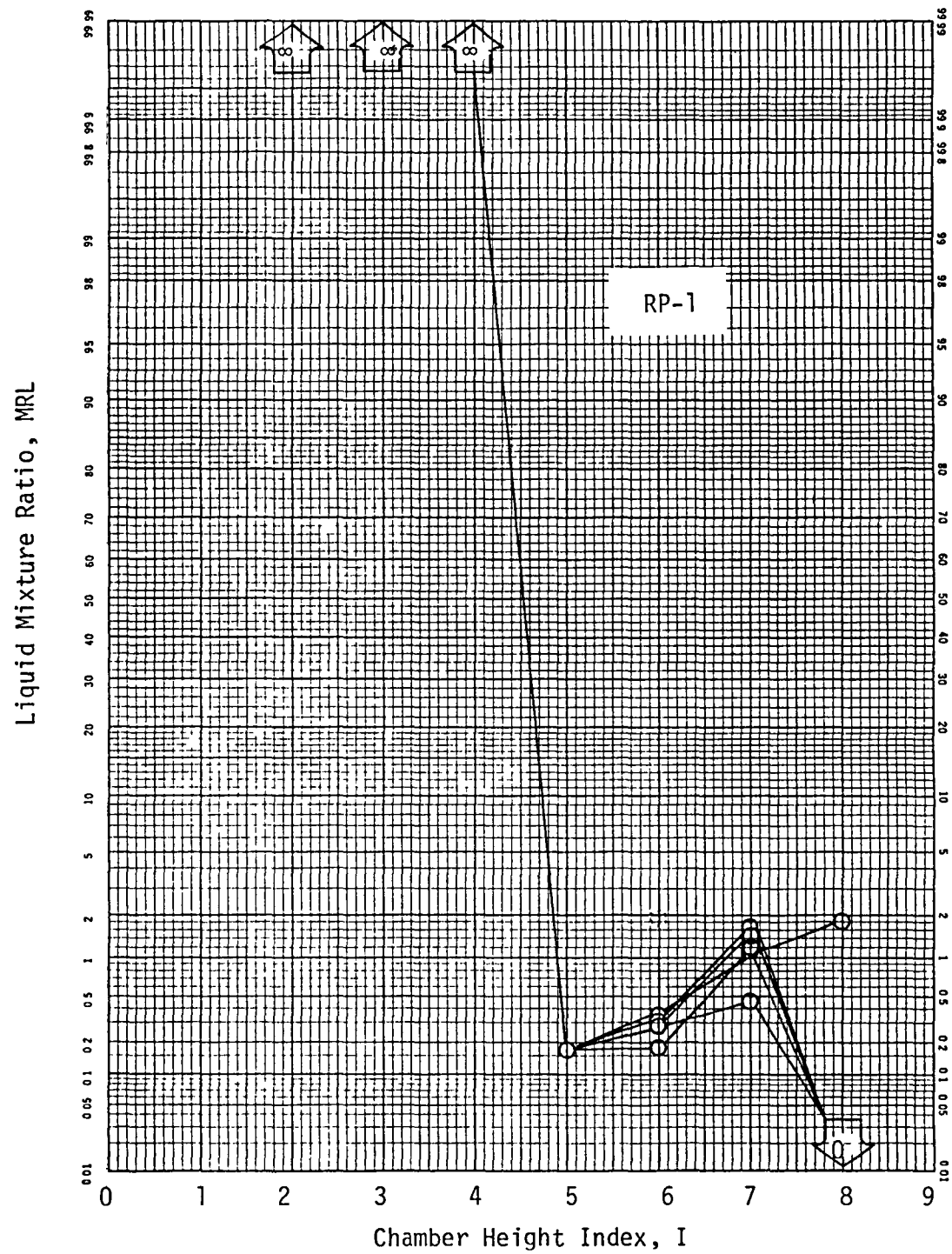


FIGURE 41. TLOL LIQUID MIXTURE RATIO DISTRIBUTION ON PLANE NO. 3 (1/2)

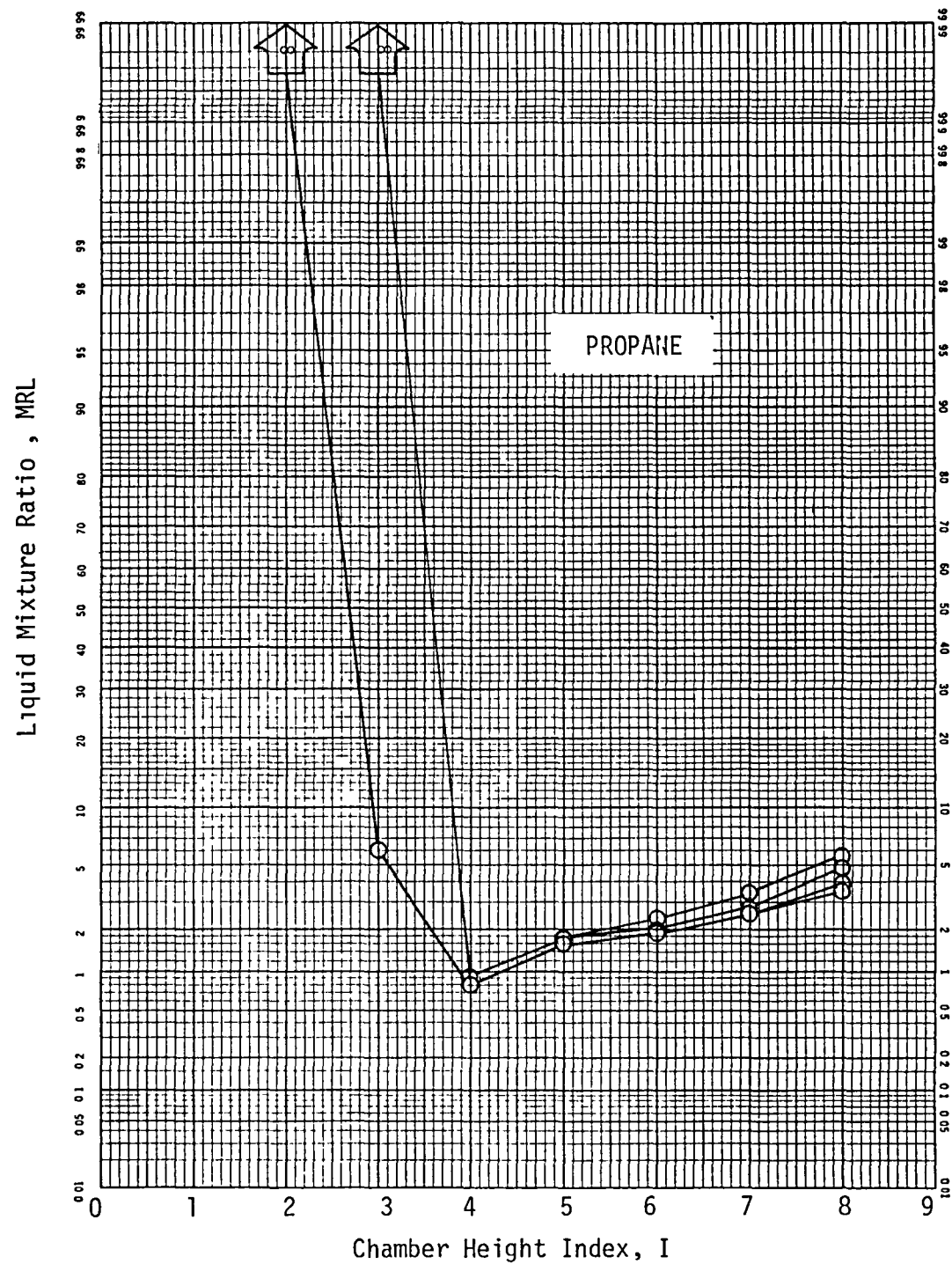


FIGURE 41. TLOL LIQUID MIXTURE RATIO DISTRIBUTION ON PLANE NO. 3 (2/2)

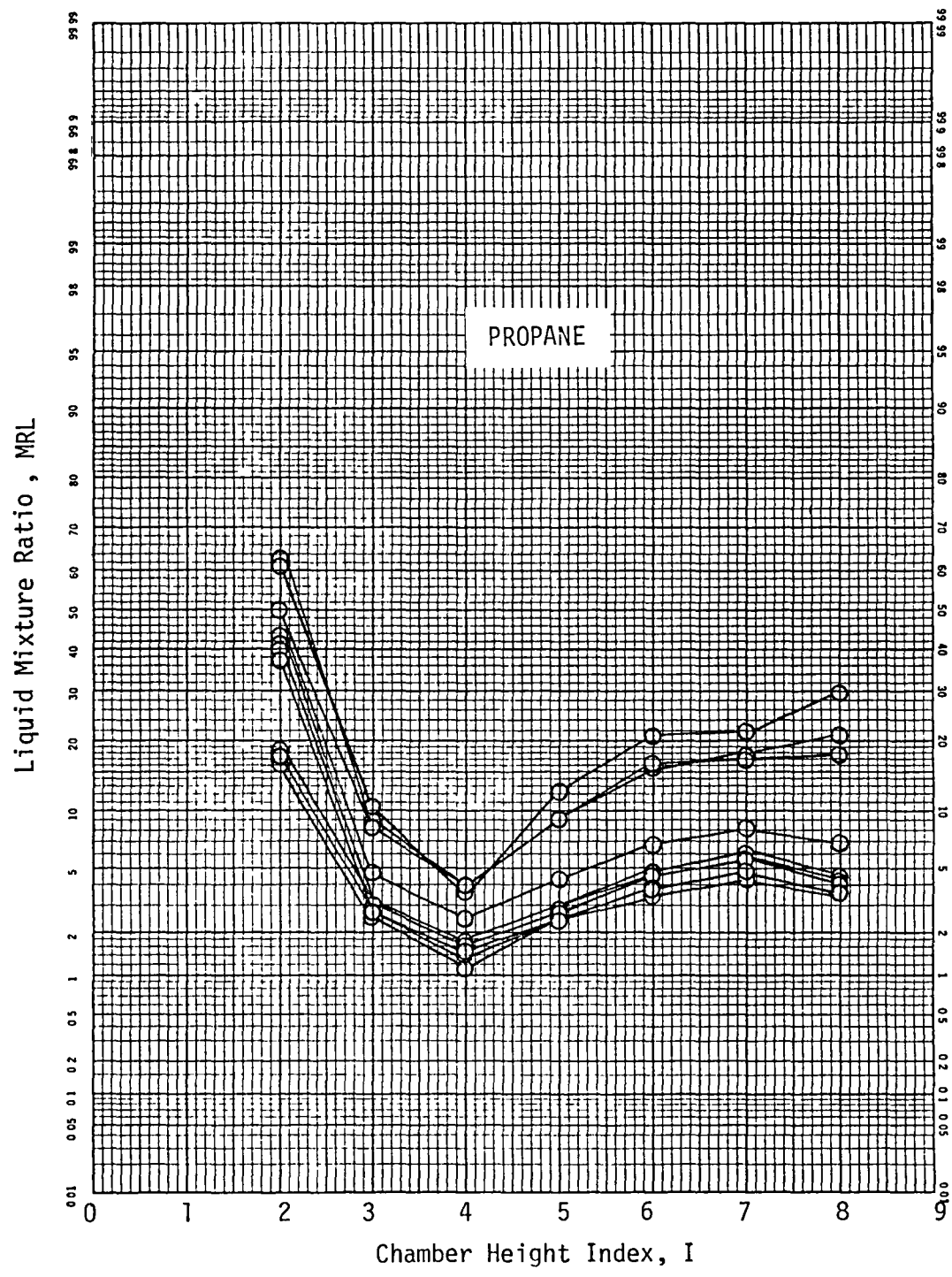


FIGURE 42. EDM-LOL LIQUID MIXTURE RATIO DISTRIBUTION ON PLANE NO. 3

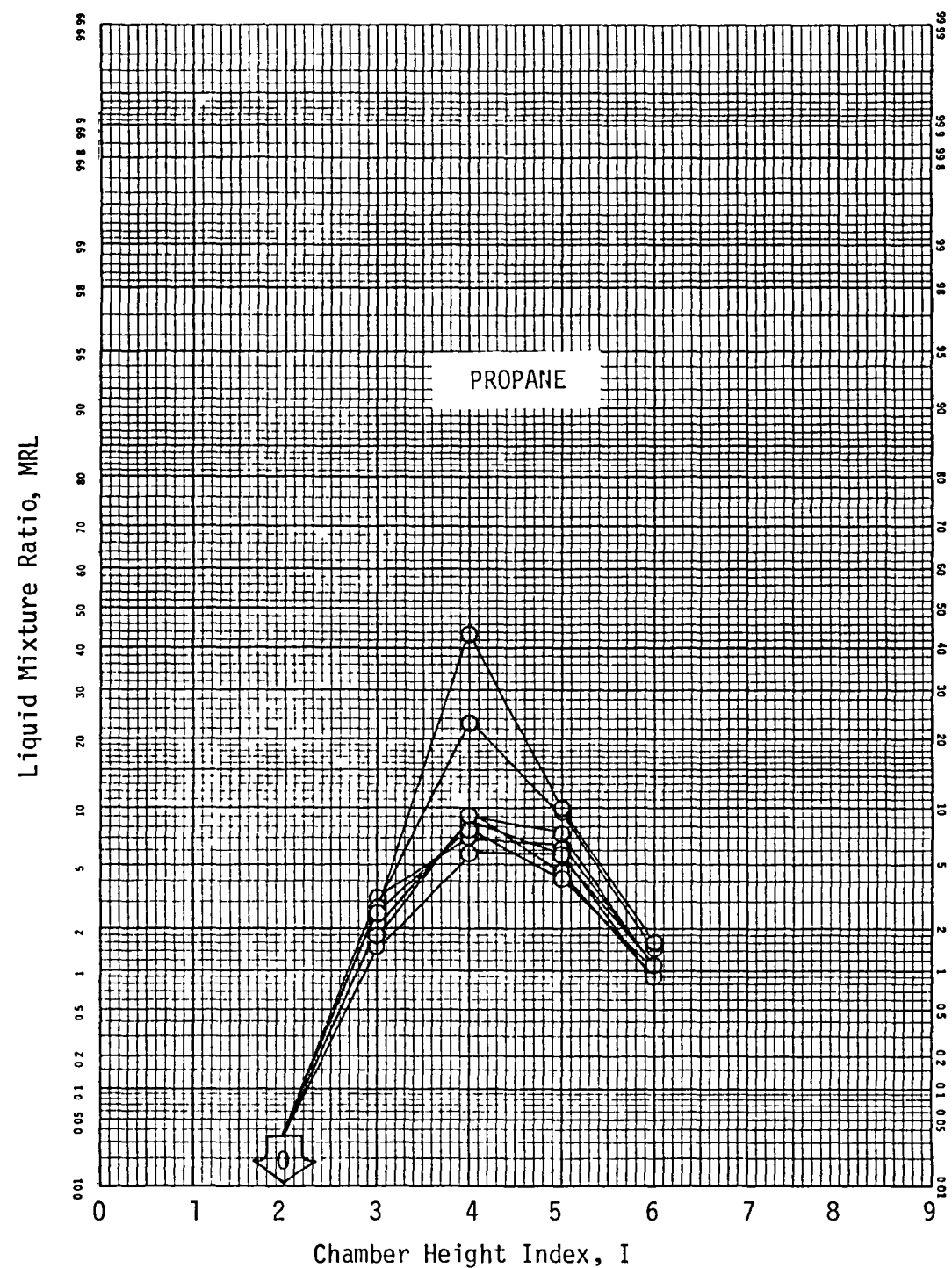


FIGURE 43. PAT LIQUID MIXTURE RATIO DISTRIBUTION ON PLANE NO. 3

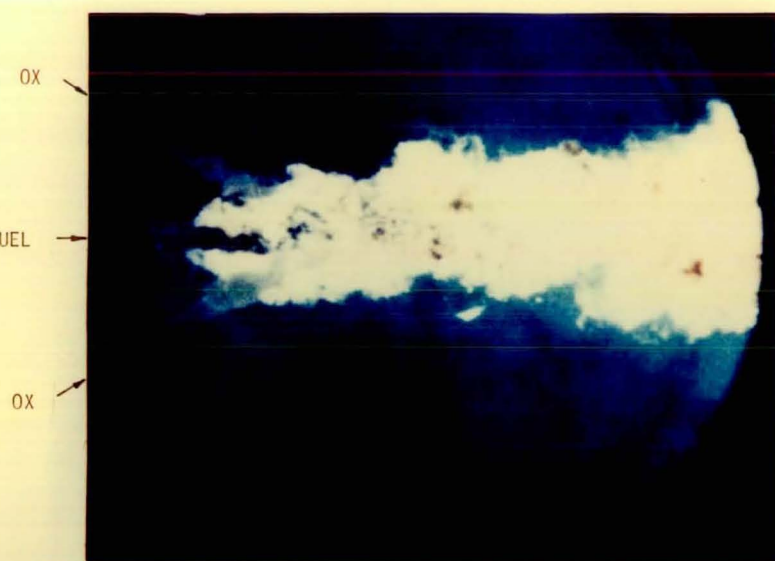


FIGURE 44. HIGH-SPEED PHOTOGRAPH OF OFO TRIPLET CARBON FORMATION PHENOMENA, TEST 116

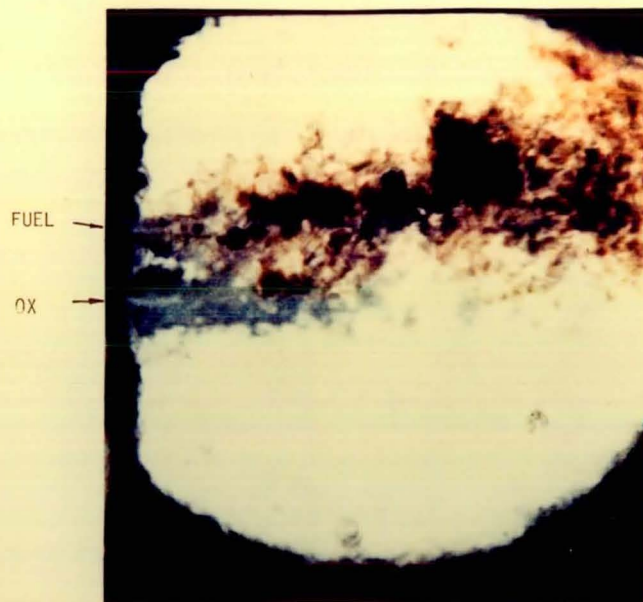


FIGURE 45. HIGH-SPEED PHOTOGRAPH OF TLOL CARBON FORMATION PHENOMENA, TEST 129



FIGURE 46. HIGH-SPEED PHOTOGRAPH OF EDM-LOL CARBON FORMATION PHENOMENA, TEST 161



FIGURE 47. HIGH-SPEED PHOTOGRAPH OF PAT CARBON FORMATION PHENOMENA, TEST 178

Comparison of Figures 33 and 34 shows that, although it has faster propane vaporization, the EDM-LOL injector produces much more carbon than the TLOL injector. The TLOL injector is a poor mixer for having a long oxidizer-fuel impingement height, therefore, the majority of the unvaporized fuel is hardly exposed to the oxidizer. The EDM-LOL injector, meanwhile, is a good mixer resulting from a much shorter oxidizer-fuel impingement height, therefore, the oxidizer is readily available to the vaporizing fuel. This difference in mixing characteristics appears to be the cause for the difference in carbon formation between these two injectors and it also leads to a conclusion that carbon formation is provoked by the exposure of liquid fuel to the oxidizer in a fuel rich environment. This also explains why the dark clouds do not occur until the fuel meets the oxidizer as shown in Figures 45 and 46.

Figure 43 shows that the unburned propellants are oxidizer-rich at the center of the flame and fuel-rich on both sides for the PAT injector. The poor mixing is due to the long unlike impingement height resulting from small impingement angle. The Splash Plate fuel element produces very fine droplets which evaporate fast. Consequently, by the time the oxidizer and fuel are mixed, there is only a small amount of unvaporized fuel left. Based on the liquid phase carbon formation mechanism, only a little carbon formation can be expected. Figures 35 and 39 uphold this conclusion. Figure 47 shows a typical PAT flame.

VII CONCLUSIONS AND RECOMMENDATIONS

A. Conclusions

Correlation of cold flow mixing data and calculated local fuel vaporization rates with photographic carbon formation data has led to the following conclusion in regard to the injector-related issues of carbon formation.

1. For all four injectors and two fuels, the carbon formation was reduced or increased when the fuel vaporization rate was increased or decreased.
2. For the TLOL injector, RP-1 formed much more carbon than propane due to the slower RP-1 vaporization rate.
3. The carbon formation originates from the areas predicted to be fuel-rich in liquid phase.
4. At a given fuel vaporization rate, early and uniform unlike mixing is conducive to carbon formation as evidenced by the EDM-LOL data.
5. The above correlation results lead to a conclusion that the carbon is formed by the liquid fuel as it is vaporizing in an oxidizer-lean environment.
6. Based on the liquid fuel carbon formation mechanism, the following injector design criteria are provided for controlling the carbon formation to meet engine design and operation requirements:
 - o Carbon formation can be increased or decreased by decreasing or increasing the fuel vaporization rate, whose primary controlling design parameters are injection orifice size, impingement angle, fuel temperature, and chamber pressure. High vaporization rate can result from small injection orifice, large impingement angle, high fuel temperature and high chamber pressure.

o For the slow vaporization injection elements, delaying the unlike mixing reduces carbon formation.

o Besides its effect on the vaporization rate, chamber pressure has an additional influence on carbon formation. High chamber pressure reduces carbon formation.

B. Recommendations

The following recommendations are made for future studies as a logical extension to the present work.

1. The cold-flow testing and vaporization analysis of the present study were conducted only at one mixture (or momentum) ratio for each injector. For a given injector design, the propellant mixing is strongly affected by the momentum ratio. Since the propellant mixing was found to be very influential on carbon formation, further cold-flow testing and vaporization analysis should be pursued to analytically evaluate the mixture ratio effect on carbon formation.

2. The present study was limited to uni-element injectors, which inherently possess large amount of hot gases recirculating in the combustion chamber. In order to have closer simulation of full scale engine combustion environment, further investigations using multi-element injectors are recommended.

3. The vaporization analysis of the present study included the effect of propellant mixing characteristics. This approach of integrating the mixing data into the propellant vaporization analysis was found to be practical in usage and realistic in modeling; yet, the computation was simple and straight forward. An engine combustion performance model can be readily developed using the present model as a frame work. Such a model is useful and convenient for engine design or data analysis.

REFERENCES

1. Lawver, B. R., "High-Performance N₂O₄/Amine Elements - Blowapart", Final Report, Contract NAS 9-14186, Report 14186-DRL-5, ALRC, March 1979
2. Judd, D. C., "Photographic Combustion Characterization of LOX/Hydrocarbon-Type Propellants", Final Report, Contract NAS 9-15724, Report MA-129T, August 1980
3. Priem, R. J. and M. F. Heidmann, "Propellant Vaporization as a Design Criterion for Rocket-Engine Combustion Chambers", NASA TR-R-67, 1960
4. Ingebo, R. D., and H. H. Foster, "Drop-Size Distribution for Cross-Current Breakup of Liquid Jets in Airstreams", NACA TN 4087, 1957
5. Mugele, R. A., "Maximum Stable Droplets in Dispersoids", A.I.Ch.E. J., Vol. 6, No. 1, 1960
6. Dombrowski, n. and P. C. Hooper, "A Study of the Sprays Formed by Impinging Jets on Laminar and Turbulent Flow", J. Fluid Mechanics, Vol. 18, Part 3, 1964
7. Jasuja, A. K., "Atomization of Crude and Residual Fuel Oils", J. Engr. for Power, Vol. 101, 1979
8. Longwell, J. OP., Ph.D. Dissertation, M.I.T. 1943
9. Marshall, Jr., W. R., "Atomization and Spray Drying", A.I.Ch.E. Pub., 1954
10. Fraser, R. p., "Liquid Fuel Atomization", 6th Combustion Symposium, 1956
11. Hagerty, W.W. and J. F. Shea, "A Study of the Stability of Plane Fluid Sheets", J. Applied Mechanics, Dec. 195512. Frazer, R.P., P. Eisenklam, N. Dombrowski, and D. Hasson, "Drop Formation from Rapidly Moving Liquids Sheets", A.I.Ch.E. J., Nov. 1962
13. Dombrowski, n. and P. C. Hooper, "The Effect of Ambient Density on Drop Formation in Sprays", Ch. Engr. Sci., Vol. 17, 1962
14. Dombrowski, N. and W. R. Johns, "The Aerodynamic Instability and Disintegration of Viscous Liquid Sheets", Ch. Engr. Sci., Vol. 18, 1963

15. Foster, H. and M. F. Heidmann, "Spatial Characteristics of Water Spray Formed by Two Impinging Jets at Several Jet Velocities in Quiescent Air", NASA TN D-301, 1960
16. Miller, K. D., J. Applied Physics, 31, 1960
17. Taylor, G. I., Proc. Roy. Soc. (London), A259, 1960
18. Hasson, D. and R. E. Peck, "Thickness Distribution in a Sheet Formed by Impinging Jets", AIChE J. Vol 10, No. 5, 1964 (J. I. Ito, Contributor)
19. McHale, R. M. and W. H. Nurick, "Noncircular Orifice Holes and Advanced Fabrication Techniques for Liquid Rocket Injectors", Contract Report, Rocketdyne, NAS 9-9528, 1974
20. Gordon, S. and B. J. McBride, "Computer Program for Calculation of Complex Chemical Equilibrium Compositions, Rocket Performance, Incident and Reflected Shocks, and Chapman-Jouguet Detonations", NASA SP-273, 1971

Name	No. of Copies	Name	No. of Copies
National Aeronautics & Space Administration Lewis Research Center 21000 Brookpark Road Cleveland, Ohio 44135		Defense Documentation Center Cameron Station, Bldg 5 5010 Duke St Alexandria, VA 22314	
Attn Contracting Officer, MS 500-306 Technical Utilization Office MS 7-3 Technical Report Control Office, MS 5-5 AFSC Liaison Office, MS 501-3 Library, MS 60-3 Office of Reliability & Quality Assurance, MS 500-211 N T Musial, MS 500-318 J P Wanhainen, Proj. Mgr., MS 501-6 E. A Bourke, MS 501-5	1 1 1 2 2 1 1 12 5	Attn TISIA Advanced Research Projects Agency Washington, D.C. 20525 Attn Library Aeronautical Systems Division Air Force Systems Command Wright-Patterson Air Force Base Dayton, Ohio 45433 Attn Library E E Bailey Air Force Rocket Propulsion Laboratory (RPM) Edwards, CA 93523 Attn Library	1 1 1 1 1 1 1 1 1
National Aeronautics & Space Administration Headquarters Washington, D.C. 20546		Attn Library Air Force FTC (FTAT-2) Edwards Air Force Base, CA 93523	
Attn. RST-5/E A. Gabris RST-5/F W. Stephenson RSS-5/R F Carlisle	1 1	Attn Library M V. Rogers, LKDH Air Force Office of Scientific Research 1400 Wilson Blvd Arlington, VA 22209	1 1
National Aeronautics & Space Administration Ames Research Center Moffett Field, CA 94035		Attn Library U S Air Force, Office of Information Office of Secretary of Air Force The Pentagon Washington, D.C. 20333	
Attn Library	1	Attn. Library	1
National Aeronautics & Space Administration Flight Research Center P.O. Box 273 Edwards, CA 93523		Attn Library Air Force Aero Propulsion Laboratory Research & Technology Division U.S. Air Force Systems Command Wright Patterson AFB, Ohio 45433	
Attn Library	1	Attn Library (APRP)	1
National Aeronautics & Space Administration Goddard Space Flight Center Greenbelt, MD 20771		Arnold Engineering Development Center Air Force Systems Command Tullahoma, TN 37388	
Attn Library	1	Attn Library	1
National Aeronautics & Space Administration George C Marshall Space Flight Center Marshall Space Flight Center, AL 35812		Bureau of Naval Weapons Department of the Navy Washington, D.C.	
Attn Library J L Sanders/PD13 R Richmond/EP24 J McCarty/EP21 C. R Bailey/EP23	1 1 1 1	Attn Library U S Naval Research Laboratory Washington, D.C. 20390 Attn Library	1 1
National Aeronautics & Space Administration John F Kennedy Space Center Kennedy Space Center, FL 32899		U.S. Army Research Office (Durham) Box CM, Duke Station Durham, NC 27706	
Attn Library	1	Attn Library	1
National Aeronautics & Space Administration Lyndon B Johnson Space Center Houston, TX 77058		U S Army Missile Command Redstone Scientific Information Center Redstone Arsenal, AL 35808	
Attn Library H O Pohl/EP R. W Polifka/EP2	1 1 1	Attn Document Section U S Naval Missile Center Point Mugu, CA 93041	1
National Aeronautics & Space Administration Langley Research Center Hampton, VA 23665		Attn Technical Library U S Naval Weapons Center China Lake, CA 93557	1
Attn Library J P Arrington	1	Attn Library	1
NASA Scientific & Technical Information Facility P O Box 8757 Baltimore-Washington International Airport Baltimore, MD 21240			
Attn Accessioning Department	10		
Office of the Director of Defense Research & Engineering Washington, D.C. 20301			
Attn Office of Assistant Director (Chemical Technology)	1		
		Attn Library	1

<u>Name</u>	<u>No of Copies</u>	<u>Name</u>	<u>No of Copies</u>
Aero Incorporated Arnold Engineering Development Center Arnold AF Station, TN 37389		Philco-Ford Corporation Aeronautics Division Ford Road Newport Beach, CA 92663	
Attn Library	1	Attn Library	1
Battelle Memorial Institute 505 King Avenue Columbus, Ohio 43201		Purdue University Lafayette, IN 47907	
Attn Library	1	Attn Library	1
Bell Aerosystems Inc. Box 1 Buffalo, NY 14240		Rocketdyne A Division of Rockwell Corporation 6633 Canoga Avenue Canoga Park, CA 91304	
Attn Library	1	Attn Library	1
Boeing Company, Space Division P O Box 868 Seattle, WA 98124		H. Diem F M. Kirby	1
Attn Library	1	Rocket Research Corporation Willow Road at 116th Street Redmond, WA 98052	
Chemical Propulsion Information Agency Applied Physics Laboratory 8621 Georgia Avenue Silver Spring, MD 20910		Attn Library	1
Chrysler Corporation Space Division P O Box 29200 New Orleans, LA 70129		Thiokol Chemical Corporation P.O. Box 1000 Newton, PA 18940	
Attn Library	1	Attn Library	1
General Dynamics/Convair P.O. Box 1128 San Diego, CA 92112		TRW Systems, Inc. 1 Space Park Redondo Beach, CA 90278	
Attn Library	1	Attn Library	1
General Electric Company Missiles & Space Systems Center Valley Forge Space Tech Center P O Box 8555 Philadelphia, PA 19101		United Aircraft Corporation Pratt & Whitney Division Florida Research & Development Center P O Box 2691 West Palm Beach, FL 33402	
Attn Library	1	Attn Library	1
Grumman Aerospace Corporation Bethpage, L I., NY 11714		United Technologies Research Center East Hartford, CT	
Attn Library	1	Attn Library	1
Ling-Temco-Vought Corporation P O. Box 5907 Dallas, TX 75222		Jet Propulsion Laboratory 4800 Oak Grove Drive Pasadena, CA 91103	
Attn Library	1	Attn Library	1
Lockheed Missiles & Space Co , P O Box 504 Sunnyvale, CA 94088		T M Auslander/125-224	1
Attn Library	1		
Marquardt Corporation 16555 Staticey Street Box 2013 South Annex Van Nuys, CA 91409			
Attn Library T. Hudson J G. Campbell	1 1 1		
Martin-Marietta Corporation P O. Box 179 Denver, CO 80201			
Attn Library	1		
McDonnell Douglas Astronautics 5301 Bolsa Avenue Huntington Beach, CA 92547			
Attn Library	1		

APPENDICES

A. HOT-FIRE DATA SUMMARY

FUEL	TEST	INJECTION	PL	MR	TF	REYN	WT	CSTRE	VF	ODE
TYPE	NO.	TYPE	(PSIA)	(F)			(LB)	(SEC)	(FT/S)	
RP-1	101	-F-O TRIPLET	450.	1.40	50.	10100.	.093	4850.	170.	SLICOK
RP-1	102	-F-O TRIPLET	0.	1.1	0.	0.	.000	0.	0.	UNDEF
RP-1	103	-F-O TRIPLET	0.	1.1	0.	0.	.000	0.	0.	UNDEF
RP-1	104	-F-O TRIPLET	460.	2.0	50.	11343.	.101	4250.	127.	UNDEF
RP-1	105	-F-O TRIPLET	480.	2.40	50.	10321.	.100	4600.	116.	SLICOK
RP-1	106	-F-O TRIPLET	485.	2.75	50.	10053.	.099	4650.	116.	SLICOK
RP-1	107	-F-O TRIPLET	470.	2.60	70.	20636.	.160	0.	200.	CLEAR
RP-1	108	-F-O TRIPLET	450.	1.70	70.	8039.	.047	4000.	76.	SLICOK
RP-1	109	-F-O TRIPLET	475.	1.42	55.	9382.	.053	4650.	89.	SLICOK
RP-1	110	-F-O TRIPLET	420.	2.70	57.	16826.	.137	4750.	165.	SLICOK
RP-1	111	-F-O TRIPLET	480.	2.70	67.	16826.	.137	4750.	165.	SLICOK
RP-1	112	L-F-O TRIPLET	900.	2.50	72.	13840.	.097	0.	120.	CLEAR
RP-1	113	-F-O TRIPLET	0.	1.0	0.	0.	.000	0.	0.	UNDEF
RP-1	114	-F-O TRIPLET	970.	2.75	56.	10315.	.075	4000.	193.	CLEAR
RP-1	115	-F-O TRIPLET	0.	1.2	0.	0.	.000	0.	0.	UNDEF
RP-1	116	-F-O TRIPLET	1500.	2.50	50.	8470.	.082	4600.	100.	CLEAR
RP-1	117	R UNLIK DOUBLE	130.	2.0	15.	2498.	.000	0.	57.	03SCUR
RP-1	118	R UNLIK DOUBLE	0.	1.1	0.	0.	.000	0.	0.	UNDEF
RP-1	119	TRANSVERSE LOL	0.	1.0	3.	0.	.000	0.	0.	UNDEF
RP-1	120	TRANSVERSE LOL	135.	2.15	41.	3815.	.062	4300.	58.	03SCUR
RP-1	121	TRANSVERSE LOL	310.	2.0	38.	3140.	.064	5300.	53.	MODCOK
RP-1	122	TRANSVERSE LOL	780.	2.75	44.	6014.	.113	4750.	95.	CLEAR
RP-1	123	TRANSVERSE LOL	475.	2.5	35.	4705.	.095	4450.	82.	SLICOK
RP-1	124	TRANSVERSE LOL	475.	2.45	34.	4797.	.095	4450.	83.	SLICOK
RP-1	125	TRANSVERSE LOL	472.	2.55	33.	4776.	.094	4450.	83.	SLICOK
RP-1	126	TRANSVERSE LOL	140.	2.10	30.	2533.	.052	4000.	49.	03SCUR
RP-1	127	TRANSVERSE LOL	250.	2.5	30.	2495.	.058	4800.	48.	MODCOK
RP-1	128	TRANSVERSE LOL	400.	3.12	39.	3426.	.077	4900.	63.	SLICOK
RP-1	129	TRANSVERSE LOL	800.	2.40	45.	5985.	.110	5100.	90.	CLEAR
C3H8	130	TRANSVERSE LOL	135.	2.5	45.	41607.	.044	4000.	63.	SLICOK
C3H8	131	TRANSVERSE LOL	290.	2.65	43.	49666.	.057	4500.	76.	CLEAR
C3H8	132	TRANSVERSE LOL	540.	3.0	43.	64458.	.079	4600.	98.	CLEAR
C3H8	133	TRANSVERSE LOL	790.	2.90	45.	78710.	.094	4650.	120.	CLEAR
C3H8	134	R UNLIK DOUBLE	0.	1.0	0.	0.	.000	0.	0.	UNDEF
C3H8	155	R UNLIK DOUBLE	770.	2.0	68.	137923.	.095	4600.	166.	MODCOK
C3H8	136	P UNLIK DOUBLE	780.	2.75	58.	121770.	.095	4600.	158.	MODCOK
C3H8	137	R UNLIK DOUBLE	790.	2.0	54.	55464.	.042	4600.	73.	MODCOK
C3H8	138	R UNLIK DOUBLE	0.	1	0.	0.	.000	0.	0.	UNDEF
C3H8	139	R UNLIK DOUBLE	540.	2.1	54.	45993.	.041	4600.	128.	MODCOK
C3H8	140	R UNLIK DOUBLE	290.	2.	54.	74036.	.063	4150.	98.	03SCUR
C3H8	141	R UNLIK DOUBLE	150.	1.15	52.	47125.	.043	4000.	63.	OBSCUR
C3H8	142	RUD - GAS GE	0.	.00	0.	0.	.000	0.	0.	UNDEF
C3H8	143	RUD - GAS GE	860.	.50	61.	128737.	.058	2000.	110.	OBSCUR
C3H8	144	RUD - GAS GE	850.	.46	59.	133986.	.059	2850.	116.	OBSCUR
'H3	145	UNLIKE-DOUBLE	505.	1.48	65.	164142.	.117	4850.	112.	CLEAR
'H3	146	UNLIKE-DOUBLE	0.	.00	0.	0.	.000	0.	0.	UNDEF
'H3	147	UNLIKE-DOUBLE	245.	1.35	45.	129509.	.095	4650.	92.	CLEAR
'H3	148	UNLIKE-DOUBLE	350.	1.50	45.	126174.	.100	4850.	92.	CLEAR
'H3	149	UNLIKE-DOUBLE	440.	1.35	63.	145380.	.099	4750.	100.	CLEAR
'H3	150	UNLIKE-DOUBLE	250.	1.38	57.	133739.	.095	4650.	94.	CLEAR
'H3	151	UNLIKE-DOUBLE	150.	1.35	48.	137729.	.100	3900.	100.	CLEAR
'H3	152	JNLIKE-DOUBLE	505.	1.10	54.	161571.	.102	4650.	115.	CLEAR
'H3	153	UNLIKE-DOUBLE	505.	1.67	56.	154827.	.128	5100.	109.	CLEAR
'H3	154	UNLIKE-DOUBLE	505.	1.64	55.	157936.	.127	5100.	111.	CLEAR
'H3	155	UNLIKE-DOUBLE	485.	1.36	61.	105097.	.071	4500.	73.	CLEAR
'H3	156	UNLIKE-DOUBLE	500.	1.40	59.	215544.	.155	4950.	150.	CLEAR
C3H8	157	LOL - ED4	800.	2.80	47.	89923.	.106	5150.	130.	MODCOK
C3H8	158	LOL - ED4	500.	2.85	29.	65659.	.090	5000.	100.	OBSCUR
C3H8	159	LOL - ED4	295.	2.90	39.	56494.	.072	4500.	84.	OBSCUR
C3H8	160	LOL - ED4	150.	2.80	30.	39452.	.050	4100.	60.	OBSCUR
C3H8	161	LOL - ED4	800.	2.90	60.	97117.	.107	5100.	132.	MODCOK
C3H8	162	LOL - ED4	550.	2.95	61.	79565.	.088	4900.	106.	03SCUR
C3H8	163	LOL - ED4	295.	3.25	64.	61592.	.074	4300.	81.	OBSCUR
C3H8	164	LOL - ED4	250.	2.90	80.	78058.	.075	4550.	91.	OBSCUR
C3H8	165	LOL - ED4	600.	2.95	147.	208855.	.097	4650.	144.	CLEAR
C3H8	166	LOL - ED4	0.	.00	0.	0.	.000	0.	0.	UNDEF
C3H8	167	LOL - ED4	0.	.00	0.	0.	.000	0.	0.	UNDEF
C3H8	168	LOL - ED4	550.	1.90	155.	157079.	.082	4600.	129.	MODCOK
C3H8	169	LOL - ED4	320.	3.10	158.	154762.	.088	3400.	117.	CLEAR
C3H8	170	LOL - ED4	0.	.00	0.	0.	.000	0.	0.	UNDEF
C3H8	171	LOL - ED4	640.	2.80	124.	104571.	.050	4900.	71.	SLICOK
C3H8	172	LOL - ED4	510.	2.95	130.	250770.	.123	4550.	165.	MODCOK
C3H8	173	LOL - ED4	640.	2.20	60.	8777.	.043	4300.	119.	OBSCUR
C3H8	174	LOL - ED4	625.	4.00	78.	83921.	.100	4250.	97.	SLICOK
C3H8	175	LOL - ED4	545.	4.10	79.	73611.	.090	4150.	85.	MODCOK
C3H8	176A	LOL - ED4	150.	2.90	75.	47110.	.047	4100.	56.	OBSCUR
C3H8	176B	LOL - ED4	100.	2.90	72.	75477.	.000	2000.	91.	CLEAR
C3H8	177	PRE ATOM TRIP	805.	2.75	70.	104118.	.086	5100.	155.	CLEAR
C3H8	178	PRE ATOM TRIP	560.	2.75	70.	87702.	.070	5400.	130.	SLICOK
C3H8	179	PRE ATOM TRIP	300.	2.05	66.	64553.	.055	4750.	99.	SLICOK

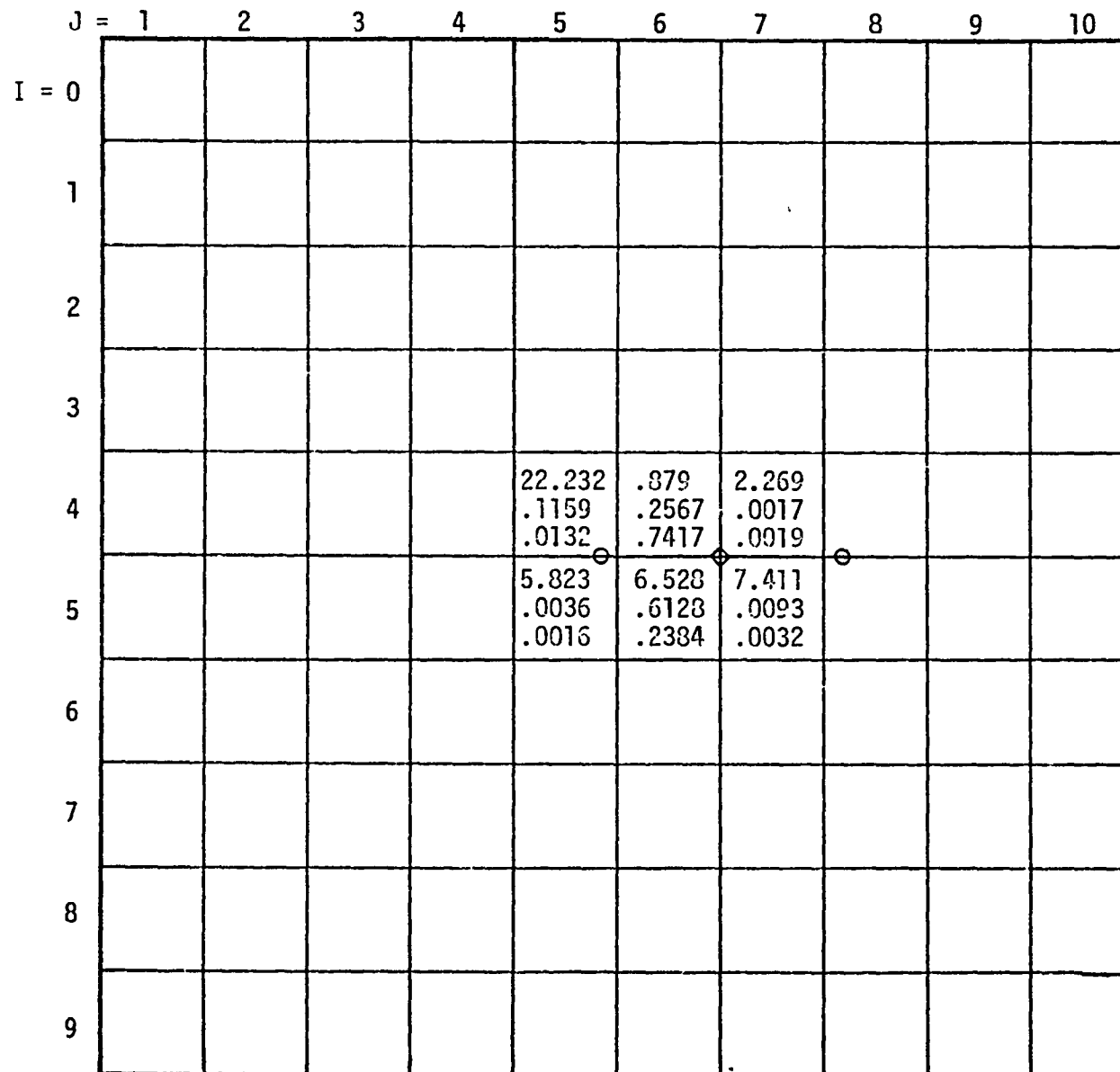
FUEL TYPE	TEST NO.	INJECTOR TYPE	PC (PSIA)	MR	TF (F)	REYN	WT (LB)	CSTRE (SEC)	VF (FT/S)	MODE
C3H4	120	PPE ATOM TRIP	0.	.00	0.	0.	.000	0.	0.	UNDEF
C3H4	161	PPE ATOM TRIP	0.	.00	0.	0.	.000	0.	0.	UNDEF
C3H4	172	PPE ATOM TRIP	150.	2.99	65.	44283.	.038	4403.	59.	MODCOK
C3H4	183	PPE ATOM TRIP	0.	.10	0.	0.	.000	0.	0.	UNDEF
C3H4	194	PPE ATOM TRIP	300.	2.85	66.	64553.	.055	4750.	99.	SLICOK
C3H4	195	PPE ATOM TRIP	565.	2.20	72.	122300.	.083	5400.	178.	SLICOK
C3H4	166	PPE ATOM TRIP	670.	3.50	69.	70033.	.073	5250.	195.	SLICOK
C3H4	147	PPE ATOM TRIP	800.	2.90	66.	60803.	.055	4600.	93.	CLEAR
C3H4	144	PPE ATOM TRIP	540.	3.00	64.	64082.	.060	5000.	100.	SLICOK
C3H4	187	PPE ATOM TRIP	155.	2.80	62.	58165.	.050	4700.	91.	MODCOK
C3H4	193	PPE ATOM TRIP	165.	2.75	63.	89331.	.078	4750.	140.	SLICOK
C3H4	191	PPE ATOM TRIP	700.	.00	110.	0.	.000	0.	0.	UNDEF
C3H4	192	PPE ATOM TRIP	0.	.00	0.	0.	.000	0.	0.	UNDEF
C3H4	193	PPE ATOM TRIP	560.	2.80	120.	170305.	.074	5150.	142.	SLICOK
C3H4	174	PPE ATOM TRIP	340.	3.00	115.	143277.	.068	4450.	122.	SLICOK
C3H4	195	PPE ATOM TRIP	670.	2.85	66.	95525.	.084	5400.	146.	SLICOK
C3H4	196	PPE ATOM TRIP	630.	3.20	66.	50112.	.051	4000.	78.	SLICOK
C3H4	197	PPE ATOM TRIP	505.	3.00	43.	68475.	.074	4700.	120.	SLICOK
C3H4	198	LOL-EDM GAS	810.	.72	79.	137519.	.079	3250.	113.	OBSCUR
C3H4	199	LOL-EDM GAS	510.	.73	75.	103371.	.063	3100.	86.	OBSCUR
GCH4	200	SLIT TRIPLET	770.	3.30	67.	269842.	.101	5150.	271.	CLEAR
GCH4	211	SLIT TRIPLET	760.	3.60	67.	277992.	.101	5100.	279.	CLEAR
GCH4	202	SLIT TRIPLET	540.	4.20	70.	173026.	.070	4300.	248.	CLEAR
GCH4	203	SLIT TRIPLET	535.	3.50	71.	211659.	.075	4600.	308.	CLEAR
GCH4	204	SLIT TRIPLET	290.	3.70	72.	136406.	.050	3200.	363.	CLEAR
GCH4	207	SLIT TRIPLET	125.	4.70	73.	103524.	.043	2700.	622.	CLEAR
GCH4	211	SLIT TRIPLET	630.	3.60	53.	283078.	.101	3500.	325.	CLEAR
GCH4	207	SLIT TRIPLET	620.	3.00	54.	345763.	.105	3300.	405.	CLEAR
CCH4	204	SLIT TRIPLET	0.	.00	0.	0.	.000	0.	0.	UNDEF
GCH4	207	SLIT TRIPLET	700.	4.00	56.	267785.	.105	5250.	279.	CLEAR
GCH4	212	SLIT TRIPLET	0.	.00	0.	0.	.000	0.	0.	UNDEF
SCH4	211	SLIT TRIPLET	0.	.00	0.	0.	.000	0.	0.	UNDEF
SCH4	212	SLIT TRIPLET	690.	3.35	50.	454803.	.150	5200.	471.	CLEAR
SCH4	213	SLIT TRIPLET	685.	2.80	45.	211966.	.060	4650.	216.	CLEAR
GCH4	214	SLIT TRIPLET	310.	3.45	44.	160539.	.051	4150.	363.	CLEAR
GCH4	215	SLIT TRIPLET	125.	4.50	40.	131234.	.050	2450.	707.	CLEAR
GCH4	216	SLIT TRIPLET	790.	2.75	38.	306921.	.087	5100.	260.	CLEAR
GCH4	217	SLIT TRIPLET	405.	4.70	38.	132693.	.054	4500.	225.	CLEAR
GCH4	218	SLIT TRIPLET	405.	2.75	38.	150993.	.041	4000.	257.	CLEAR
GCH4	219	SLIT TRIPLET	790.	3.20	40.	215515.	.067	4900.	183.	CLEAR
CCH4	220	SLIT TRIPLET	450.	3.00	40.	303088.	.088	4900.	468.	CLEAR
CCH4	221	SLIT TRIPLET	410.	4.00	46.	101752.	.038	4400.	174.	CLEAR
LCH4	227	LOL-EDM GAS GF	805.	.82	-220.	189924.	.082	3050.	140.	CLEAR
LCH4	223	LOL-EDM GAS GF	775.	.61	-230.	194587.	.084	2900.	157.	CLEAR
LCH4	224	LOL-EDM GAS GE	A05.	.50	-206.	210361.	.068	2875.	146.	CLEAR
LCH4	226	LOL-EDM GAS GE	515.	.78	-226.	145129.	.066	3200.	113.	CLEAR
LCH4	225	LOL-EDM GAS GE	495.	.60	-245.	132636.	.066	2900.	120.	CLEAR
LCH4	227	LOL-EDM GAS GE	495.	.44	-211.	212882.	.070	2700.	150.	CLEAR

B. INJECTOR COLD-FLOW DATA SUMMARY

Injector: OFO TRIPLET

Axial Distance: 1.27 cm (0.5")

B₁



○ Oxidizer Hole Projection
◇ Fuel Hole Projection

Injector: OFO TRIPLET

Axial Distance: 2.54 cm (1")

J =	1	2	3	4	5	6	7	8	9	10
I =	0									
1										
2										
3					0.993 .0023 .0052	0.654 .0013 .0047				
4			∞ .0383 0	18.527 .0646 .0083	2.129 .0582 .0647	.660 .1477 .5304	1.588 .0111 .0165			
5					5.293 .0092 .0041	1.915 .1893 .2342	5.898 .2401 .0964	56.374 .0656 .0023	7.622 .0044 .0014	0 0 .0019
6					5.553 .0065 .0028	9.755 .0397 .0096	13.498 .0785 .0138	32.554 .0379 .0028	∞ .0040	
7						5.293 .0009 .0004				
8										
9										

○ Oxidizer Hole Projection
◊ Fuel Hole Projection

Injector: OFO Triplet

Axial Distance: 3.31 cm (1.5")

	J = 1	2	3	4	5	6	7	8	9	10
I = 0										
1										
2										
3	.0496 .0005 .0022	1.401 .0076 .0023	1.501 .0059 .0076	.794 .0066 .0163	.397 .0020 .0093		0 0 .0110			
4	24.879 .0516 .0041	2.779 .0308 .0218	.611 .0220 .0703	.555 .0934 .3263	.858 .0439 .1008	.382 .0110 .0245				
5	.794 .0015 .0038	.397 .0009 .0044	6.511 .0036 .0056	1.168 .0275 .0463	16.939 .0035 .0004	2.250 .0934 .0817	5.528 .0198 .0041	13.498 .0019 .0003		
6	.079 .0001 .0027	.794 .0010 .0025	.1687 .0093 .0109	2.321 .0417 .0354	4.389 .1285 .0517	6.443 .1560 .0477	28.584 .0989 .0068	30.933 .0230 .0007	∞ .0060 0	
7	.041 .0001 .0053	.937 .0022 .0046	.274 .0055 .0395	2.522 .0148 .0116	7.146 .0297 .0082	9.346 .0341 .0068	25.408 .0176 .0014	∞ .0049		
8		0 0 .0027	0 0 .0116	0 0 .0014						
9										

B-3

O Oxidizer Hole Projection
◊ Fuel Hole Projection

Injector: EDM-LOL

Axial Distance: 1.27 cm (0.5")

B-4

J =	1	2	3	4	5	6	7	8	9	10
I =	0									
1										
2	0 0 .0060	0 0 .0011	1.059 .0012 .0024	7.940 .0083 .0023	1.444 .0083 .0125	.934 .0009 .0018				
3			.794 .0027 .0063	8.951 .055 .013	43.67 .049 .0023	1.236 .0015 .0024				
4			.635 .0035 .011	2.257 .230 .215	1.720 .230 .272	.681 .0027 .0079				
5		0 0 .0023	.977 .0071 .015	2.000 .150 .153	1.701 .199 .233	1.290 .0115 .018	0 0 .0011			
6			2.647 .0044 .0034	3.363 .0032 .0019	4.764 .0053 .0023	4.129 .0115 .0057				
7			8.999 .0015 .0003			5.955 .0027 .0009				
8						1.588 .0009 .0011				
9						.				

○ Oxidizer Hole Projection
◇ Fuel Hole Projection

Injector: EDM-LOL

Axial Distance: 2.54 cm (1")

	J = 1	2	3	4	5	6	7	8	9	10
I = 0				4.764 .0025 .0010	3.970 .0038 .0017	3.289 .0024 .0014	.471 .0007 .0026		0 0 .0021	
1			.794 .0017 .0039	9.210 .0073 .0015	20.64 .0109 .0010	6.352 .0067 .0019	1.412 .0013 .0017			
2		0 0 .0024	.577 .0034 .0058	5.717 .015 .0049	98.46 .026 .0005	12.175 .0097 .0015	1.036 .0013 .0022			
3		0 0 .0026	.681 .0050 .0136	2.382 .038 .029	6.268 .063 .018	1.720 .022 .023	.353 .0017 .0087	0 0 .0010		
4	0 0 .0015	0 0 .0041	.669 .0067 .0184	1.568 .084 .097	1.405 .1930 .252	1.006 .089 .146	.489 .0067 .0252	.294 .0004 .0026		
5		.326 .0007 .0038	1.290 .0109 .0155	2.779 .0381 .058	2.117 .113 .073 ◇	2.498 .099 .073	1.450 .013 .022	.467 .0003 .0032		
6		.667 .0008 .0015	3.176 .010 .0058	4.367 .019 .0078	3.176 .0050 .0029	4.058 .019 .0037	3.298 .023 .013	1.966 .0022 .0020		
7		2.647 .0013 .0009	3.176 .0050 .0029	2.269 .0008 .0007		1.588 .0004 .0005	6.352 .010 .0029	2.925 .0029 .0018		
8		1.059 .0005 .0009	2.647 .0013 .0009		0 0 .0015		6.987 .0018 .0005	5.823 .0028 .0009	0 0 .0076	
9			0 0 .0019				1.191 .0010 .0016			

○ Oxidizer Hole Projection
◇ Fuel Hole Projection

Injector: EDM-LOL

Axial Distance: 3.31 cm (1.5")

B-6

	J = 1	2	3	4	5	6	7	8	9	10
I = 0		0 0 .0017	.706 .0011 .0027	9.074 .0022 .0004	∞ .0036 0	∞ .0040 0	∞ .0023 0	1.832 .0008 .0008	0 0 .0006	0 0 .0024
1	0 0 .0007	.127 .0002 .0030	.529 .0016 .0055	7.146 .0049 .0012	47.64 .0081 .0003	∞ .0080 0	∞ .0038 0	1.588 .0011 .0012		
2		.155 .0004 .0025	.567 .0027 .0085	2.38 .0081 .0061	47.64 .0162 .0006	41.29 .0140 .0006	5.293 .0054 .0018	.529 .0011 .0036	0 0 .0018	0 0 .0010
3	0 0 .0009	.065 .0001 .0030	.418 .0027 .0097	1.489 .0162 .0195	3.176 .0324 .0182	2.454 .0275 .0201	3.032 .0113 .0067	.441 .0027 .0109	.222 .0001 .0026	0 0 .0009
4	0 0 .0015	.113 .0003 .0040	.681 .0049 .0128	1.344 .030 .040	1.355 .078 .1030	1.023 .078 .137	.728 .030 .073	.418 .0054 .023	.176 .0005 .0055	0 0 .0018
5	0 0 .0018	.218 .0005 .0044	1.191 .0081 .0122	2.077 .046 .040	2.382 .097 .073 \diamond	2.098 .0998 .085	1.755 .057 .058	.998 .0119 .021	.289 .0011 .0067	0 0 .0021
6	0 0 .0012	.529 .0008 .0027	2.250 .0092 .0073	3.535 .037 .019	4.764 .041 .015	3.494 .030 .015	3.403 .041 .021	2.235 .021 .016	1.059 .0032 .0055	
7		1.323 .0013 .0018	3.630 .0086 .0043	5.293 .0108 .0036	4.764 .0049 .0018	5.029 .0021 .0007	4.764 .0081 .0030	3.516 .017 .0085	2.911 .0059 .0036	.397 .0003 .0012
8		1.985 .0013 .0012	5.558 .0038 .0012	2.117 .0011 .0009			0 0 .0006	5.558 .0076 .0024	.983 .0070 .0128	.635 .0005 .0015
9		2.117 .0011 .0009	3.000 .0009 .0005					3.970 .0013 .0006	3.705 .0038 .0018	1.588 .0011 .0012

\circ Oxidizer Hole Projection
 \diamond Fuel Hole Projection

Injector: EDM-LOL

Axial Distance: 5.08 cm (2")

	J =	1	2	3	4	5	6	7	8	9	10
I =	0	0 .0007 .0020	.299 .0016 .0040	.681 .0038 .0003	22.23 .0055 .0003	31.76 ∞ 0	.0055 .0033 0	∞ .0014 .0005	4.963 .0011 .0009	1.254 .0008 .0011	0 0 .0009
1	.079 .0001 .0023	.430 .0013 .0049	1.011 .0038 .0064	6.352 .0065 .0017	26.99 .0093 .0006	25.41 .0087 .0006	14.29 .0049 .0006	1.588 .0022 .0023	.316 .0007 .0022	0 0 .0014	
	.596 .0016 .0052	1.121 .0065 .0099	2.329 .0120 .0087	5.082 .017 .0058	3.441 .014 .0070	1.290 .0071 .0093	.561 .0033 .0099	.265 .0008 .0052	0 0 .0021		
	.176 .0003 .0026	.433 .0016 .0064	1.036 .0082 .0075	1.512 .022 .024	1.475 .035 .041	1.087 .035 .052	.761 .019 .042	.492 .0071 .042	.280 .0016 .0099	.108 .0002 .0034	
4	.223 .0004 .0033	.489 .0022 .0075	1.198 .012 .017	1.720 .035 .035	1.664 .060 .061	1.248 .060 .081	1.011 .038 .064	.749 .014 .031	.505 .0038 .013	.190 .0004 .0039	
	.237 .0004 .0027	.983 .0035 .0061	1.985 .016 .014	2.495 .042 .028	2.729 .060 .037 ◊	2.382 .057 ◊41	1.896 .044 .039	1.152 .020 .024	.970 .0060 .0104	.454 .0011 .0041	
	.741 .0008 .0017	1.390 .0038 .0046	2.779 .015 .0093	3.557 .031 .0145	3.590 .028 .013	3.427 .022 .011	3.176 .025 .013	2.529 .023 .016	1.800 .0093 .0087	.907 .0022 .0041	
7	1.323 .0011 .0014	2.382 .0043 .0030	7.543 .010 .023	3.772 .010 .0046	4.764 .0065 .0023	4.083 .0039 .0016	3.176 .0055 .0029	3.609 .0136 .0064	2.779 .011 .0070	1.588 .0027 .0029	
	1.429 .0010 .0012	2.558 .0038 .0021	2.226 .0038 .0018	2.802 .0016 .0010	1.588 .0005 .0006		1.815 .0004 .0004	3.348 .0043 .0021	3.630 .0087 .0041	2.779 .0038 .0023	
	1.286 .0009 .0012	3.176 .0015 .0008	2.823 .0009 .0005					1.600 .0004 .0003	4.764 .0043 .0016	3.740 .0040 .0018	

○ Oxidizer Hole Projection
◊ Fuel Hole Projection

Injector: PAT

Axial Distance: 1.27 cm (0.5")

	J = 1	2	3	4	5	6	7	8	9	10
I = 0										
1										
2										
3					0 0 .044	0 0 .032	0 0 .0009			
4		1.547 .0051 .0073	.027 .0009	3.606 .327 .201	2.084 .141 .150	∞ .022 0	∞ .0042 0	4.764 .0020 .0009	∞ .0020 0	
5	∞ .0009 0	∞ .0040 0	∞ .012 0	108.0 .046 .0009	1.832 .202 .244	1.755 .141 .178	57.17 .024 .0009	63.52 .0054 .0002	30.17 .0026 .0002	31.76 .0027 .0002
6	∞ .0078 0		∞ .0003 0	∞ .0019 0	.347 .0094 .060	.378 .0067 .039	6.881 .0017 .0006	1.588 .0003 .0004		
7					.983 .0017 .0039	0 0 .0024	0 0 .0004			
8	0 0 .0041									
9										

O Oxidizer Hole Projection
◊ Fuel Hole Projection

Injector: PAT

Axial Distance: 2.54 cm (1")

	J = 1	2	3	4	5	6	7	8	9	10
I = 0										
1										
2					0 0 .0134	0 0 .0209	0 0 .0078			
3				∞ .0083 0 .0453	1.588 .035 .024 .0744	.658 .024 .0118	.722 .0069 .0118	34.14 .0059 .0004	28.58 .0025 .0002	∞ .0003 0
4	∞ .0010 .0004	27.79 .0048 0	∞ .0091 .00	14.29 .037 .00	1.926 .204 .0054	12.17 .318 .236	1.516 .087 .161	∞ .021 0	∞ .0083 0	∞ .0021 0
5	19.06 .0017 .0002	∞ .0051 0	∞ .013 0	19.06 .0249 .0027	1.588 .040 .0526	1.642 .084 .107	1.732 .033 .040	150.9 .013 .0002	∞ .0064 0	∞ .0018 0
6		∞ .0007 0	∞ .0011 0	2.117 .0006 .0005	0 0 .0103	0 0 .0290	0 0 .0051	0 0 .0004	0 0 .0011	
7						0 0 .0040				
8										
9										

O Oxidizer Hole Projection
◊ Fuel Hole Projection

Injector: PAT

Axial Distance: 3.31 cm (1.5")

	J =	1	2	3	4	5	6	7	8	9	10
I =	0										
1					0 0 .0044	0 0 .0057					
2				.132 .0004 .0048	.053 .0004 .013	0 0 .0112	0 0 .0022				
3			5.445 .0044 .0015	.889 .026 .024	1.732 .044 .048	.934 .0182 .028	1.157 .078 .013	7.940 .0055 .0013	∞ .0027 .0015	∞	
4	∞ .0009 0	∞ .0046 0	16.67 .019 .0022	2.300 .077 .063	1.971 .197 .190	1.906 .164 .164	1.254 .055 .083	10.32 .017 .0031	∞ .0069 0	∞ .0027 0	
5	∞ .0036 0	∞ .0098 0	15.88 .018 .0022	2.199 .033 .028	1.974 .084 .081	2.129 .108 .103	1.516 .038 .048	11.998 .012 .0020	∞ .0053 0	∞ .0029 0	
6	6.35 .0015 .0004	∞ .0036 0	1.429 .0033 .0004	.855 .0026 .0057	.425 .0055 .019	.433 .0055 .024	.907 .0036 .0077	5.399 .0031 .0011	∞ .0026 0	∞ .0013 0	
7					0 0 .0061	0 0 .0066	0 0 .0039				
8											
9											

O Oxidizer Hole Projection
◊ Fuel Hole Projection

Injector: PAT

Axial Distance: 5.08 cm (2")

B-11

	J = 1	2	3	4	5	6	7	8	9	10
I = 0					0 0 .0016	0 0 .0032	0 0 .0012			
1				0 0 .0023	0 0 .0046	0 0 .0056	0 0 .0028			
2			1.475 .0028 .0032	1.207 .0081 .0116	1.134 .0106 .016	.575 .0053 .016	.265 .0013 .0083	.706 .0017 .0042	3.705 .0015 .0007	
3		4.764 .0013 .0005	7.940 .0106 .0023	1.764 .043 .042	1.684 .074 .076	1.390 .060 .051	.866 .0255 .051	1.583 .013 .014	14.29 .0057 .0007	∞ .0021 0
4	∞ .0021 0	∞ .0070 0	15.88 .021 .0023	2.382 .057 .042	1.768 .125 .123	2.779 .149 .093	1.191 .083 .120	2.722 .026 .016	15.88 .0106 .0012	∞ .0034 0
5	∞ .0043 0	∞ .0089 0	9.528 .013 .0023	1.672 .0213 .022	1.629 .043 .045	2.303 .062 .046	1.257 .040 .056	1.710 .015 .015	4.446 .0060 .0023	∞ .0017 0
6	∞ .0021 0	∞ .0028 0	7.940 .0032 .0007	.681 .0026 .0065	.893 .0057 .0111	.864 .0079 .016	.676 .0043 .013	1.038 .0036 .0060	15.88 .0021 .0002	∞ .0015 0
7					0 0 .0042	0 0 .0053	0 0 .0039	0 0 .0016		
8					0 0 .0023	0 0 .0046				
9										

○ Oxidizer Hole Projection
◇ Fuel Hole Projection

Injector: T-LOL

Axial Distance: 1.27 cm (0.5")

B-12

		J = 1	2	3	4	5	6	7	8	9	10	
		I = 0										
	2		2.647 .0005 .0005	19.85 .0026 .0003	21.17 .0042 .0005	7.94 .0021 .0007						
	3				14.93 .0050 .0009	34.94 .023 .0017	25.94 .010 .0010	.529 .0002 .0010				
	4					9.528 .0038 .0010	57.17 .190 .0086○	25.81 .137 .014	1.588 .0011 .0017			
	5						6.352 .0017 .0007	1.380 .237 .445	2.787 .287 .266	1.059 .0008 .0021		
	6							3.970 .0016 .0010	.440 .019 .112	1.089 .051 .120	6.108 .0053 .0022	
	7								1.985 .0011 .0014	1.003 .0025 .0065	1.444 .0042 .0076	8.258 .0055 .0017
	8								∞ .0011 0	1.732 .0013 .0019	15.88 .0021 .0003	
	9											

○ Oxidizer Hole Projection
◊ Fuel Hole Projection

Injector: T-LOL

Axial Distance: 2.54 cm (1")

	J = 1	2	3	4	5	6	7	8	9	10
I = 0										
1				∞ .0018 0	∞ .0043 0	∞ .0018 0				
2				∞ .0052 0	∞ .015 0	∞ .0046 0	∞ .0029 0	∞ .0006 0		
3		2.647 .0006 .0005	23.82 .0087 .0008	49.23 .036 .0017	∞ .050 0	25.41 .0092 .0008	1.815 .0009 .0012			
4			7.058 .0046 .0013	6.785 .054 .018	27.79 .162 .013	5.955 .017 .0049	.397 .0002 .0013			
5			5.029 .0044 .0022	1.489 .087 .132	1.538 .248 .365	3.298 .031 .021	.318 .0002 .0016			
6			5.558 .0040 .0016	1.509 .044 .066	.962 .096 .225	4.870 .053 .025	2.779 .0024 .0020			
7			2.417 .0040 .0038	1.543 .0080 .0117	.095 .0007 .016	2.671 .021 .018	2.911 .0051 .0039			
8			3.176 .0021 .0015	.496 .0006 .0026	0 0 .0038	1.701 .0035 .0046	4.446 .0049 .0025			
9				0 0 .0008	0 0 .0008	0 0 .0008	0 0 .0008			

O Oxidizer Hole Projection
◊ Fuel Hole Projection

Injector: T-LOL

Axial Distance: 3.81 cm (1.5")

	J = 1	2	3	4	5	6	7	8	9	10
I = 0					4.537 .0023 .0011	20.64 .0015 .0002				
1			3.705 .0008 .0005	31.76 .0023 .0002	∞ .0041 0	∞ .0035 0	∞ .0017 0	2.541 .0009 .0008		
2			11.645 .0026 .0003	21.04 .0062 .0037	∞ .015 0	∞ .017 0	43.67 .0064 .0003	7.940 .0017 .0005		
3			3.705 .0008 .0005	8.999 .0079 .0028	21.84 .032 .0031	177.9 .065 .0008	25.41 .019 .0016	4.764 .0035 .0016		
4			0 0 .0008	2.565 .0049 .0041	3.176 .037 .025	8.293 .109 .028	6.352 .033 .011	2.071 .0035 .0036		
5				2.481 .0058 .0050	1.358 .062 .097	1.225 .157 .273	2.762 .046 .036	2.565 .0049 .0041		
6				3.006 .0062 .0044	1.477 .046 .067	.912 .099 .231	3.032 .073 .052	3.550 .0088 .0053	.397 .0002 .0012	
7				1.951 .0050 .0055	1.732 .014 .017	.424 .0046 .023	2.541 .037 .031	2.722 .014 .011	1.588 .0016 .0022	
8				1.985 .0035 .0037	.934 .0023 .0050	0 0 .0055	1.511 .0045 .0064	3.176 .012 .0078	2.382 .0028 .0025	
9				2.117 .0023 .0023	0 0 .0022	0 0 .0031	0 0 .0028	3.176 .0046 .0031	3.176 .0023 .0016	

○ Oxidizer Hole Projection
◊ Fuel Hole Projection

Injector: T-LOL

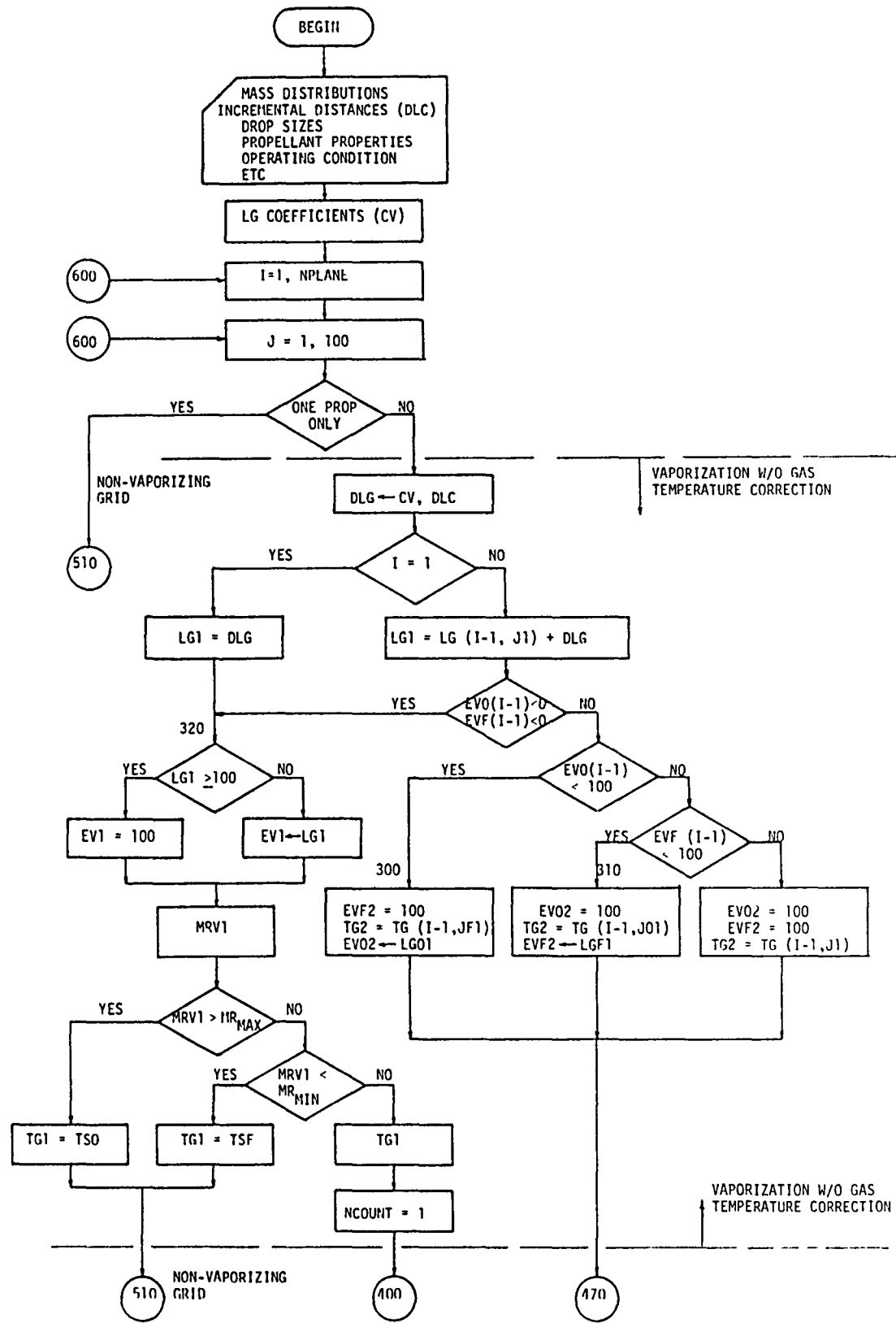
Axial Distance: 5.03 cm (2")

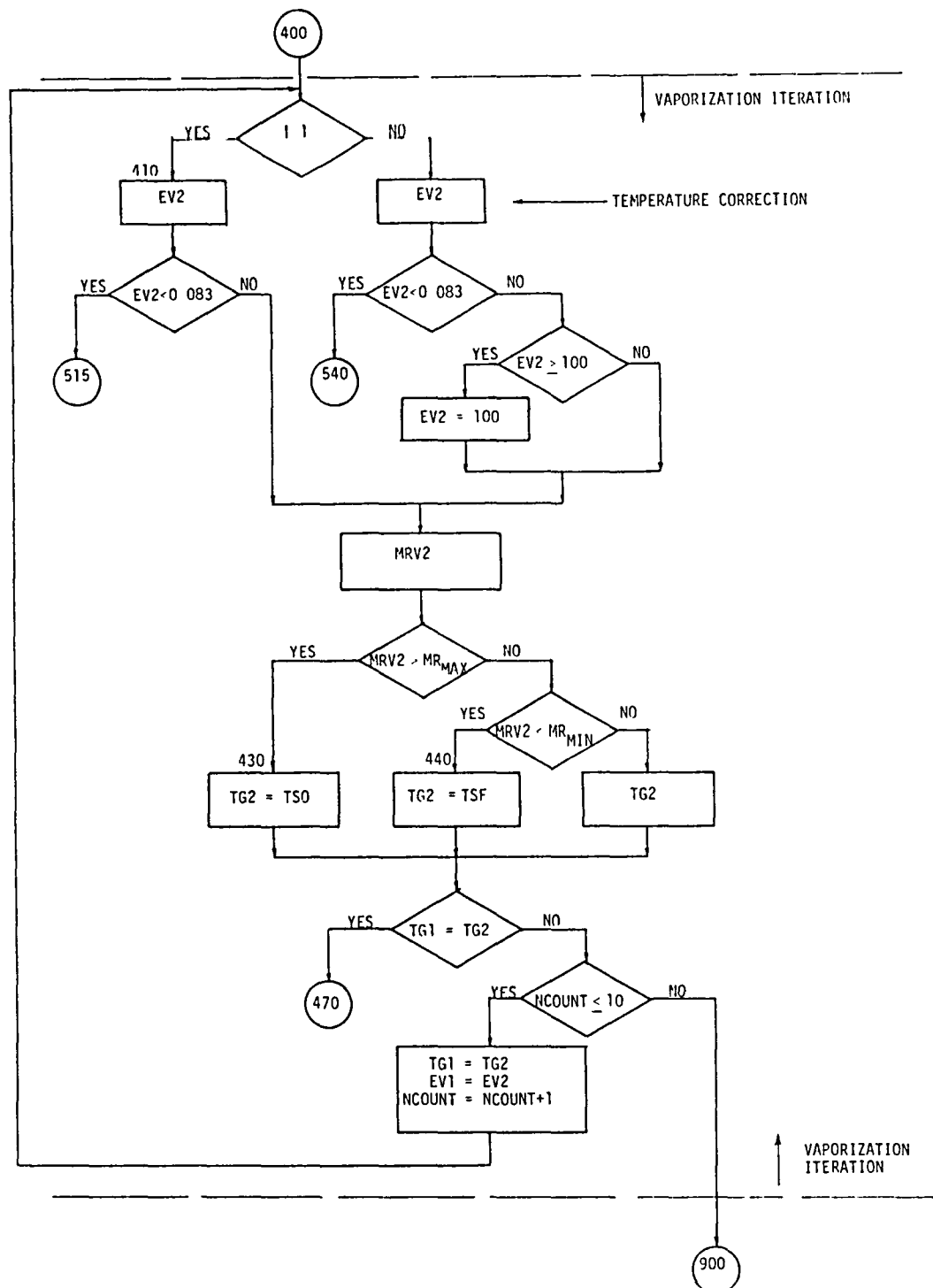
B-15

		J = 1	2	3	4	5	6	7	8	9	10
		I = 0			.0017 0	.0017 0	.0012 0				
	1				∞	∞	∞				
	1				.0017 0	.0039 0	.0069 0	.0060 0	.0022 0	.0009 0	
	2				26.99 .0029 .0002	17.47 .0094 .0010	∞ .022 0	∞ .022 0	∞ .0086 0	6.352 .0014 .0003	
	3				3.176 .0017 .0010	5.325 .0098 .0035	22.76 .037 .0031	96.87 .052 .0010	17.87 .015 .0017	4.083 .0031 .0015	0 0 .0017
	4				0 0 .0012	1.723 .0088 .0097	3.176 .045 .027	6.670 .072 ○	4.446 .024 .010	2.055 .0038 .0035	
	5				.662 .0009 .0025	1.832 .013 .014	.993 .069 ◇	1.344 .094 .133	2.383 .031 .025	2.382 .0051 .0041	0 0 .0021
	6				.706 .0007 .0019	1.815 .014 .015	.989 .065 .127	1.083 .103 .183	2.117 .048 .044	2.941 .0086 .0056	.529 .0003 .0012
	7				.529 .0007 .0029	2.077 .012 .011	.191 .021 .033	1.036 .026 .048	2.558 .050 .037	2.548 .014 .010	1.444 .0017 .0023
	8				.159 .0003 .0041	1.732 .0062 .0068	.675 .0029 .0083	.069 .0003 .0095	2.193 .015 .013	3.176 .017 .010	1.800 .0029 .0031
	9				.681 .0010 .0029	1.059 .0017 .0031	.0993 .0002 .0033	0 0 .0031	.496 .0009 .0033	3.176 .0069 .0041	2.647 .0034 .0025

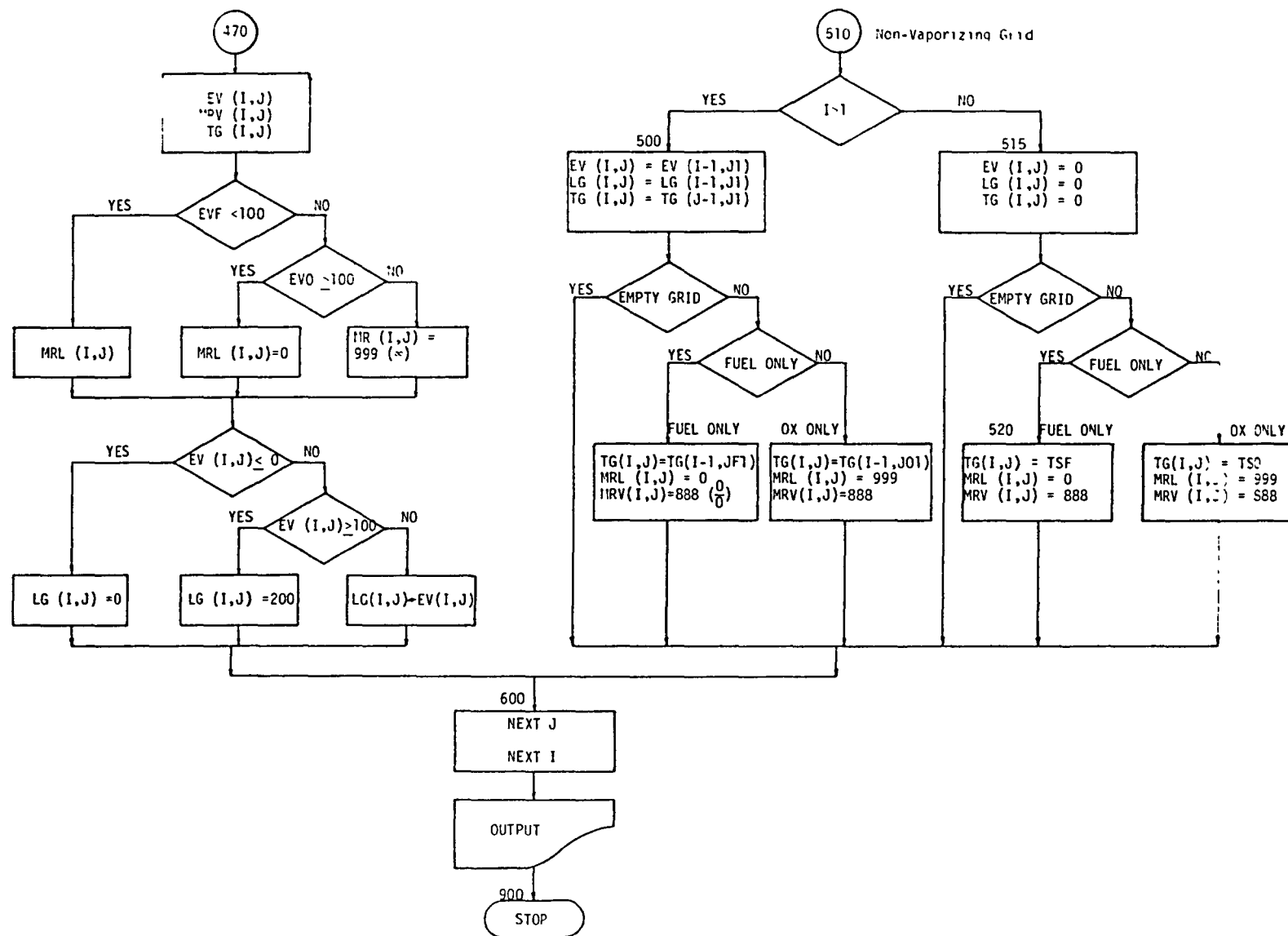
○ Oxidizer Hole Projection
◇ Fuel Hole Projection

C. VAPORIZATION COMPUTATION FLOWCHART
AND COMPUTER PROGRAM LISTING





C-3



1234567890123456789012345678901234567890123456789012345678901234567890123456789012345678901234567890***SEQ NO 01

VV	VV	AAAAAAA	PPPPPPPPP	00000000	RRRRRRRRR
VV	VV	AAAAAA	PPPPPPPPP	000000000	RRRRRRRRRR
VV	VV	AA	PP	00	RR
VV	VV	AA	PP	00	RR
VV	VV	AA	PP	00	RR
VV	VV	AAAAA	PPPPPPPPP	00	RRRRRRRRR
VV	VV	AAAAAA	PPPPPPPPP	00	RRRRRRRRR
VV	VV	AA	PP	00	RR
VVVV		AA	PP	00	RR
VVVV		AA	PP	00	RR
VV		AA	PP	00000000000	RR
VV		AA	PP	000000000	RR

PRINTED BY VAPOR
USER NAME ALRC
ACCOUNT 0427AA133
ON SYSTEM B
EXEC LEVEL 37R2B-B42
EXEC DATE 05/06

CREATED BY VAPOR

STARTED PRINTING 5/14/82 07 58 20
QUEUED 5/14/82 07 57 53
CREATED 5/14/82 07 57 23
PART NAME -BK1-\$*-BK2-
PART NO 00
FILE NAME 000427*BKFIL\$VAPOR(4)

ESTIMATED PAGES 12
INPUT DEVICE DG1924
QUEUED TO AJ1
PRINTED ON AJ1PR1

C-4

* * * CDC / INFORMATION SYSTEMS DESIGN * 3205 CORONADO DR * SANTA CLARA, CA 95051 * (408) 727-8100 * * * 1108 1XO * * *

FORTRAN
FORTRAN V: ISD VERSION 4.9S-08/30/82-14:33:25 (26.)

MAIN PROGRAM

STORAGE USED: CODE(1) 002174; DATA(0) 010770; BLANK COMMON(2) 000000

EXTERNAL REFERENCES (BLOCK, NAME)

0003 SINTP
0004 VINTRS
0005 VRDUS
0006 NI03\$
0007 VI02\$
0010 VRNLS
0011 VI01\$
0012 VWDUS
0013 VERR2\$
0014 XERR
0015 VSTOP\$

STORAGE ASSIGNMENT (BLOCK, TYPE, RELATIVE LOCATION, NAME)

0001	000310	100L	0000	010324	1000F	0000	010325	1010F	0001	000317	110L	0001	000325	120L
0001	000335	130L	0001	000032	135G	0001	000034	140G	0001	000344	140L	0001	000353	150L
0001	000351	160L	0001	000612	170L	0001	000617	175L	0001	000630	180L	0001	000637	145L
0001	000647	190L	0001	000052	20L	0000	010331	2000F	0000	010345	2010F	0000	010365	2220F
0000	010367	2030F	0000	010373	2040F	0000	010410	2050F	0000	010432	2060F	0000	010454	2070F
0000	010461	2080F	0000	010466	2090F	0000	010504	2100F	0000	010516	2200F	0000	010522	2210F
0000	010524	2220F	0000	C10537	2230F	0000	010545	2240F	0000	010553	2250F	0000	010560	2260F
0000	010565	2270F	0000	010572	2280F	0000	010577	2300F	0001	000205	231G	0000	010605	2310F
0000	010612	2320F	0000	010620	2330F	0000	010631	2340F	0000	010642	2350F	0000	010653	2360F
0000	010664	2370F	0000	010675	2380F	0001	000223	241G	0001	000264	262G	0001	000265	265G
0001	000076	30L	0001	000776	300L	0001	001021	310L	0001	001044	320L	0001	000577	330G
0001	001064	330L	0001	001066	340L	0001	001106	350L	0001	000555	353G	0001	000675	356G
0001	001110	360L	0001	001122	365L	0001	001142	368L	0001	001166	370L	0001	001171	380L
0001	001174	390L	0001	000254	40L	0001	001176	400L	0001	001255	410L	0001	001303	420L
0001	001315	425L	0001	001335	426L	0001	001361	430L	0001	001364	440L	0001	001366	450L
0001	001410	460L	0001	001422	470L	0001	001443	472L	0001	001445	473L	0001	001457	474L
0001	001504	475L	0001	001511	480L	0001	001512	485L	0001	001537	490L	0001	001541	495L
0001	001546	510L	0001	001550	515L	0001	001603	520L	0001	001611	540L	0001	001663	550L
0001	001673	600L	0001	001705	653G	0001	001730	665G	0001	001770	702G	0001	002003	710G
0001	001741	710L	0001	002016	716G	0001	002031	724G	0001	002044	732G	0001	002057	740G
0001	002072	746G	0001	002103	810L	0001	002114	820L	0001	002125	830L	0001	002136	840L
0001	002147	850L	0001	002160	860L	0001	002170	900L	0000	R 010214	CR	0000	R 010227	CVF
0000	R 010226	CVO	0000	R 003114	DLCF	0000	R 002440	DLC0	0000	R 002375	EV	0000	R 006524	EVF
0000	R 010240	EVF1	0000	R 010234	EVF2	0000	R 006050	EVO	0000	R 010237	EV01	0000	R 010233	EV02
0000	R 010224	HVF	0000	P 010222	HVO	0000	I 010220	I	0000	I 010204	IDF	0000	I 010203	ID0
0000	010250	INPUT	0000	I 010236	ISITOK	0000	I 010221	J	0000	I 004244	JFC	0000	I 010232	JF1
0000	I 010245	JJ	0000	I 010244	JJJ	0000	I 003570	J00	0000	I 010231	J01	0000	I 010246	J1
0000	I 010247	J2	0000	I 010230	K	0000	R 000002	LG	0000	R 00521	LGF	0000	R 002372	LGF1
0000	R 000045	LGG	0000	R 002371	LGO1	0000	R 002326	MR	0000	R 002324	MRJ	0000	R 001651	MRL
0000	R 001175	MRV	0000	K 002373	MRV1	0000	R 002374	MRV2	0000	R 000001	MWF	0000	R 000000	MW0
0000	I 010242	NCOUNT	0000	I 010217	NPLANE	0000	R 010213	PC	0000	R 010210	RMF	0000	R 010207	RMO
0000	R 007464	T	0000	R 010225	TCF	0000	R 010223	TC0	0000	R 010243	TEST	0000	R 010206	TF

0000 R 007527 TG	0000 R 010241 TG1	0000 R 010235 TG2	0000 R 007414 TITLE1	0000 R 007440 TITLE2
0000 R 010205 TO	0000 R 007200 TP100	0000 R 007243 TP1000	0000 R 007306 TR100	0000 R 007351 TR1000
0000 R 010216 TSF	0000 R 010215 TSO	0000 R 010212 VF	0000 R 010211 VO	0000 R 005374 XCF
0000 R 004720 XC0				

```

00101      1*
00101      2*      C DECLARATION
00101      3*
00101      4*      REAL MW0,MWF,LG,LGO,LGF,MRV,MRL,MRJ,MR,LGO1,LGF1,MRV1,MRV2
00103      5*      DIMENSION LG(35),EV(35),DLCO(3,100),DLCF(3,100),JOO(3,100),
00103      6*          1      JF0(3,100),XC0(3,100),XCF(3,100),MRV(3,100),MRL(3,100),
00103      7*          2      LGO(3,100),LGF(3,100),EVO(3,100),EVF(3,100),MR(35),
00103      8*          3      TP100(35),TP1000(35),TR100(35),TR1000(35),TITLE1(20),
00103      9*          4      TITLE2(20),T(35),TG(3,100)
00104     10*      NAMELIST /INPUT/IDO, IDF, TO, TF, RM0, RMF, VO, VF, PC, CR, TSO, TSF,
00104     11*          1      MRJ,NPLANE
00105     12*      DATA LG/0.01,0.02,0.04,0.06,0.1,0.2,0.4,0.6,0.8,1.0,1.5,2.0,
00105     13*          1      3.0,4.0,5.0,6.0,7.0,8.0,9.0,10.0,13.0,15.0,17.0,
00105     14*          2      20.0,25.0,30.0,35.0,40.0,45.0,50.0,60.0,70.0,80.0,90.0,
00105     15*          3      100.0/
00107     16*      DATA EV/0.083,0.31,0.91,1.61,3.10,6.5,12.2,17.3,21.8,25.9,34.2,
00107     17*          1      41.5,52.2,60.0,66.0,70.5,74.5,77.8,80.5,82.7,87.8,90.2,
00107     18*          2      92.0,94.0,96.2,97.6,98.5,99.1,99.4,99.6,99.82,99.92,
00107     19*          3      99.96,99.98,99.99/
00111     20*      DATA MR/0.1,0.2,0.4,0.6,0.8,1.0,1.2,1.4,1.6,1.8,2.0,2.2,2.4,
00111     21*          1      2.6,2.8,3.0,3.2,3.4,3.6,3.8,4.0,4.5,5.0,5.5,6.0,7.0,8.0,
00111     22*          2      9.0,10.0,15.0,20.0,30.0,40.0,50.0,100.0/
00113     23*      DATA TP100/1421.0,1618.0,1844.0,1992.0,2125.0,2280.0,2712.0,
00113     24*          1      3587.0,4336.0,4922.0,5347.0,5632.0,5806.0,5905.0,
00113     25*          2      5959.0,5984.0,5990.0,5986.0,5974.0,5956.0,5936.0,
00113     26*          3      5873.0,5801.0,5725.0,5646.0,5482.0,5313.0,5137.0,
00113     27*          4      4957.0,4026.0,3257.0,2311.0,1774.0,1425.0,638.0/
00115     28*      DATA TP1000/1551.0,1817.0,2109.0,2289.0,2438.0,2586.0,2838.0,
00115     29*          1      3590.0,4364.0,5027.0,5555.0,5974.0,5254.0,6429.0,
00115     30*          2      6526.0,6575.0,6591.0,6589.0,6575.0,6551.0,6521.0,
00115     31*          3      6433.0,6330.0,6220.0,6109.0,5876.0,5637.0,5398.0,
00115     32*          4      5155.0,4055.0,3261.0,2311.0,1774.0,1425.0,673.0/
00117     33*      DATA TR100/1517.0,1708.0,1934.0,2102.0,2291.0,2554.0,3090.0,
00117     34*          1      4024.0,4769.0,5304.0,5651.0,5857.0,5955.0,6019.0,
00117     35*          2      6040.0,6044.0,6037.0,6020.0,6001.0,5975.0,5950.0,
00117     36*          3      5876.0,5797.0,5714.0,5630.0,5455.0,5275.0,5088.0,
00117     37*          4      4894.0,3909.0,3133.0,2204.0,1684.0,1348.0,592.0/
00121     38*      DATA TR1000/1672.0,1929.0,2213.0,2404.0,2584.0,2791.0,3131.0,
00121     39*          1      4037.0,4845.0,5498.0,5988.0,6314.0,6506.0,6607.0,
00121     40*          2      6652.0,6665.0,6658.0,6638.0,6611.0,6577.0,6541.0,
00121     41*          3      6436.0,6325.0,6208.0,6087.0,5839.0,5587.0,5329.0,
00121     42*          4      5074.0,3929.0,3135.0,2204.0,1684.0,1348.0,633.0/
00123     43*      C INPJT DATA
00123     44*      READ(5,1000) (TITLE1(I),I=1,20)
00123     45*      READ(5,1000) (TITLE2(I),I=1,20)
00123     46*      READ(5,INPUT)
00123     47*      DO 10 I=1,NPLANE
00123     48*      10
00123     49*      10

```

00137 50* DO 10 J=1,100 000034
 00142 51* XCO(I,J)=0.0 000034
 00143 52* XCF(I,J)=0.0 000035
 00144 53* DLCO(I,J)=0.0 000036
 00145 54* DLCF(I,J)=0.0 000037
 00146 55* J00(I,J)=J 000040
 00147 56* JF0(I,J)=J 000042
 00150 57* 10 CONTINUE 000052
 00153 58* 20 READ(5,1010,END=30) I,J,XCO(I,J),DLCO(I,J),J00(I,J), 000052
 00153 59* 1 XCF(I,J),DLCF(I,J),JF0(I,J) 000052
 00155 60* GO TO 20 000074
 00166 61* 30 WRITE(6,2000) 000076
 00170 62* WRITE(6,2010) 000102
 00172 63* WRITE(6,2020) (TITLE1(I),I=1,20) 000107
 00175 64* WRITE(6,2020) (TITLE2(I),I=1,20) 000122
 00200 65* WRITE(6,2030) 000132
 00202 66* WRITE(6,2040) PC,MRJ,CR,NPLANE 000137
 00210 67* WRITE(6,2050) ID0,T0,V0,RM0,TS0 000150
 00217 68* WRITE(6,2060) IDF,TF,VF,RMF,TSF 000162
 00225 69* WRITE(6,2070) 000174
 00230 70* DO 40 I=1,NPLANE 000205
 00233 71* WRITE(6,2080) I 000205
 00236 72* WRITE(6,2090) 000213
 00240 73* DO 40 J=1,100 000223
 00243 74* IF(XCO(I,J) .LE. 0.0 .AND. XCF(I,J) .LE. 0) GO TO 40 000223
 00245 75* WRITE(6,2100) J,XCO(I,J),DLCO(I,J),J00(I,J),XCF(I,J),DLCF(I,J), 000237
 00245 76* 1 JF0(I,J) 000237
 00256 77* 40 CONTINUE 000265
 00261 78* 000265
 00261 79* C INITIALIZATION 000265
 00261 80* 000265
 00261 81* DO 50 I=1,NPLANE 000265.
 00264 82* DO 50 J=1,100 000265
 00267 83* TG(I,J)=0.0 000265
 00270 84* MVR(I,J)=0.0 000265
 00271 85* MRL(I,J)=0.0 000266
 00272 86* LG0(I,J)=0.0 000267
 00273 87* LGF(I,J)=0.0 000270
 00274 88* EVO(I,J)=0.0 000271
 00275 89* EVF(I,J)=0.0 000272
 00276 90* 50 CONTINUE 000300
 00301 91* 000300
 00301 92* C PROPELLANT PROPERTY ASSIGNMENT 000300
 00301 93* 000300
 00301 94* GO TO (100,110),ID0 000300
 00302 95* 000310
 00302 96* C * L02 000310
 00302 97* 000310
 00302 98* 100 HVO=91.6 000310
 00303 99* TCO=278.0 000311
 00304 100* MW0=32.0 000313
 00305 101* GO TO 120 000315
 00306 102* 110 WRITE(6,2300) 000317
 00310 103* GO TO 900 000323
 00311 104* 120 GO TO (130,140,150),IDF 000325
 00312 105* 000335
 00312 106* C * PROPANE 000335

```

00312   107*          000335
00312   108*          130 HVF=183.0          000335
00313   109*          TCF=670.0          000336
00314   110*          MWF=44.0          000340
00315   111*          GO TO 160          000342
00316   112*          000344
00316   113*          C     * RP-1          000344
00316   114*          000344
00316   115*          140 HVF=125.0          000344
00317   116*          TCF=1218.0          000345
00320   117*          MWF=172.0          000347
00321   118*          GO TO 160          000351
00322   119*          150 WRITE(6,2310)      000353
00324   120*          GO TO 900          000357
00325   121*          000361
00325   122*          C     * LG COEFFICIENT 000361
00325   123*          000361
00325   124*          160 CVO=((PC/300.0)**0.66/CR**0.44)/((1.0-TO/TCO)**0.4*(HVO/140.0) 000361
00325   125*          1    **0.8*(MVO/100.0)**0.35*(RMO/0.003)**1.45*(V0/100.0)**0.75) 000361
00325   126*          CVF=((PC/300.0)**0.66/CR**0.44)/((1.0-TF/TCF)**0.4*(HVF/140.0) 000455
00325   127*          1    **0.8*(MWF/100.0)**0.35*(RMF/0.003)**1.45*(VF/100.0)**0.75) 000455
00327   128*          000577
00327   129*          C     * TEMPERATURE INTERPOLATION 000577
00327   130*          000577
00327   131*          DO 190 K=1,35          000577
00332   132*          IF(IDO .NE. 1) GO TO 110          000577
00334   133*          GO TO (170,180,150),IDF          000601
00335   134*          170 IF(PC .LT. 1000.0) GO TO 175          000612
00337   135*          T(K)=TP1000(K)          000613
00340   136*          GO TO 190          000615
00341   137*          175 T(K)=TP100(K)+((PC-100.0)/(1000.0-100.0))*(TP1000(K)-TP100(K)) 000617
00342   138*          GO TO 190          000626
00343   139*          180 IF(PC .LT. 1000.0) GO TO 185          000630
00345   140*          T(K)=TR1000(K)          000633
00346   141*          GO TO 190          000635
00347   142*          185 T(K)=TR100(K)+((PC-100.0)/(1000.0-100.0))*(TR1000(K)-TR100(K)) 000637
00350   143*          190 CONTINUE          000655
00352   144*          000655
00352   145*          C VAPORIZATION CALCULATION          000655
00352   146*          000655
00352   147*          DO 600 I=1,NPLANE          000655
00355   148*          DO 600 J=1,100          000675
00360   149*          J01=J00(I,J)          000675
00361   150*          JF1=JF0(I,J)          000677
00362   151*          IF(XCO(I,J) .LE. 0.0 .OR. XCF(I,J) .LE. 0.0) GO TO 510          000701
00364   152*          000715
00364   153*          C     * VAPORIZING GRIDS (BOTH OXIDIZER AND FUEL PRESENT) 000715
00364   154*          000715
00364   155*          C     ** FIRST TRIAL (BASFD ON LC AND NOT TG CORRECTED) 000715
00364   156*          000715
00364   157*          C     *** FIRST PLANE LG          000715
00364   158*          000715
00364   159*          LG01=CVO*DLC0(I,J)          000715
00365   160*          LGF1=CVF*DLCF(I,J)          000720
00366   161*          IF(I .EQ. 1) GO TO 320          000723
00370   162*          000731
00370   163*          C     ***SECOND OR THIRD PLANE LG          000731

```

00370	164*		000731
00370	165*	LG01=LG01+LG0(I-1,J01)	000731
00371	166*	LGF1=LGF1+LGF(I-1,JF1)	000733
00372	167*	IF(EVO(I-1,J01) .LT. 100.0 .AND. EVF(I-1,JF1) .LT. 100) GO TO 320	000735
00374	168*	IF(EVO(I-1,J01) .LT. 100.0) GO TO 300	000753
00376	169*	IF(EVF(I-1,JF1) .LT. 100.0) GO TO 310	000757
00400	170*	EVO2=100.0	000763
00401	171*	EVF2=100.0	000765
00402	172*	MRV2=888.0	000766
00403	173*	TG2=(TG(I-1,J01)+TG(I-1,JF1))/2.0	000770
00404	174*	GO TO 470	000774
00405	175*	300 TG2=TG(I-1,JF1)	000776
00406	176*	EVF2=100.0	001002
00407	177*	CALL SINTP(LG(1),EV(1),35,LG01,EVO2,ISITOK)	001004
00410	178*	IF(ISITOK .LT. 0) GO TO 810	001014
00412	179*	GO TO 470	001017
00413	180*	310 TG2=TG(I-1,J01)	001021
00414	181*	EVC2=100.0	001025
00415	182*	CALL SINTP(LG(1),EV(1),35,LGF1,EVF2,ISITOK)	001027
00416	183*	IF(ISITOK .LT. 0) GO TO 420	001037
00420	184*	GO TO 470	001042
00421	185*		001044
00421	186*	C *** VAPORIZATION	001044
00421	187*		001044
00421	188*	320 IF(LG01 .GT. 100.0) GO TO 330	001044
00423	189*	CALL SINTP(LG(1),EV(1),35,LG01,EVO1,ISITOK)	001047
00424	190*	IF(ISITOK .LT. 0) GO TO 810	001057
00426	191*	GO TO 340	001062
00427	192*	330 EVO1=100.0	001064
00433	193*	340 IF(LGF1 .GT. 100.0) GO TO 350	001066
00432	194*	CALL SINTP(LG(1),EV(1),35,LGF1,EVF1,ISITOK)	001071
00433	195*	IF(ISITOK .LT. 0) GO TO 820	001101
00435	196*	GO TO 360	001104
00436	197*	350 EVF1=100.0	001106
00437	198*	360 IF(I .GT. 1) GO TO 365	001110
00441	199*	MRV1=MRJ*(XCO(I,J)/XCF(I,J))*(EVO1/EVF1)	001111
00442	200*	GO TO 368	001120
00443	201*	365 MRV1=MRJ*(XCO(I,J)/XCF(I,J))*((EVO1-EVO(I-1,J01)) / 1 (EVF1-EVF(I-1,JF1)))	001122
00443	202*	368 IF(MRV1 .GE. MR(35)) GO TO 370	001122
00444	203*	IF(MRV1 .LE. MR(1)) GO TO 380	001142
00446	204*	CALL SINTP(MR(1),T(1),35,MRV1,TG1,ISITOK)	001145
00450	205*	IF(ISITOK .LT. 0) GO TO 830	001151
00451	206*	GO TO 390	001161
00453	207*	370 TG1=TS0	001164
00454	208*	GO TO 510	001166
00455	209*	380 TG1=TSF	001167
00456	210*	GO TO 510	001171
00457	211*	390 VCOJVT=1	001172
00458	212*		001174
00451	213*		001176
00461	214*	C ** SECOND TRIAL (BASED ON TG)	001176
00461	215*		001176
00461	216*	400 IF(I .EQ. 1) GO TO 410	001176
00463	217*		001177
00453	218*	C ** SECOND OR THIRD PLANE EV	001177
00453	219*		001177
00463	220*	EV02=((TG1+TG(I-1,J01)-2.0*TS0)/((5000.0-TS0)*2.0))	001177

00463 221* 1 *(EVO1-EVO(I-1,J01))+EVO(I-1,J01) 001177
 00464 222* IF(EVO2 .LT. 0.083) GO TO 540 001213
 00465 223* IF(EVO2 .GT. 100.0) EVO2=100.0 001222
 00470 224* EVF2=((TG1+TG(I-1,JF1)-2.0*TSF)/((5000.0-TSF)*2.0)) 001230
 00470 225* 1 *(EVF1-EVF(I-1,JF1))+EVF(I-1,JF1) 001230
 00471 226* IF(EVF2 .LT. 0.083) GO TO 540 001242
 00473 227* IF(EVF2 .GT. 100.0) EVF2=100.0 001245
 00475 228* GO TO 420 001253
 00475 229*
 00476 230* C *** FIRST PLANE EV 001255
 00476 231*
 00476 232* 410 EVO2=((TG1-TS0)/(5000.0-TS0))+EVO1 001255
 00477 233* EVF2=((TG1-TSF)/(5000.0-TSF))+EVF1 001261
 00500 234* IF(EVO2 .LT. 0.083 .OR. EVF2 .LT. 0.083) GO TO 515 001266
 00502 235*
 00502 236* C *** MRV2 AND TG2 001303
 00502 237*
 00502 238* 420 IF(I .GT. 1) GO TO 425 001303
 00504 239* MRV2=MRJ*(XCO(I,J)/XCF(I,J))*((EVO2/EVF2)
 00505 240* GO TO 428 001313
 00506 241* 425 MRV2=MRJ*(XCO(I,J)/XCF(I,J))*((EVO2-EVO(I-1,J01))/
 00506 242* 1 *(EVF2-EVF(I-1,JF1))) 001315
 00507 243* 428 IF(MRV2 .GE. MR(35)) GO TO 430 001335
 00511 244* IF(MRV2 .LE. MR(1)) GO TO 440 001340
 00513 245* CALL SINTP(MR(1),T(1),35,MRV2,TG2,ISITOK) 001344
 00514 246* IF(ISITOK .LT. 0) GO TO 840 001354
 00516 247* GO TO 450 001357
 00517 248* 430 TG2=TS0 001361
 00520 249* GO TO 450 001362
 00521 250* 440 TG2=TSF 001364
 00522 251*
 00522 252* C ** COMPARISON OF 1 AND 2 001366
 00522 253*
 00522 254* 450 TEST=ABS(TG2/TG1-1.0) 001366
 00523 255* IF(TEST .LE. 0.05) GO TO 470 001372
 00525 256*
 00525 257* C *** FURTHER ITERATION REQUIRED 001375
 00525 258*
 00525 259* IF(NCOUNT .LE. 10) GO TO 460 001375
 00527 260* WRITE(6,2320) 001401
 00531 261* GO TO 900 001406
 00532 262* 460 TG1=TG2 001410
 00533 263* EVO1=EVO2 001411
 00534 264* EVF1=EVF2 001413
 00535 265* NCOUNT=NCOUNT+1 001415
 00536 266* GO TO 400 001420
 00537 267*
 00537 268* C *** ITERATION COMPLETED 001422
 00537 269*
 00537 270* 470 EVO(I,J)=EVO2 001422
 00540 271* EVF(I,J)=EVF2 001423
 00541 272* MRV(I,J)=MRV2 001425
 00542 273* TG(I,J)=TG2 001427
 00543 274* IF(EVF2 .LT. 100.0) GO TO 473 001431
 00545 275* IF(EVO2 .GE. 100.0) GO TO 472 001434
 00547 276* MRL(I,J)=999.0 001437
 00550 277* GO TO 474 001441

00551 278* 472 MRL(I,J)=0.0 001443
 00552 279* GO TO 474 001443
 00553 280* 473 MRL(I,J)=MRJ*(XCO(I,J)/XCF(I,J))*((100.-EVO(I,J))/(100.-EVF(I,J))) 001445
 00554 281* 474 IF(EVO2 .LE. 0.0) GO TO 480 001457
 00556 282* IF(EVO2 .GE. 99.99) GO TO 475 001461
 00560 283* CALL SINTP(EV(1),LG(1),35,EVO2,LGO(I,J),ISITOK) 001465
 00561 284* IF(ISITOK .LT. 0) GO TO 850 001477
 00553 285* GO TO 485 001502
 00554 286* 475 LGO(I,J)=200.0 001504
 00565 287* EVO2=100.0 001505
 00566 288* GO TO 485 001507
 00557 289* 480 LGO(I,J)=0.0 001511
 00570 290* 485 IF(EVF2 .LE. 0.0) GO TO 490 001512
 00572 291* IF(EVF2 .GE. 99.99) GO TO 495 001514
 00574 292* CALL SINTP(EV(1),LG(1),35,EVF2,LGF(I,J),ISITOK) 001520
 00575 293* IF(ISITOK .LT. 0) GO TO 860 001532
 00577 294* GO TO 600 001535
 00580 295* 490 LGF(I,J)=0.0 001537
 00601 295* GO TO 600 001537
 00602 297* 495 LCF(I,J)=200.0 001541
 00603 298* EVF2=100.0 001542
 00604 299* GO TO 600 001544
 00605 300*
 00605 301* C * NONVAPORIZING GRIDS (EITHER OXIDIZER OR FUEL OR BOTH ABSENT) 001546
 00605 302*
 00605 303* 510 IF(I .GT. 1) GO TO 540 001546
 00607 304*
 00607 305* C ** FIRST PLANE 001550
 00607 305*
 00607 307* 515 EVO(I,J)=0.0 001550
 00610 308* EVF(I,J)=0.0 001550
 00611 309* LGO(I,J)=0.0 001551
 00612 310* LGF(I,J)=0.0 001552
 00613 311* IF(XCO(I,J) .LE. 0.0 .AND. XCF(I,J) .LE. 0.0) GO TO 600 001553
 00615 312* IF(XCF(I,J) .GT. XCO(I,J)) GO TO 520 001567
 00617 313*
 00617 314* C *** OXIDIZER PRESENT ONLY 001573
 00617 315*
 00617 315* TG(I,J)=TS0 001573
 00620 317* MRL(I,J)=999.0 001575
 00621 318* MRV(I,J)=888.0 001577
 00622 319* GO TO 600 001601
 00623 320*
 00623 321* C *** FUEL PRESENT ONLY 001603
 00623 322*
 00623 323* 520 TG(I,J)=TSF 001603
 00624 324* MRL(I,J)=0.0 001604
 00625 325* MRV(I,J)=888.0 001605
 00626 325* GO TO 600 001607
 00627 327*
 00627 328* C ** SECOND OR THIRD PLANE 001611
 00627 329*
 00627 330* 480 EVO(I,J)=EVO(I-1,J01) 001611
 00630 331* LVF(I,J)=LVF(I-1,JF1) 001615
 00631 332* LGO(I,J)=LGO(I-1,J01) 001623
 00632 333* LGF(I,J)=LGF(I-1,JF1) 001625
 00633 334* TG(I,J)=(TG(I-1,J01)+TG(I-1,JF1))/2.0 001627

00634 335* IF(XCO(I,J) .LE. 0.0 .AND. XCF(I,J) .LE. 0.0) GO TO 600 001633
 00636 336* IF(XCF(I,J) .GT. XCO(I,J)) GO TO 550 001647
 00640 337*
 00640 338* C *** OXIDIZER PRESENT ONLY 001653
 00640 339*
 00640 340* TG(I,J)=TG(I-1,J01) 001653
 00641 341* MRL(I,J)=999.0 001655
 00642 342* MRV(I,J)=888.0 001657
 00643 343* GO TO 600 001661
 00644 344*
 00644 345* C ** FUEL PRESENT ONLY 001663
 00644 346*
 00644 347* 550 TG(I,J)=TG(I-1, JF1) 001663
 00645 348* MRL(I,J)=0.0 001667
 00646 349* MRV(I,J)=888.0 001670
 00647 350* 600 CONTINUE 001705
 00652 351*
 00652 352* C PRINT OJTPUT 001705
 00652 353*
 00654 354* DO 800 I=1,NPLANE 001705
 00655 355* WRITE(6,2000)
 00657 356* WRITE(6,2010)
 00661 357* WRITE(6,2200) I
 00664 358* DO 800 JJJ=1,10 001730
 00667 359* IF(JJJ .NE. 6) GO TO 710 001730
 00671 360* WRITE(6,2210)
 00673 361* 710 JJ=(JJJ-1)*10 001741
 00674 362* J1=JJ+1 001744
 00675 363* J2=JJ+10 001750
 00676 364* WRITE(6,2220) J1,J2,(LGO(I,J),J=J1,J2) 001753
 00706 365* WRITE(6,2230) (LGF(I,J),J=J1,J2) 001773
 00714 366* WRITE(6,2240) (TG(I,J),J=J1,J2) 002006
 00722 367* WRITE(6,2250) (EVO(I,J),J=J1,J2) 002021
 00730 368* WRITE(6,2260) (EVF(I,J),J=J1,J2) 002034
 00735 369* WRITE(6,2270) (MRV(I,J),J=J1,J2) 002047
 00744 370* WRITE(6,2280) (MRL(I,J),J=J1,J2) 002062
 00752 371* 800 CONTINUE 002101
 00755 372* GO TO 900 002101
 00756 373*
 00756 374* C CUTSIDE TABLE RANGE 002103
 00756 375*
 00756 376* 810 WRITE(6,2330) I,J,LG01 002103
 00753 377* GO TO 900 002112
 00754 378* 820 WRITE(6,2340) I,J,LGF1 002114
 00771 379* GO TO 900 002123
 00772 380* 830 WRITE(6,2350) I,J,MRV1 002125
 00777 381* GO TO 900 002134
 01000 382* 840 WRITE(6,2360) I,J,MRV2 002136
 01005 383* GO TO 900 002145
 01006 384* 850 WRITE(6,2370) I,J,EVO2 002147
 01013 385* GO TO 900 002156
 01014 386* 860 WRITE(6,2380) I,J,EVF2 002160
 01021 387*
 01021 388* C FORMATS 002170
 01021 389*
 01021 390* 1000 FORMAT(20A4) 002170
 01022 391* 1010 FORMAT(2I10.2(2F10.4,I10)) 002170

01023	392*	2000 FORMAT(1H1,/38X,"A E R O J E T L I Q U I D R O C K E T C O M P	002170
01023	393*	1A V Y")	002170
01024	394*	2010 FORMAT(/25X,"PROPELLANT VAPORIZATION ANALYSIS BASED ON COLD-FLOW L	002170
01024	395*	1IQUID MASS DISTRIBUTION DATA")	002170
01025	396*	2020 FORMAT(10X,20A4)	002170
01026	397*	2030 FORMAT(/5X,"NAMELIST INPUT")	002170
01027	398*	2040 FORMAT(/10X,"PC(PSIA)=",F6.1,3X,"MRJ=",F5.3,3X,"CR=",F7.3,3X,	002170
01027	399*	1 "NPLANE=",I2)	002170
01030	400*	2050 FORMAT(/10X,"IDO=",I2,3X,"TO(R)=",F6.1,3X,"VO(FT/SEC)=",F6.1,3X,	002170
01030	401*	1 "RMO(IN)=",E10.4,3X,"TS0(R)=",F6.1)	002170
01031	402*	2060 FORMAT(/10X,"IDF=",I2,3X,"TF(R)=",F5.1,3X,"VF(FT/SEC)=",F6.1,3X,	002170
01031	403*	1 "RMF(IN)=",E10.4,3X,"TSF(R)=",F6.1)	002170
01032	404*	2070 FORMAT(/5X,"COLD-FLOW INPUT")	002170
01033	405*	2080 FORMAT(1H1,//30X,"PLANE NO.",I2)	002170
01034	406*	2090 FORMAT(/10X,"J",4X,"XCO",7X,"DLC0",6X,"J00",7X,	002170
01034	407*	1 "XCF",7X,"DLCF",6X,"JF0")	002170
01035	408*	2100 FORMAT(8X,I3,T14,F6.4*T26,F5.3*T36,I3,T46+F6.4*T56,F5.3*T66,I3)	002170
01036	409*	2200 FORMAT(10X,"PLANE NO.",I2)	002170
01037	410*	2210 FORMAT(1H1,////)	002170
01040	411*	2220 FORMAT(/1X,"J=",I2,1X,"TO",1X,I3,2X,"LG0 (IN)",3X,10(F7.5,2Y))	002170
01041	412*	2230 FORMAT(14X,"LGF (1)",3X,10(F7.3,3X))	002170
01042	413*	2240 FORMAT(14X,"TG (R)",6X,10(F6.1,4X))	002170
01043	414*	2250 FORMAT(14X,"EVG",9X,10(F6.2,4X))	002170
01044	415*	2260 FORMAT(14X,"EVF",9X,10(F6.2,4X))	002170
01045	416*	2270 FORMAT(14X,"MRV",9X,10(F6.2,4X))	002170
01046	417*	2280 FORMAT(14X,"MRL",5X,10(F6.2,4X))	002170
01047	418*	2300 FORMAT(/10X,"UNIDENTIFIABLE OXIDIZER")	002170
01050	419*	2310 FORMAT(/15X,"UNIDENTIFIABLE FULL")	002170
01051	420*	2320 FORMAT(/10X,"EXCEEDS 10 ITERATIONS")	002170
01052	421*	2330 FORMAT(/5X,"AT I=",I2,3X,"J=",I4,3X,"LG01=",F7.3)	002170
01053	422*	2340 FORMAT(/5X,"AT I=",I2,3X,"J=",I4,3X,"LGF1=",F7.3)	002170
01054	423*	2350 FORMAT(/5X,"AT I=",I2,3X,"J=",I4,3X,"MRV1=",F7.3)	002170
01055	424*	2360 FORMAT(/5X,"AT I=",I2,3X,"J=",I4,3X,"MRV2=",F7.3)	002170
01056	425*	2370 FORMAT(/5X,"AT I=",I2,3X,"J=",I4,3X,"EV02=",F7.3)	002170
01057	426*	2380 FORMAT(/5X,"AT I=",I2,3X,"J=",I4,3X,"EVF2=",F7.3)	002170
01060	427*		002170
01060	428*	900 STOP	002170
01061	429*	END	002173

END FOR

MAP,S,VAPOR

MAP 30R1V2-2 74R1-2 08/30/82 14:33:43

DEMAND INPUT IS ILLEGAL. SOURCE IMAGES IGNORED.

AFCM STATUS OF OUTPUT ELEMENT=UNKNOWN

QUARTER/THIRD WORD INSENSITIVE

ADDRESS LIMITS 001000 016605 7046 IBANK WORDS DECIMAL
040000 055360 6897 DBANK WORDS DECIMAL

STARTING ADDRESS 014250

SEGMENT \$MAIN\$	001000 016605	040000 055360			
VSWTC\$/FOR69	\$1)	001000 001032		27 JUL 76	14:02:51
VWBL\$(\$/FOR58	\$1)	001033 001221	\$0) 040000 040001 \$4) 040002 040053	36 AUG 76	13:42:47
VFIL\$(\$/FOR-E2	\$1)	001222 001337	\$0) 040054 040055 \$4) 040056 040130	6 AUG 76	13:42:16
VDEF\$/FOR-E2	\$1)	001340 001573	\$2) 040131 040150	7 SEP 76	11:45:58
VRND\$/FOR-E2	\$1)	001574 001655	\$2) 040151 040152	6 AUG 76	13:42:24
VCLSS\$/FOR-E3	\$1)	001656 002121	\$2) 040163 040212	23 MAR 76	14:51:32
VLIIV\$/FOR-E3	\$1)	002122 003700	\$2) 040213 040402	23 MAR 76	14:52:38
VFTCH\$/FOR-E2	\$1)	003701 004166	\$2) 040403 040416	27 JUL 76	13:58:56
VIVPT\$/FOR-E3	\$1)	004167 005575	\$2) 040417 040452	30 APR 76	16:45:16
VIVIV\$/FOR-E3	\$1)	005576 006035	\$2) 040453 040453	27 JUL 74	14:00:54
VI3JF\$/FOR-E2	\$1)	006036 C06075	\$2) 040454 040454	29 APR 74	13:47:55
VGNVT\$/FOR68	\$1)	006076 006317	\$2) 040455 040552	23 MAY 76	14:51:36
VOTIV\$/FOR-E3	\$1)	006320 006614	\$2) 040553 040556	16 APR 75	13:29:59
VBSBL\$/FOR-E3	\$1)	006615 006667	\$0) 040557 040557 \$4) 040560 040615	23 MAR 76	14:51:29
VUPDAS/FOR68	\$1)	006670 006723		16 JUL 72	21:41:26
NTAB\$/ISD			\$2) 040616 040655	23 MAR 76	14:53:06
VFCHK\$/FOR-E3	\$1)	006724 007714	\$2) 040656 041027 \$3) 007715 007715 \$4) 041030 041101	24 MAY 76	15:30:02
VICDR\$/FOR-E3	\$1)	007716 C10145	\$2) 041102 041251	24 MAY 76	19:57:04
V3FOO\$/ISD			\$2) 041252 043457	23 APR 74	14:51:07
V3OCV\$/FOR-E3	\$1)	010146 010276	\$2) 043460 043535	23 APR 74	14:51:23
VFTV\$/FOR-E2	\$1)	010277 010321		24 APR 74	13:47:54
VFMTS\$/FOR-E3	\$1)	010322 011204	\$2) 043536 043611	23 MAR 76	14:52:00
VOUT\$/FOR-E3	\$1)	011205 013002	\$2) 043612 043655	14 SEP 77	20:51:42
VOBDFS/FOR68	\$1)	013003 013043		16 JUL 72	21:41:08
FORCOM\$/FORFTN			\$2) 043657 043664	24 MAY 76	15:28:58
VINTR\$/FOR-E3	\$1)	013044 013203	\$2) 043665 043715	17 JAN 77	17:26:16
VERCOM\$/FOR-TE3	\$1)	013204 013263	\$2) 043716 043731	11 MAR 75	15:33:59
CRUB\$/SYS74-ISD				14 DEC 79	09:57:05
VERR\$/FOR-E3	\$1)	013264 013627	\$2) 043732 044122	16 APR 75	13:17:20
FORVC04\$/FOR-TE3			\$2) 044123 044132	14 MAY 75	15:29:07
VSTOP\$/FOR-TE3	\$1)	013630 013673	\$2) 044133 044141	17 JAN 77	13:40:51
VERPS\$/FOR-E3	\$1)	013674 014071	\$2) 044142 044213	17 APR 74	13:51:41
VIERR\$/FOR-E3	\$1)	014072 C14247	\$2) 044214 044334	24 MAY 74	15:57:15
SLAVES\$COMMON(COMMONBLOCK)					
VAPOR	\$1)	014250 016443	\$0) 044335 055324 \$2) BLANK\$COMMON	30 AUG 72	14:33:36

```
SUBROUTINE SINTP(U,V,N,X,Y,ISITOK)
DIMENSION U(N),V(N)
DO 1 I=2,N
J=I
IF (X.LT.U(1))GO TO 3
IF(X.GT.U(N))GO TO 3
IF((X-U(I))/(U(N)-U(1)))2,2,1
1 CONTINUE
2 Y=V(J-1)+(V(J)-V(J-1)*(X-U(J-1))/U(J)-U(J-1))
ISITOK=1
GO TO 10
3 WRITE(6,4)X,Y
4 FORMAT(2X,15HTABLE TOO SMALL,5X,3HX= ,F13.5,5X,3HY= ,F13.5)
ISITOK=-1
10 RETURN
END
```

A E R O J E T L I Q U I D R O C K E T C O M P A N Y

PROPELLANT VAPORIZATION ANALYSIS BASED ON COLD-FLOW LIQUID MASS DISTRIBUTION DATA

EDM LOL INJECTOR
TEST 171

NAMELIST INPUT

PC(PSIA)= 640 0 MRJ=2 800 CR=616 000 NPLANE= 3
IDO= 1 TO(R)= 200 0 VO(FT/SEC)= 44 0 RMO(IN)= 1186-02 TSO(R)= 270 0
IDF= 1 TF(R)= 584 0 VF(FT/SEC)= 71 0 RMF(IN)= 6430-03 TSF(R)= 665 0

COLD-FLOW INPUT

PLANE NO 1

J	XCO	DLCO	JOO	XCF	DLCF	JFO
25	0088	300	25	0023	300	25
26	0088	300	26	0125	300	26
35	0550	300	35	0130	300	35
36	0490	300	36	0023	300	36
44	0035	300	44	0110	300	44
45	2390	300	45	2150	300	45
46	2300	300	46	2720	300	46
47	0027	300	47	0079	300	47
54	0071	300	54	0150	300	54
55	1500	300	55	1530	300	55
56	1990	300	56	2380	300	56
57	0115	300	57	0180	300	57
67	0115	300	67	0057	300	67

PLANE NO 2

J	XCO	DLCO	JOO	XCF	DLCF	JFO
15	0109	800	25	0010	800	26
24	0150	800	35	0049	800	25
25	0260	800	35	0005	800	36
26	0097	800	26	0015	800	26
33	0050	800	44	0136	800	35
34	0380	800	44	0290	800	45
35	0630	800	45	0180	800	45
36	0220	800	36	0230	800	46
37	0017	800	47	0087	800	47
43	0067	800	54	0184	800	44
44	0840	800	45	0970	800	45
45	1930	800	45	2520	800	46
46	0800	800	46	1460	800	56
47	0067	800	46	0252	800	57
53	0109	800	55	0155	800	54
54	0881	800	55	0580	800	55
55	1180	800	56	0730	800	55
56	0990	800	56	0730	800	56
57	0180	800	46	0220	800	56
63	0100	800	55	0058	800	54
64	0190	800	55	0078	800	55
66	0190	800	56	0087	800	56
67	0230	800	57	0130	800	56
77	0100	800	56	0029	800	67

PLANE NO 3

J	XCO	DLCO	JOO	XCF	DLCF	JFO
23	0027	1 300	24	0085	1 300	33
24	0081	1 300	24	0061	1 300	24
25	0162	1 300	25	0006	1 300	25
26	0140	1 300	26	0006	1 300	26
33	0027	1 300	24	0097	1 300	33
34	0162	1 300	34	0195	1 300	34
35	0324	1 300	35	0182	1 300	35
36	0275	1 300	35	0201	1 300	36
37	0113	1 300	26	0067	1 300	26
38	0027	1 300	37	0109	1 300	37
43	0049	1 300	33	0128	1 300	43
44	0300	1 300	44	0400	1 300	44
45	0780	1 300	45	1030	1 300	45
46	0780	1 300	46	1370	1 300	45
47	0300	1 300	36	0730	1 300	46
48	0054	1 300	37	0230	1 300	46
53	0081	1 300	43	0122	1 300	53
54	0460	1 300	54	0400	1 300	44
55	0970	1 300	45	0730	1 300	55
56	0998	1 300	56	0850	1 300	56
57	0570	1 300	46	0580	1 300	46
58	0119	1 300	47	0210	1 300	46
63	0092	1 300	53	0073	1 300	53
64	0370	1 300	54	0190	1 300	54
65	0410	1 300	55	0150	1 300	55
66	0300	1 300	55	0150	1 300	66
67	0410	1 300	56	0210	1 300	57
68	0210	1 300	57	0160	1 300	47
73	0086	1 300	63	0043	1 300	63
74	0108	1 300	64	0036	1 300	64
77	0081	1 300	66	0030	1 300	67
78	0170	1 300	67	0085	1 300	57
88	0076	1 300	66	0024	1 300	77
89	0070	1 300	77	0128	1 300	67

C-19

A E R O J E T L I Q U I D R O C K E T C O M P A N Y
P R O P E L L A N T V A P O R I Z A T I O N A N A L Y S I S B A S E D O N C O L D - F L O W L I Q U I D M A S S D I S T R I B U T I O N D A T A

PLANE NO 1

J= 1 TO 10	LGD (IN)	000	000	000	000	000	000	000	000	000	000
	LGF (IN)	000	000	000	000	000	000	000	000	000	000
	TG (R)	0	0	0	0	0	0	0	0	0	0
	EVD	00	00	00	00	00	00	00	00	00	00
	EVF	00	00	00	00	00	00	00	00	00	00
	MRV	00	00	00	00	00	00	00	00	00	00
	MRL	00	00	00	00	00	00	00	00	00	00
J=11 TO 20	LGD (IN)	000	000	000	000	000	000	000	000	000	000
	LGF (IN)	000	000	000	000	000	000	000	000	000	000
	TG (R)	0	0	0	0	0	0	0	0	0	0
	EVD	00	00	00	00	00	00	00	00	00	00
	EVF	00	00	00	00	00	00	00	00	00	00
	MRV	00	00	00	00	00	00	00	00	00	00
	MRL	00	00	00	00	00	00	00	00	00	00
J=21 TO 30	LGD (IN)	000	000	000	000	767	670	000	000	000	000
	LGF (IN)	000	000	000	000	923	791	000	000	000	000
	TG (R)	0	0	0	0	5233 5	4744 8	0	0	0	0
	EVD	00	00	00	00	21 06	18 88	00	00	00	00
	EVF	00	00	00	00	24 32	21 59	00	00	00	00
	MRV	00	00	00	00	9 28	1 72	00	00	00	00
	MRL	00	00	00	00	11 17	2 04	00	00	00	00
J=31 TO 40	LGD (IN)	000	000	000	000	727	000	000	000	000	000
	LGF (IN)	000	000	000	000	868	000	000	000	000	000
	TG (R)	0	0	0	0	5014 5	270 0	0	0	0	0
	EVD	00	00	00	00	20 16	00	00	00	00	00
	EVF	00	00	00	00	23 19	00	00	00	00	00
	MRV	00	00	00	00	10 30	888 00	00	00	00	00
	MRL	00	00	00	00	12 31	999 00	00	00	00	00
J=41 TO 50	LGD (IN)	000	000	000	274	979	838	280	000	000	000
	LGF (IN)	000	000	000	277	1 238	1 020	285	000	000	000
	TG (R)	0	0	0	2374 6	6241 4	5546 4	2420 4	0	0	0
	EVD	00	00	00	8 60	25 46	22 58	8 78	00	00	00
	EVF	00	00	00	8 69	29 85	26 23	8 92	00	00	00
	MRV	00	00	00	88	2 66	2 04	94	00	00	00
	MRL	00	00	00	89	3 31	2 48	96	00	00	00

A E R O J E T L I Q U I D R O C K E T C O M P A N Y
P R O P E L L A N T V A P O R I Z A T I O N A N A L Y S I S B A S E D O N C O L D - F L O W L I Q U I D M A S S D I S T R I B U T I O N D A T A

PLANE NO 2

J= 1 TO 10	LGO (IN)	000	000	000	000	000	000	000	000	000	000
	LGF (IN)	000	000	000	000	000	000	000	000	000	000
	TG (R)	0	0	0	0	0	0	0	0	0	0
	EVO	00	00	00	00	00	00	00	00	00	00
	EVF	00	00	00	00	00	00	00	00	00	00
	MRV	00	00	00	00	00	00	00	00	00	00
	MRL	00	00	00	00	00	00	00	00	00	00
J=11 TO 20	LGO (IN)	000	000	000	000	1 673	000	000	000	000	000
	LGF (IN)	000	000	000	000	1 600	000	000	000	000	000
	TG (R)	0	0	0	0	2234 0	0	0	0	0	0
	EVO	00	00	00	00	36 73	00	00	00	00	00
	EVF	00	00	00	00	35 66	00	00	00	00	00
	MRV	00	00	00	00	31 43	00	00	00	00	00
	MRL	00	00	00	00	30 01	00	00	00	00	00
J=21 TO 30	LGO (IN)	000	000	000	2 823	727	2 192	000	000	000	000
	LGF (IN)	000	000	000	3 580	000	2 586	000	000	000	000
	TG (R)	0	0	0	5591 5	5014 5	3807 2	0	0	0	0
	EVO	00	00	00	50 30	20 16	43 55	00	00	00	00
	EVF	00	00	00	56 72	00	47 77	00	00	00	00
	MRV	00	00	00	7 60	888 00	16 51	00	00	00	00
	MRL	00	00	00	9 84	999 00	19 57	00	00	00	00
J=31 TO 40	LGO (IN)	000	000	367	329	3 422	000	881	000	000	000
	LGF (IN)	000	000	1 398	3 841	4 202	1 020	867	000	000	000
	TG (R)	0	0	1945 0	2195 3	5318 4	5546 4	2131 6	0	0	0
	EVO	00	00	11 25	10 17	55 49	00	23 46	00	00	00
	EVF	00	00	32 51	58 76	61 21	26 23	23 17	00	00	00
	MRV	00	00	36	64	8 88	888 00	55	00	00	00
	MRL	00	00	1 35	7 99	11 25	00	55	00	00	00
J=41 TO 50	LGO (IN)	000	000	631	3 605	3 483	2 535	2 179	000	000	000
	LGF (IN)	000	000	521	4 469	3 763	2 945	1 808	000	000	000
	TG (R)	0	0	2791 8	5831 8	5593 0	3603 5	2339 4	0	0	0
	EVO	00	00	18 01	56 92	55 97	47 22	43 42	00	00	00
	EVF	00	00	15 29	62 82	58 15	51 61	38 70	00	00	00
	MRV	00	00	1 20	2 20	2 06	1 40	84	00	00	00
	MRL	00	00	99	2 81	2 26	1 67	69	00	00	00

A E R O J E T L I Q U I D R O C K E T C O M P A N Y
P R O P E L L A N T V A P O R I Z A T I O N A N A L Y S I S B A S E D O N C O L D - F L O W L I Q U I D M A S S D I S T R I B U T I O N D A T A

PLANE NO 3

J= 1 TO 10	LGO (IN)	000	000	000	000	000	000	000	000	000	000
	LGF (IN)	000	000	000	000	000	000	000	000	000	000
	TG (R)	0	0	0	0	0	0	0	0	0	0
	EVO	00	00	00	00	00	00	00	00	00	00
	EVF	00	00	00	00	00	00	00	00	00	00
	MRV	00	00	00	00	00	00	00	00	00	00
	MRL	00	00	00	00	00	00	00	00	00	00
J=11 TO 20	LGO (IN)	000	000	000	000	1 673	000	000	000	000	000
	LGF (IN)	000	000	000	000	1 600	000	000	000	000	000
	TG (R)	0	0	0	0	2234 0	0	0	0	0	0
	EVO	00	00	00	00	36 73	00	00	00	00	00
	EVF	00	00	00	00	35 66	00	00	00	00	00
	MRV	00	00	00	00	00	00	00	00	00	00
	MRL	00	00	00	00	00	00	00	00	00	00
J=21 TO 30	LGO (IN)	000	000	4 592	6 982	1 334	3 357	000	000	000	000
	LGF (IN)	000	000	1 497	8 734	484	3 758	000	000	000	000
	TG (R)	0	0	4527 4	6343 3	270 0	1244 0	0	0	0	0
	EVO	00	00	63 55	74 43	31 45	54 98	00	00	00	00
	EVF	00	00	34 15	79 78	14 34	58 11	00	00	00	00
	MRV	00	00	1 66	3 47	165 80	61 81	00	00	00	00
	MRL	00	00	49	4 70	60 50	70 22	00	00	00	00
J=31 TO 40	LGO (IN)	000	000	4 107	369	7 295	7 329	5 346	1 773	000	000
	LGF (IN)	000	000	1 457	3 874	8 985	6 497	6 350	1 708	000	000
	TG (R)	0	0	3632 4	2041 5	6177 1	6287 7	6218 8	2249 5	0	0
	EVO	00	00	60 64	11 32	75 47	75 58	67 56	38 19	00	00
	EVF	00	00	33 49	59 02	80 46	72 49	71 90	37 24	00	00
	MRV	00	00	1 41	45	4 68	3 99	4 44	71	00	00
	MRL	00	00	46	5 03	6 26	3 40	5 45	68	00	00
J=41 TO 50	LGO (IN)	000	000	1 219	7 344	7 158	2 940	1 992	1 182	000	000
	LGF (IN)	000	000	1 634	9 042	8 268	5 522	4 522	3 617	000	000
	TG (R)	0	0	2369 6	5405 8	5524 2	2798 3	2280 2	1914 6	0	0
	EVO	00	00	29 53	75 63	75 02	51 56	41 39	28 92	00	00
	EVF	00	00	36 16	80 59	78 52	68 35	63 13	57 02	00	00
	MRV	00	00	88	1 97	2 03	1 20	75	33	00	00
	MRL	00	00	1 18	2 64	2 47	2 44	-1 83	1 09	00	00

J=51	TO	60	LGO (IN)	000	000	954	8 156	7 599	7 897	5 581	2. 577	000	000	
			LGF (IN)	000	000	4 636	9 809	10 298	9 922	6 577	3 750	000	000	
			TG (R)	0	0	2260 9	6342 3	6346 5	6343 7	6214 5	3200 3	0	0	
			EVO	00	00	24 96	78 22	76 48	77 46	68 61	47 68	00	00	
			EVF	00	00	63 82	82 28	83 21	82 53	72 81	58 05	00	00	
			MRV	00	00	73	3 06	3 42	3 09	2 59	1 30	00	00	
			MRL	00	00	3 86	3 96	5 21	4 24	3 18	1. 98	00	00	
J=61	TO	70	LGO (IN)	000	000	7 871	8 000	7 491	7 693	7 750	7 243	000	000	
			LGF (IN)	000	000	8 084	10 062	9 716	9 194	8 744	4 641	000	000	
			TG (R)	0	0	6341 2	6094 7	5697 7	6058 0	6065 9	6234 8	0	0	
			EVO	00	00	77 38	77 80	76 12	76 79	76 97	75 30	00	00	
			EVF	00	00	78 03	82 81	82 08	80 93	79 81	63 84	00	00	
			MRV	00	00	3 50	5 12	7 10	5 31	5 27	4 33	00	00	
			MRL	00	00	3 63	7 04	10 20	6 82	6 23	2. 51	00	00	
C-25	J=71	TO	80	LGO (IN)	000	000	7. 645	7 329	000	000	7 232	7 130	000	000
			LGF (IN)	000	000	7 648	9 042	000	000	9 253	8 756	000	000	
			TG (R)	0	0	6002 5	5533 1	0	0	5714 2	6069 2	0	0	
			EVO	00	00	76 63	75 58	00	00	75 26	74. 93	00	00	
			EVF	00	00	76 64	80 59	00	00	81 06	79 84	00	00	
			MRV	00	00	5 60	7 88	00	00	7 02	5 26	00	00	
			MRL	00	00	5 60	10 57	00	00	9 87	6 97	00	00	
J=81	TO	90	LGO (IN)	000	000	000	000	000	000	000	7 087	5 719	000	
			LGF (IN)	000	000	000	000	000	000	000	8 513	7 767	000	
			TG (R)	0	0	0	0	0	0	0	5427 4	3493 7	0	
			EVO	00	00	00	00	00	00	00	74 79	69 23	00	
			EVF	00	00	00	00	00	00	00	79 18	77 03	00	
			MRV	00	00	00	00	00	00	00	8 37	1 38	00	
			MRL	00	00	00	00	00	00	00	10 74	2 05	00	
J=91	TO	100	LGO (IN)	000	000	000	000	000	000	000	000	000	000	
			LGF (IN)	000	000	000	000	000	000	000	000	000	000	
			TG (R)	0	0	0	0	0	0	0	0	0	0	
			EVO	00	00	00	00	00	00	00	00	00	00	
			EVF	00	00	00	00	00	00	00	00	00	00	
			MRV	00	00	00	00	00	00	00	00	00	00	
			MRL	00	00	00	00	00	00	00	00	00	00	

^=QT VAPOR

D. VAPORIZATION ANALYSIS INPUT DATA

PLANE NO 1

OFO TRIPLET

J	XCO	DLCO	JOO	XCF	DLCF	JFO
45	1159	300	45	0132	300	45
46	2567	300	46	7417	300	46
56	6123	300	56	2384	300	56

PLANE NO 2 OFO TRIPLET

J	XCO	DLCO	JOO	XCF	DLCF	JFO
43	0388	800	45	0000	800	43
44	0640	800	45	0083	800	45
45	0582	800	46	0647	800	46
46	1477	800	46	5304	800	46
47	0111	800	46	0165	800	46
55	0092	800	45	0041	800	45
56	1893	800	56	2342	800	56
57	2401	800	56	0964	800	46
58	0656	800	56	0028	800	46
59	0777	800	45	0096	800	56
60	0785	800	56	0138	800	46
63	0379	800	56	0028	800	46

PLANE NO 3

OFO TRIPLET

J	XCO	DLCO	JOO	XCF	DLCF	JFO
34	0066	1 300	45	0163	1 300	46
37	0000	1 300	37	0110	1 300	47
41	0516	1 300	42	0041	1 300	44
42	0308	1 300	43	0218	1 300	45
43	0220	1 300	44	0709	1 300	46
44	0934	1 300	45	3266	1 300	46
45	0439	1 300	45	1008	1 300	46
46	0110	1 300	46	0245	1 300	46
53	0036	1 300	54	0056	1 300	55
54	0115	1 300	55	0463	1 300	46
55	0035	1 300	56	0004	1 300	46
56	0934	1 300	56	0817	1 300	57
57	0142	1 300	57	0041	1 300	58
63	0093	1 300	54	0109	1 300	56
64	0417	1 300	55	0354	1 300	56
65	1285	1 300	55	0517	1 300	56
66	1580	1 300	56	0417	1 300	56
67	0939	1 300	57	0068	1 300	56
68	0280	1 300	57	0007	1 300	68
73	0055	1 300	65	0395	1 300	56
74	0143	1 300	65	0110	1 300	56
75	0297	1 300	66	0082	1 300	66
76	0341	1 300	66	0068	1 300	67
77	0176	1 300	67	0014	1 300	68
83	0000	1 300	83	0110	1 300	56

D-3

PLANE NO. 1

TLOL

J	XCO	DLCO	JOO	XCF	DLCF	JFO
35	.0230	.300	35	.0017	.300	35
36	.0100	.300	36	.0010	.300	36
45	.1900	.300	45	.0086	.300	45
46	.1370	.300	46	.0140	.300	46
55	.2370	.300	55	.4450	.300	55
56	.2870	.300	56	.2660	.300	56
65	.0190	.300	65	.1120	.300	65
66	.0510	.300	66	.1200	.300	66
76	.0042	.300	76	.0076	.300	76

PLANE NO. 2

TLOL

J	XCO	DLCO	JOO	XCF	DLCF	JFO
25	.0150	.800	35	.0000	.800	35
35	.0360	.800	45	.0017	.800	35
36	.0500	.800	36	.0000	.800	36
37	.0092	.800	36	.0008	.800	36
45	.0540	.800	45	.0160	.800	45
46	.1620	.800	46	.0130	.800	46
47	.0170	.800	46	.0049	.800	46
55	.0870	.800	55	.1320	.800	55
56	.2460	.800	56	.3650	.800	56
57	.0310	.800	56	.0210	.800	56
65	.0440	.800	55	.0660	.800	55
66	.0960	.800	66	.2250	.800	66
67	.0530	.800	66	.0250	.800	66
75	.0060	.800	65	.0117	.800	65
76	.0007	.800	76	.0160	.800	76
77	.0210	.800	76	.0180	.800	76

	PLANE NO. 3			TLOL		
J	XCO	DLC0	JOC	XCF	DLCF	JFO
25	.0150	1.300	25	.0000	1.300	25
26	.0170	1.300	36	.0000	1.300	26
35	.0320	1.300	35	.0031	1.300	35
36	.0650	1.300	46	.0008	1.300	46
37	.0190	1.300	36	.0016	1.300	47
45	.0370	1.300	45	.0250	1.300	45
46	.1090	1.300	46	.0280	1.300	56
47	.0330	1.300	46	.0110	1.300	56
54	.0058	1.300	55	.0050	1.300	55
55	.0620	1.300	55	.0970	1.300	55
56	.1570	1.300	56	.2730	1.300	56
57	.0460	1.300	56	.0360	1.300	56
64	.0062	1.300	65	.0044	1.300	65
65	.0460	1.300	65	.0670	1.300	65
66	.0990	1.300	66	.2310	1.300	66
67	.0730	1.300	56	.0520	1.300	57
68	.0088	1.300	66	.0053	1.300	57
74	.0050	1.300	75	.0055	1.300	75
75	.0140	1.300	75	.0170	1.300	75
76	.0046	1.300	76	.0230	1.300	76
77	.0370	1.300	66	.0310	1.300	67
78	.0140	1.300	66	.0110	1.300	67
87	.0045	1.300	76	.0064	1.300	77
88	.0120	1.300	76	.0078	1.300	77

		PLANE NO	1		EDM-LOL	
J	XCO	DLCO	JOO	XCF	DLCF	JFO
25	0058	300	25	0023	300	25
26	0058	300	26	.0125	.300	26
27	0150	300	35	0130	300	35
28	0450	300	50	0023	300	36
29	0035	300	44	.0110	300	44
30	2390	300	45	.2150	300	45
31	2300	300	46	2720	.300	46
32	0027	300	47	0079	300	47
33	4571	200	54	0150	300	54
34	1500	300	55	1530	.300	55
35	1470	300	56	2380	300	56
36	0115	300	57	.0180	300	57
37	0115	300	57	0057	300	57

PLANE NO 2

EDM-LOL

J	XCO	DLCO	JOO	XCF	DLCF	JFO
15	0109	800	25	. 0010	. 800	26
24	0150	800	35	. 0049	. 800	25
25	0260	800	35	. 0005	. 800	36
26	0097	800	26	. 0015	. 800	26
29	0050	800	44	0136	800	35
31	0380	800	44	0290	. 800	45
35	0830	800	45	0180	. 800	45
36	0120	800	36	0230	. 800	46
37	0017	800	47	0087	800	47
43	0067	800	54	0184	800	44
44	0440	800	45	0970	800	45
45	1930	800	45	2520	. 800	46
46	0800	800	46	1460	. 800	56
47	0557	800	46	0252	800	57
53	0107	800	55	0155	800	54
54	0881	800	55	0580	. 800	55
55	1120	800	56	0730	800	55
56	0440	800	56	0730	800	56
57	0180	800	46	0220	. 800	56
58	0100	800	55	0058	800	54
59	0190	800	55	0078	800	55
60	0120	800	55	0087	800	56
67	0230	800	57	0130	800	56
77	0100	800	56	0029	800	67

		PLANE NO	3		EDM-LOL	
J	XCO	DLCO	JOO	XCF	DLCF	JFO
23	0027	1 300	24	0085	1. 300	33
24	0051	1 300	24	0061	1. 300	24
25	0142	1 300	25	0006	1 300	25
26	0140	1 300	26	0006	1 300	26
27	0027	1 300	24	0097	1. 300	33
28	0162	1 300	34	0195	1 300	34
29	0324	1 300	35	0182	1. 300	35
30	0275	1 300	35	0201	1 300	36
31	0113	1 300	26	. 0067	1 300	26
32	0027	1 300	37	0109	1 300	37
33	0149	1 300	33	0123	1 300	43
34	0100	1 300	44	0400	1 300	44
35	0763	1 300	45	1030	1 300	45
36	0760	1 300	46	1370	1 300	45
37	0350	1 300	36	0730	1 300	46
38	0054	1 300	37	0230	1 300	46
39	0061	1 300	43	0122	1. 300	53
40	0460	1 300	54	0400	1 300	44
41	0470	1 300	45	0730	1 300	55
42	0492	1 300	56	0850	1 300	56
43	0570	1 300	46	0580	1 300	46
44	0119	1 300	47	0210	1. 300	46
45	0092	1 300	53	0073	1 300	53
46	0370	1 300	54	0190	1 300	54
47	0410	1 300	55	0150	1 300	55
48	0300	1 300	55	0150	1. 300	66
49	0410	1 300	56	0210	1. 300	57
50	0210	1 300	57	0160	1. 300	47
51	0086	1 300	63	0043	1. 300	63
52	0108	1 300	64	0036	1 300	64
53	0081	1 300	66	0030	1. 300	67
54	0170	1 300	67	0085	1 300	57
55	0076	1 300	66	0024	1 300	77
56	0070	1 300	77	0128	1. 300	67

PLANE NO. 1

PAT

J	XCO	DLCO	J00	XCF	DLCF	JFO
35	.0000	.300	35	.0690	.300	35
36	.0000	.300	36	.0320	.300	36
44	.0270	.300	44	.0000	.300	44
45	.3270	.300	45	.2010	.300	45
46	.1410	.300	46	.1500	.300	46
47	.0220	.300	47	.0000	.300	47
53	.0120	.300	53	.0000	.300	53
54	.0460	.300	54	.0000	.300	54
55	.2020	.300	55	.2440	.300	55
56	.1410	.300	56	.1780	.300	56
57	.0240	.300	57	.0000	.300	57
65	.0094	.300	65	.0600	.300	65
66	.0674	.300	66	.0390	.300	66

PLANE NO. 2

PAT

J	XCO	DLCO	J00	XCF	DLCF	JF0
25	.0000	.800	35	.0134	.800	35
26	.0000	.800	36	.0210	.800	36
35	.0350	.800	45	.0450	.800	35
36	.0240	.800	46	.0740	.800	36
37	.0070	.800	47	.0120	.800	36
44	.0370	.800	44	.0054	.800	45
45	.2040	.800	45	.2213	.800	45
46	.3180	.800	46	.2358	.800	46
47	.0870	.800	47	.1161	.800	46
48	.0210	.800	47	.0000	.800	48
53	.0130	.800	53	.0000	.800	53
54	.0250	.800	54	.0027	.800	55
55	.0400	.800	55	.0530	.800	55
56	.0840	.800	56	.1070	.800	56
57	.0330	.800	57	.0400	.800	56
58	.0130	.800	57	.0000	.800	58
65	.0094	.800	65	.0103	.800	65
66	.0067	.800	66	.0290	.800	66

PLANE NO. 3

PAT

J	XCO	DLC0	J00	XCF	DLCF	JF0
25	.0000	1.300	25	.0130	1.300	25
26	.0000	1.300	26	.0110	1.300	26
34	.0260	1.300	35	.0240	1.300	35
35	.0440	1.300	35	.0480	1.300	35
36	.0182	1.300	36	.0280	1.300	36
37	.0078	1.300	37	.0130	1.300	37
43	.0190	1.300	44	.0022	1.300	44
44	.0770	1.300	45	.0632	1.300	45
45	.1970	1.300	45	.1902	1.300	45
46	.1640	1.300	46	.1640	1.300	46
47	.0550	1.300	47	.0830	1.300	47
48	.0170	1.300	48	.0031	1.300	47
53	.0180	1.300	53	.0022	1.300	54
54	.0330	1.300	54	.0280	1.300	55
55	.0840	1.300	55	.0810	1.300	55
56	.1680	1.300	56	.1030	1.300	56
57	.0380	1.300	57	.0480	1.300	57
58	.0120	1.300	58	.0020	1.300	57
65	.0055	1.300	65	.0190	1.300	65
66	.0055	1.300	66	.0240	1.300	66

INJECTOR	TEST NO	PC	MRJ	CR	NPLANE	IDO	IDF	TO	TF	VO	VF	RMO	RMF	TSO	TSF
OFO	101	475	2.40	490	3	1	2	208	520	80	91	2.924×10^{-4}	6.797×10^{-4}	255	1218
OFO	105	480	2.80	251	3	1	2	185	510	112	116	2.716×10^{-4}	5.714×10^{-4}	256	1218
OFO	106	480	2.80	251	3	1	2	185	510	112	116	2.716×10^{-4}	5.714×10^{-4}	256	1218
OFO	109	475	2.40	490	3	1	2	208	520	80	91	2.924×10^{-4}	6.797×10^{-4}	255	1218
OFO	110	480	2.70	176	3	1	2	205	525	162	164	1.892×10^{-4}	4.316×10^{-4}	256	1218
OFO	111	480	2.70	176	3	1	2	205	525	162	164	1.892×10^{-4}	4.316×10^{-4}	256	1218
OFO	116	1500	2.60	963	3	1	2	205	510	95	100	2.925×10^{-4}	6.416×10^{-4}	278	1218
TLOL	120	135	2.35	122	3	1	2	199	505	46	58	1.495×10^{-3}	2.889×10^{-3}	212	1100
TLOL	121	310	2.80	212	3	1	2	227	491	55	51	1.108×10^{-3}	3.347×10^{-3}	245	1210
TLOL	122	800	2.75	349	3	1	2	188	503	82	92	1.090×10^{-3}	2.131×10^{-3}	278	1218
TLOL	123	475	2.65	270	3	1	2	209	498	78	83	9.920×10^{-4}	2.354×10^{-3}	255	1218
TLOL	124	475	2.65	270	3	1	2	209	498	78	83	9.920×10^{-4}	2.354×10^{-3}	255	1218
TLOL	127	250	2.85	212	3	1	2	189	489	45	48	1.621×10^{-3}	3.484×10^{-3}	222	1180
TLOL	128	400	3.00	251	3	1	2	188	493	62	62	1.311×10^{-3}	2.900×10^{-3}	250	1218
TLOL	129	800	2.75	349	3	1	2	188	503	82	92	1.090×10^{-3}	2.131×10^{-3}	278	1218
TLOL	130	135	2.50	176	3	1	1	192	505	24	64	2.444×10^{-3}	1.164×10^{-3}	212	530
TLOL	131	290	2.65	270	3	1	1	185	502	44	80	1.693×10^{-3}	1.009×10^{-3}	238	595
TLOL	132	540	3.00	349	3	1	1	186	504	61	99	1.365×10^{-3}	8.730×10^{-4}	260	655
TLOL	133	790	2.80	428	3	1	1	186	505	40	122	1.803×10^{-3}	7.600×10^{-4}	278	666
EDM-LOL	157	800	2.80	349	3	1	1	190	506	89	131	8.380×10^{-4}	5.660×10^{-4}	278	666
EDM-LOL	158	560	2.85	322	3	1	1	180	488	72	101	9.640×10^{-4}	7.110×10^{-4}	263	645
EDM-LOL	159	295	2.90	212	3	1	1	185	500	61	85	1.075×10^{-3}	7.570×10^{-4}	237	595
EDM-LOL	160	150	2.80	176	3	1	1	210	490	52	68	1.000×10^{-3}	9.230×10^{-4}	215	540
EDM-LOL	161	800	2.90	349	3	1	1	185	520	93	133	8.140×10^{-4}	5.370×10^{-4}	278	666
EDM-LOL	162	550	2.95	322	3	1	1	195	521	76	104	8.560×10^{-4}	6.310×10^{-4}	263	640
EDM-LOL	164	290	2.90	212	3	1	1	195	538	64	92	9.570×10^{-4}	6.500×10^{-4}	238	595
EDM-LOL	165	800	2.85	428	3	1	1	194	607	84	144	7.950×10^{-4}	3.530×10^{-4}	278	666
EDM-LOL	168	550	2.90	349	3	1	1	184	617	67	122	1.011×10^{-3}	3.680×10^{-4}	263	640
EDM-LOL	169	320	3.10	270	3	1	1	190	616	70	119	9.820×10^{-4}	3.740×10^{-4}	240	605
EDM-LOL	171	640	2.80	616	3	1	1	200	584	44	71	1.186×10^{-3}	6.430×10^{-4}	270	665

<u>INJECTOR</u>	<u>TEST NO.</u>	<u>PC</u>	<u>MRJ</u>	<u>CR</u>	<u>NPLANE</u>	<u>IDO</u>	<u>IDF</u>	<u>TO</u>	<u>TF</u>	<u>VO</u>	<u>VF</u>	<u>RMO</u>	<u>RMF</u>	<u>TSO</u>	<u>TSF</u>
PAT	178	560	2 75	349	3	1	1	180	530	60	132	7.820×10^{-4}	2.580×10^{-4}	264	660
PAT	179	300	2 85	279	3	1	1	190	526	42	95	6.300×10^{-4}	2.400×10^{-4}	230	600
PAT	182	150	2.90	212	3	1	1	180	525	31	65	1.210×10^{-3}	4.120×10^{-4}	215	540
PAT	184	300	2 85	279	3	1	1	190	526	42	95	6.300×10^{-4}	2.400×10^{-4}	230	600
PAT	187	800	2 90	754	3	1	1	190	527	45	94	9.480×10^{-4}	3.230×10^{-4}	278	666
PAT	189	150	2 90	212	3	1	1	180	525	31	65	1.210×10^{-3}	4.120×10^{-4}	215	540
PAT	190	165	2.75	109	3	1	1	180	525	65	143	7.420×10^{-4}	2.450×10^{-4}	220	550
PAT	193	560	2 80	349	3	1	1	185	580	60	161	7.820×10^{-4}	1.920×10^{-4}	264	660
PAT	194	340	3 00	270	3	1	1	190	578	57	136	8.090×10^{-4}	2.140×10^{-4}	243	610
PAT	197	505	3 00	349	3	1	1	180	504	62	122	7.660×10^{-4}	2.920×10^{-4}	260	640

E. PREDICTED FUEL VAPORIZATION AND LIQUID PHASE
MIXTURE RATIO

TEST NO 105

INJECTOR OFO

GRID NO.	PLANE NO. 1		PLANE NO. 2		PLANE NO. 3	
	EVF	MRL	EVF	MRL	EVF	MRL
34					65.46	0.03
37					41.73	0
41					0	∞
42					52.16	8.26
43			0	∞	56.98	2.01
44			0	∞	58.81	0.05
45	0	∞	40.89	0.24	66.00	0.03
46	15.85	0.35	55.78	0	66.25	0.00
47			41.73	0.16	41.73	0
53					19.74	1.04
54					55.78	0
55			0	∞	61.03	59.05
56	0	∞	0	0	29.27	2.17
57			15.85	∞	15.90	15.64
58			15.85	∞	15.85	0
63					18.41	1.43
64					0	∞
65					0	∞
66			0	∞	0	∞
67			15.85	∞	0	∞
68			15.85	∞	15.85	∞
73					1.06	0.35
74					0	∞
75					0	∞
76					15.88	16.26
77					15.64	41.20
83					0	0

DEPTH AVG

J=1

2					0	∞
3			0	∞	31.70	1.41
4			0	∞	52.40	0.03
5	0	∞	38.45	0.21	41.45	0.83
6	11.99	0.15	38.21	0	26.65	2.46
7			5.43	0.01	23.44	7.46
8			0	∞	15.85	∞
9						
10						
PLANE AVG.	11.84	0.14	33.47	0.02	42.26	2.00

TEST NO 109

INJECTOR: OFO

GRID NO	PLANE NO. 1		PLANE NO. 2		PLANE NO. 3	
	EVF	MRL	EVF	MRL	EVF	MRL
34					50.72	0.02
37					31.91	0
41					0	∞
42					40.84	5.73
43			0	∞	36.19	1.17
44			0	∞	47.18	1.42
45	0	∞	31.14	0.22	51.12	0.02
46	10.98	0.32	91.95	0.06	51.28	0.02
47			31.91	0.15	31.91	0
53					15.07	0.86
54					38.03	2.30
55			0	∞	47.27	37.87
56	0	∞	0	∞	21.94	1.74
57			10.98	∞	10.99	12.74
58			10.98	∞	10.98	0
63					13.90	1.20
64					0	∞
65					0	∞
66			0	∞	0	∞
67			10.98	∞	0	∞
68			10.98	∞	10.98	∞
73					1.10	0.30
74					0	∞
75					0	∞
76					10.98	13.24
77					10.92	33.56
83					0	0

DEPTH AVG.

J=1

2					40.84	5.73
3			0	∞	20.53	0.90
4			0	∞	41.26	0.31
5	0	∞	29.28	0.20	32.10	0.52
6	8.31	0.14	21.89	0.03	20.19	1.98
7			4.16	0.01	17.65	6.06
8			0	∞	0	∞
9						
10						
PLANE AVG.	8.20	0.13	19.81	0.03	32.37	1.59

TEST NO. 110/111

INJECTOR OFO

GRID NO	PLANE NO. 1		PLANE NO. 2		PLANE NO. 3	
	EVF	MRL	EVF	MRL	EVF	MRL
34					65.84	0
37					51.22	0
41					0	∞
42					50.47	∞
43			0	∞	54.49	1.83
44			0	∞	55.83	0
45	0	∞	50.47	0.03	66.56	0
46	20.99	0.16	52.64	0	66.88	0
47			51.22	0.02	51.22	0
53					24.47	0.96
54					52.64	0
55			0	∞	60.15	33.76
56	0	∞	16.25	1.22	21.60	0.03
57			20.99	∞	21.16	15.91
58			20.99	∞	20.99	0
63					59.53	2.44
64					16.25	∞
65					16.25	∞
66			0	∞	46.20	1.53
67			20.99	∞	42.93	67.07
68			20.99	∞	20.99	∞
73					25.73	0.51
74					16.25	∞
75					0	∞
76					21.13	16.54
77					20.67	42.01
83					16.25	0

DEPTH AVG.

J=1

2					50.47	∞
3			0	∞	42.26	1.49
4			0	∞	51.60	0
5	0	∞	47.46	0.03	47.01	0.11
6	15.88	0.07	40.98	0.51	35.38	2.48
7			24.93	0	41.68	54.53
8			20.99	∞	20.99	∞
9						
10						
PLANE AVG	15.67	0.06	38.91	0.25	46.25	6.78

TEST NO. 116

INJECTOR: OFO

GRID NO.	PLANE NO. 1		PLANE NO. 2		PLANE NO. 3	
	EVF	MRL	EVF	MRL	EVF	MRL
34					63.06	0
37					47.44	0
41					0	∞
42					64.43	10.32
43			0	∞	56.59	1.85
44			0	∞	57.87	1.28
45	0	∞	46.55	0.06	65.66	0
46	18.57	0.18	55.70	0	65.85	0
47			47.44	0.04	47.44	0
53					23.55	0.88
54			0	∞	55.70	0
55			14.80	1.17	60.85	8.47
56	0	∞	18.57	∞	18.69	0.11
57			18.57	∞	18.72	14.85
58					18.57	0
63					23.55	0.88
64					55.70	0
65					60.85	8.47
66			0	∞	18.69	0.11
67			18.57	∞	18.72	14.85
68			18.57	∞	18.57	0
73					55.00	2.05
74					34.22	4.65
75					14.80	∞
76					41.32	1.65
77					41.57	63.08
83					18.57	∞

DEPTH AVG.

J=1						
2					64.43	0 01
3			0	0	42.49	0 61
4			0	0	54.77	0.86
5	0	0	43.78	4.38	45.92	0.97
6	14.05	1.76	42.64	3.77	32.26	16.12
7			22.33	0.17	30.94	1 99
8			18.57	0	18.57	0
9						
10						
PLANE AVG	13.87	1.60	39.60	2.22	47.31	4.96

TEST NO. 120

INJECTOR: TLOL

GRID NO	PLANE NO 1		PLANE NO 2		PLANE NO 3	
	EVF	MRL	EVF	MRL	EVF	MRL
25			0	∞	0	∞
26					0	∞
35	0	∞	0	∞	0	∞
36	0	∞	0	∞	0	∞
37			0	∞	0	
45	0	∞	0	∞	0	∞
46	0	∞	0	∞	0	∞
47			0	∞	0	∞
54					0	∞
55	0	0	0	0	0	0
56	0	∞	0	0	0	0
57			0	∞	0	∞
64					0	∞
65	1.03	0.35	0	0	0	0
66	0.70	0.91	4.11	0.74	9.97	0.53
67			0.75	4.49	0	∞
68					0	∞
74					9.37	1.15
75			4.84	1.12	9.51	1.04
76	0	0	0.09	0.10	7.15	0.28
77			0	∞	0.75	1.82
78					0.76	1.95
87					0	0
88					0	∞

DEPTH AVG.

I=0

1						
2			0	∞	0	∞
3	0	∞	0	∞	0	∞
4	0	∞	0	∞	0	∞
5	0	0	0	0	0	0
6	0.86	0.69	2.99	1.31	6.40	0.27
7	0	0	1.27	0.31	4.68	1.45
8					0	
9						
PLANE AVG.	0.20	0.07	1.09	0.33	2.88	0.20

TEST NO. 121

INJECTOR-TL01

GRID NO.	PLANE NO. 1		PLANE NO. 2		PLANE NO. 3	
	EVF	MRL	EVF	MRL	EVF	MRL
25			0	0	0	0
26					0	0
35	0	0	0	0	0	0
36	0	0	0	0	0	0
37			0	0	0	0
45	0	0	0	0	0	0
46	0	0	0	0	0	0
47			0	0	0	0
54					0	0
55	0	0	0	0	0	0
56	0	0	0	0	0	0
57			0	0	0	0
64					0	0
65	1.13	0.37	0	0	0	0
66	0	0	0	0	0	0
67			0	0	0	0
68					0	0
74					1.41	1.90
75			1.40	1.45	1.42	1.72
76	0	0	0.47	0.11	9.03	0.19
77			0	0	0	0
78					0	0
87					0	0
88					0	0

DEPTH AVG.

I=0

1						
2			0	0	0	0
3	0	0	0	0	0	0
4	0	0	0	0	0	0
5	0		0		0	
6	0.55	0.14	0	0	0	-
7	0	0	0.52	0.40	2.74	0.47
8					0	-
9						
PLANE AVG.	0.13	0.01	0.03	0.01	0.25	0.04

TEST NO 123/124

INJECTOR TLOL

GRID NO	PLANE NO. 1		PLANE NO. 2		PLANE NO. 3	
	EVF	MRL	EVF	MRL	EVF	MRL
25			0	∞	0	∞
26					0	∞
35	0	∞	0	∞	0	∞
36	0	∞	0	∞	0	∞
37			0	∞	0	∞
45	0	∞	0	∞	0	∞
46	0	∞	0	∞	0	∞
47	∞		0	∞	0	∞
54					0	∞
55	0	0	0	0	0	0
56	0	∞	0	0	0	0
57			0	∞	0	∞
64					0	∞
65	2.16	0.34	0	0	0	0
66	1.37	0.94	6.77	0.65	15.69	0.37
67			1.51	4.59	0	∞
68					0	∞
74					14.80	0.83
75			8.09	0.92	15.01	0.74
76	0	0	0.31	0.11	12.02	0.19
77			0	∞	1.52	1.50
78					1.52	1.60
87					0	0
88					0	∞

DEPTH AVG.

I=0

1						
2			0	∞	0	∞
3	0	∞	0	∞	0	∞
4	0	∞	0	∞	0	∞
5	0	-	4.77	0.45	0	-
6	1.75	0.71	4.94	1.29	10.18	0.19
7	0	0	3.18	0.26	7.74	1.17
8					0	-
9						
PLANE AVG.	0.42	0.07	4.50	0.52	4.61	0.15

TEST NO: 127

INJECTOR: TLOL

GRID NO.	PLANE NO. 1		PLANE NO. 2		PLANE NO. 3	
	EVF	MRL	EVF	MRL	EVF	MRL
25			0	∞	0	∞
26					0	∞
35	0	∞	0	∞	0	∞
36	0	∞	0	∞	0	∞
37			0	∞	0	∞
45	0	∞	0	∞	0	∞
46	0	∞	0	∞	0	∞
47			0	∞	0	∞
54					0	∞
55	0	0	0	0	0	0
56	0	∞	0	0	0	0
57			0	∞	0	∞
64					0	∞
65	1.04	0.43	0	0	0	0
66	0	0			0	0
67					0	∞
68					0	∞
74					8.72	1.45
75			4.69	1.38	8.09	1.30
76	0	0	0.20	0.12	7.62	0.34
77			0	∞	0	∞
78					0	∞
87					0	0
88					0	∞

DEPTH AVG.

I=0

1						
2			0	∞	0	∞
3	0	∞	0	∞	0	∞
4	0	∞	0	∞	0	∞
5	0	-	0	-	0	-
6	0.50	0.17	0	-	0	-
7	0	0	1.27	0.38	6.80	1.24
8					0	-
9						
PLANE AVG.	0.12	0.02	0.06	0.01	0.63	0.10

TEST NO. 128

INJECTOR: TLOL

GRID NO	PLANE NO. 1		PLANE NO. 2		PLANE NO. 3	
	EVF	MRL	EVF	MRL	EVF	MRL
25			0	∞	0	∞
26					0	∞
35	0	∞	0	∞	0	∞
36	0	∞	0	∞	0	∞
37			0	∞	0	∞
45	0	∞	0	∞	0	∞
46	0	∞	0	∞	0	∞
47			0	∞	0	∞
54					0	∞
55	0	0	0	0	0	0
56	0	∞	0	0	0	0
57			0	∞	0	∞
64					0	∞
65	1.71	0.43	0	0	0	0
66	1.09	1.13	5.72	0.87	13.43	0.58
67			1.20	5.54	0	∞
68					0	∞
74					12.42	1.29
75			6.88	1.29	12.63	1.15
76	0	0	0.26	0.13	10.28	0.30
77			0	∞	1.22	2.10
78					1.22	2.25
87					0	0
88					0	∞

DEPTH AVG.

I=0

1						
2			0	∞	0	∞
3	0	∞	0	∞	0	∞
4	0	∞	0	∞	0	∞
5	0	-	0	-	0	-
6	1.39	0.86	4.17	1.64	8.62	0.29
7	0	0	1.85	0.36	6.52	1.68
8					0	-
9						
PLANE AVG.	0.33	0.08	1.53	0.41	3.90	0.22

TEST NO. 129

INJECTOR-TLOL

GRID NO	PLANE NO. 1		PLANE NO. 2		PLANE NO. 3	
	EVF	MRL	EVF	MRL	EVF	MRL
25			0	∞	0	∞
26					0	∞
35	0	∞	0	∞	0	∞
36	0	∞	0	∞	0	∞
37			0	∞	0	∞
45	0	∞	0	∞	0	∞
46	0	∞	0	∞	0	∞
47			0	∞	0	∞
54					18.91	1.22
55	2.36	1.22	9.50	1.05	20.44	0.62
56	0	∞	0	0	0	0
57			0	∞	0	∞
64					18.16	1.53
65	3.55	0.36	9.48	1.06	20.25	0.68
66	2.72	0.95	11.06	0.62	23.21	0.37
67			3.41	4.48	0	∞
68					0	∞
74					21.86	0.82
75			12.09	0.94	22.09	0.74
76	2.29	1.27	6.55	0.08	14.71	0.25
77			7.91	2.01	3.41	1.35
78					3.41	1.46
87					16.83	0.93
88					14.37	2.25

DEPTH AVG.

I=0

1						
2			0	∞	0	∞
3	0	∞	0	∞	0	∞
4	0	∞	0	∞	0	∞
5	1.48	0.62	2.42	0.26	5.05	0.17
6	3.12	0.72	10.12	1.50	18.90	0.35
7	2.29	1.27	8.50	1.46	11.14	1.08
8					15.48	1.83
9						
PLANE AVG.	1.84	0.38	5.27	0.53	10.69	0.28

TEST NO. 130

INJECTOR: TLOL

GRID NO.	PLANE NO. 1		PLANE NO. 2		PLANE NO. 3	
	EVF	MRL	EVF	MRL	EVF	MRL
25			0	∞	0	∞
26					0	∞
35	0	∞	0	∞	0	∞
36	0	∞	0	∞	0	∞
37			0	∞	18.45	35.97
45	0	∞	7.10	7.32	28.61	3.44
46	0	∞	0	∞	22.46	∞
47			6.66	8.48	22.46	∞
54					36.00	2.64
55	5.44	1.31	18.62	1.57	34.13	1.46
56	7.52	2.65	22.46	1.60	35.98	1.30
57			23.24	3.48	38.50	2.88
64					36.04	3.20
65	1.95	0.42	18.69	1.59	34.76	1.57
66	1.72	1.06	4.87	1.05	7.39	1.04
67			15.54	5.09	39.86	3.24
68					39.14	4.91
74					32.36	2.08
75			12.36	1.65	32.07	1.89
76	5.69	1.36	13.39	0.11	17.97	0.47
77			20.18	2.77	34.49	3.23
78					34.42	3.45
87					24.39	1.94
88					37.91	4.31

DEPTH AVG.

I=0

1			0	∞	0	∞
2			0	∞	5.37	5.98
3	0	∞	0	∞	5.37	5.98
4	0	∞	4.47	2.46	24.86	0.79
5	6.22	1.96	21.51	1.72	35.76	1.58
6	1.83	0.81	8.60	1.97	18.00	1.85
7	5.69	1.36	15.80	2.08	29.53	2.59
8					31.82	3.56
9						
PLANE AVG.	5.01	1.05	16.06	1.79	27.42	2.01

TEST NO 131

INJECTOR: TL01

GRID NO.	PLANE NO. 1		PLANE NO. 2		PLANE NO. 3	
	EVF	MRL	EVF	MRL	EVF	MRL
25			0	∞	0	∞
26					0	∞
35	0	∞	0	∞	0	∞
36	0	∞	0	∞	0	∞
37			0	∞	8.62	∞
45	0	∞	9.28	7.69	36.01	3.52
46	0	∞	0	∞	29.80	∞
47			8.62	8.90	29.80	∞
54					46.21	2.70
55	8.17	1.38	25.89	1.64	44.22	1.50
56	10.56	2.78	29.80	1.67	45.84	1.34
57			30.74	3.63	48.54	2.94
64					46.17	3.28
65	8.74	0.44	25.96	1.65	44.93	1.60
66	5.83	1.11	11.68	1.09	18.87	1.06
67			22.66	5.28	49.97	3.33
68					52.65	5.72
74					41.92	2.14
75			16.91	1.72	41.61	1.94
76	8.50	1.43	18.89	0.11	24.34	0.49
77			27.79	2.89	45.07	3.40
78					44.97	3.63
87					33.53	2.15
88					48.14	4.78

DEPTH AVG.

I=0

1						
2			0	∞	0	∞
3	0	∞	0	∞	2.51	∞
4	0	∞	5.83	2.58	32.23	0.80
5	9.06	2.06	28.84	1.80	45.70	1.63
6	4.34	0.85	15.53	2.05	29.05	1.92
7	8.50	1.43	21.89	2.18	38.74	2.72
8					41.56	3.95
9						
PLANE AVG.	7.70	1.10	22.94	1.87	37.46	1.52

TEST NO 132

INJECTOR: TLOL

GRID NO	PLANE NO. 1		PLANE NO. 2		PLANE NO. 3	
	EVF	MRL	EVF	MRL	EVF	MRL
25			0	∞	0	∞
26					0	∞
35	0	∞	0	∞	0	∞
36	0	∞	0	∞	0	∞
37			0	∞	0	∞
45	0	∞	11.60	8.62	44.45	3.89
46	0	∞	0		39.53	∞
47			0		39.53	∞
54					59.07	2.89
55	12.93	1.54	36.44	1.77	57.26	1.60
56	14.93	3.10	39.53	1.81	57.88	1.42
57			39.66	3.92	60.40	3.14
64					58.94	3.51
65	4.06	0.50	36.51	1.79	57.91	1.72
66	9.95	1.24	27.43	1.17	38.98	1.13
67			31.58	5.78	60.56	3.47
68					59.61	5.40
74					53.58	2.28
75			23.46	1.90	53.38	2.06
76	13.28	1.60	26.93	0.12	33.26	0.53
77			37.67	3.12	56.42	3.49
78					56.32	3.72
87					45.76	2.60
88					47.33	5.87

DEPTH AVG.

I=0

1						
2			0	∞	0	∞
3	0	∞	0	∞	0	∞
4	0	∞	5.82	2.11	41.45	0.88
5	13.68	2.31	38.75	1.95	57.97	1.73
6	7.11	0.96	29.65	2.25	46.17	2.02
7	13.28	1.60	30.27	2.39	49.55	2.83
8					46.62	4.85
PLANE AVG.	11.76	1.21	33.80	1.90	51.05	1.61

TEST NO. 133

INJECTOR. TLOL

GRID NO.	PLANE NO. 1		PLANE NO. 2		PLANE NO. 3	
	EVF	MRL	EVF	MRL	EVF	MRL
25			0	∞	0	∞
26					0	∞
35	0	∞	0	∞	0	∞
36	0	∞	0	∞	0	∞
37			0	∞	13.60	∞
45	0	∞	14.70	8.12	52.61	3.79
46	0	∞	0		45.18	
47			13.60	9.40	45.18	∞
54					62.51	2.96
55	12.63	1.46	36.98	1.74	59.03	1.64
56	18.65	2.95	45.18	1.80	62.25	1.47
57			47.12	3.91	66.02	3.25
64					62.54	3.60
65	4.82	0.47	37.13	1.76	60.04	1.76
66	4.20	1.18	13.48	1.15	18.04	1.14
67			31.96	5.65	68.39	3.86
68					77.09	11.32
74					58.56	2.34
75			25.66	1.82	57.87	2.12
76	13.28	1.52	27.20	0.12	34.61	0.52
77			40.47	3.08	61.07	4.23
78					60.89	4.51
87					50.60	2.75
88					56.91	6.91

DEPTH AVG.

I=0

1			0	∞	0	∞
2			0	∞	3.96	∞
3	0	∞	0	∞	48.08	0.86
4	0	∞	9.23	2.71	61.82	1.79
5	14.88	2.19	43.17	1.93	24.56	2.30
6	4.50	0.91	19.88	2.20	53.31	3.30
7	13.28	1.52	32.03	2.33	34.07	5.60
8						
9						
PLANE AVG.	12.02	1.16	33.15	1.99	49.23	1.77

TEST NO	157	INJECTOR	EDM-LOL			
GRID NO	PLANE NO. 1		PLANE NO. 2		PLANE NO. 3	
	EVF	MRL	EVF	MRL	EVF	MRL
15			40.51	36.11	40.51	
23					30.66	0.39
24			46.59	7.61	73.48	2.85
25	17.89	10.10	0	∞	7.49	57.93
26	26.55	1.81	50.66	15.22	57.54	51.94
33			27.89	1.13	30.35	0.39
34			61.53	4.62	80.44	2.18
35	16.45	11.21	56.80	8.06	75.91	3.64
36	0	∞	27.66	0	72.80	2.46
37			25.25	0.50	69.47	3.58
38					39.06	0.59
43			22.16	0.68	48.23	1.43
44	1.39	0.88	61.35	1.95	80.18	1.47
45	27.54	2.85	60.83	1.73	79.65	1.49
46	27.66	2.17	56.89	1.26	77.29	1.41
47	2.03	0.95	46.84	0.59	68.68	1.66
48					64.16	1.14
53			51.40	1.27	75.13	1.67
54	18.54	1.25	61.07	3.43	80.94	2.28
55	27.76	2.51	60.89	3.67	80.35	2.61
56	27.63	2.14	61.19	3.06	80.83	2.28
57	25.29	1.65	61.16	1.84	76.48	2.00
58					68.95	1.88
63			50.66	3.14	77.48	2.12
64			59.22	5.55	79.90	3.83
65					78.81	5.45
66			59.58	4.96	78.45	3.74
67	24.52	5.22	60.48	4.27	80.00	3.81
68					66.29	1.48
73					75.25	3.41
74					76.79	6.10
77			53.64	7.40	78.56	5.67
78					79.99	4.28
88					71.99	5.30
89					76.70	1.36

DEPTH AVG.

I=0

1			40.51	36.11		
2	25.20	5.30	44.10	5.33	47.33	36.89
3	13.98	6.11	43.79	4.90	65.79	2.70
4	26.64	2.47	57.88	1.61	74.86	1.47
5	27.26	2.25	60.44	3.22	78.75	2.29
6	24.52	5.22	58.37	4.62	76.99	3.77
7			53.43	7.40	78.12	4.78
8					71.99	3.52
9						
PLANE AVG	26.67	2.76	57.02	3.23	75.05	3.77

TEST NO: 158

INJECTOR: EDM-LOL

GRID NO.	PLANE NO. 1		PLANE NO. 2		PLANE NO. 3	
	EVF	MRL	EVF	MRL	EVF	MRL
15			31.89	35.67	31.89	
23					30.06	0.57
24			34.88	7.68	61.32	2.88
25	11.95	10.32	0	∞	0	∞
26	19.47	1.84	40.23	15.38	42.16	54.26
33			27.01	1.01	28.91	0.53
34			48.74	4.10	70.09	2.04
35	11.07	11.45	44.32	8.17	64.14	3.73
36	0	∞	19.72		60.03	2.56
37			21.33	0.50	58.42	3.65
38					33.03	0.60
43			22.35	0.64	41.35	1.23
44	2.34	0.89	48.81	1.97	70.08	1.51
45	19.34	2.91	48.97	1.76	69.98	1.53
46	19.72	2.21	46.59	1.26	67.99	1.30
47	4.48	0.95	38.02	0.63	59.54	1.54
48					55.15	0.98
53			43.68	1.45	66.94	1.42
54	15.44	1.26	48.33	3.46	70.46	2.36
55	19.60	2.56	48.15	3.68	69.38	2.61
56	19.73	2.19	48.72	3.08	70.10	2.35
57	19.01	1.68	49.12	1.86	67.42	2.01
58					60.19	1.93
63			42.60	3.59	67.93	2.35
64			46.63	5.61	68.86	3.94
65					67.62	5.56
66			47.24	5.01	67.34	3.89
67	16.99	5.34	48.03	4.13	69.68	4.00
68					56.35	1.79
73					65.34	3.77
74					65.31	6.21
77			41.21	7.56	67.47	5.72
78					69.64	4.29
88					59.73	5.60
89					66.45	1.33

DEPTH AVG.

I=0

1			31.89	35.67		
2	18.30	5.41	33.52	5.38	41.45	17.27
3	9.41	6.24	34.86	4.79	56.08	2.75
4	18.94	2.52	46.87	1.63	65.51	1.42
5	19.12	2.30	48.29	3.25	68.58	2.32
6	16.99	5.34	46.63	4.67	66.38	3.94
7			41.21	7.56	67.55	4.89
8					59.73	3.66
9						
PLANE AVG.	18.85	2.82	45.89	3.24	65.30	3.06

TEST NO. 159 INJECTOR EDM-LOL

GRID NO.	PLANE NO. 1		PLANE NO. 2		PLANE NO. 3	
	EVF	MRL	EVF	MRL	EVF	MRL
15			26.20	34.83	26.20	0
23					19.95	0.48
24			31.53	8.10	56.25	3.18
25	10.61	10.68	0	∞	0	∞
26	16.16	1.93	35.05	16.66	37.11	58.97
33			12.37	1.13	17.04	0.42
34			42.53	4.23	63.90	2.25
35	9.84	11.84	38.89	8.91	58.48	4.15
36	0	∞	16.43	0	52.87	2.80
37			17.81	0.53	52.91	4.05
38					28.37	0.64
43			18.78	0.77	28.48	1.43
44	1.60	0.91	42.57	2.18	63.91	1.73
45	16.19	3.05	42.66	1.93	63.81	1.75
46	16.43	2.32	40.59	1.39	62.01	1.43
47	3.23	0.98	32.66	0.68	53.41	1.55
48					48.86	0.96
53			37.64	1.63	60.66	1.66
54	12.68	1.31	42.20	3.82	64.21	2.70
55	16.36	2.69	42.06	4.06	63.16	3.01
56	16.42	2.30	42.47	3.41	63.86	2.71
57	15.76	1.76	42.78	2.05	61.20	2.27
58					53.13	1.96
63			36.80	4.00	61.62	2.73
64			40.82	6.16	62.70	4.50
65					61.55	6.34
66			41.28	5.51	61.22	4.48
67	14.49	5.57	41.92	4.54	63.48	4.57
68					50.22	2.19
73					59.31	4.35
74					59.43	6.98
77			36.45	8.41	61.37	6.42
78					63.45	4.82
88					54.80	6.59
89					60.58	1.42

DEPTH AVG.

I=0

1		26.20	22.55			
2	15.30	5.63	30.01	5.75	33.86	18.79
3	8.36	6.44	28.54	5.16	49.38	3.03
4	15.80	2.64	40.80	1.79	59.19	1.57
5	16.24	2.41	42.00	3.59	62.28	2.65
6	14.49	5.57	40.57	5.14	60.23	4.53
7			36.45	8.41	61.46	5.52
8					54.80	4.24
9						
PLANE AVG.	15.86	2.95	39.76	3.51	58.95	3.44

TEST NO	160	INJECTOR	EDM-LOL			
GRID NO	PLANE NO. 1		PLANE NO. 2		PLANE NO. 3	
	EVF	MRL	EVF	MRL	EVF	MRL
15			17.12	32.37	17.12	0
23					30.89	0.79
24			16.88	7.30	36.87	2.54
25	4.75	10.11	0	∞	0	∞
26	10.07	1.75	23.13	14.16	23.72	50.44
33			16.20	0.67	28.43	0.69
34			28.33	2.86	47.67	1.41
35	4.35	11.23	24.86	7.54	40.84	3.23
36	0	∞	9.87	∞	36.94	2.33
37			20.58	0.44	36.84	3.22
38					23.90	0.54
43			24.74	0.72	41.66	0.62
44	8.12	0.81	28.87	1.78	48.42	1.21
45	9.43	2.79	29.62	1.59	48.94	1.23
46	9.87	2.11	29.49	1.12	48.52	0.93
47	8.66	0.87	24.39	0.58	38.07	1.37
48					39.12	0.64
53			29.86	1.45	49.98	1.16
54	10.04	1.18	28.32	3.14	48.15	1.94
55	9.65	2.45	28.16	3.32	46.48	2.10
56	9.88	2.09	28.90	2.78	47.53	1.93
57	10.13	1.59	29.59	1.67	48.55	1.59
58					51.09	1.80
63			28.59	3.61	48.71	2.05
64			26.87	5.13	45.97	3.26
65					44.59	4.64
66			27.64	4.55	44.41	3.28
67	7.72	5.16	28.27	3.62	47.66	3.31
68					39.46	1.82
73					45.83	3.40
74					42.06	5.32
77			10.68	7.38	40.53	4.78
78					47.60	3.49
88					11.02	4.97
89					40.50	1.68

DEPTH AVG.

I=0

1			17.12	32.37		
2	9.24	5.26	17.02	5.03	31.75	16.03
3	3.70	6.12	20.54	4.12	37.58	2.36
4	9.63	2.41	29.04	1.47	45.88	1.14
5	9.81	.19	28.66	2.94	48.90	2.35
6	7.72	5.16	27.86	4.26	44.98	3.33
7			10.68	7.38	45.70	4.13
8					11.02	3.48
9						
PLANE AVG.	9.60	2.71	27.88	2.91	45.62	2.76

TEST NO. 161

INJECTOR· EDM-LOL

GRID NO	PLANE NO 1		PLANE NO 2		PLANE NO 3	
	EVF	MRL	EVF	MRL	EVF	MRL
15			40.93	37.15	40.93	0
23					25.89	0.31
24			50.75	8.38	76.53	3.30
25	20.16	10.67	0	∞	8.82	59.72
26	28.04	1.94	52.60	16.81	59.66	57.84
33			19.05	1.29	23.06	0.26
34			60.53	5.22	82.87	2.62
35	18.68	11.82	59.88	9.00	78.48	4.24
36	0	∞	29.78	0	75.72	2.86
37			25.80	0.53	71.72	4.09
38					40.18	0.64
43			21.19	0.78	28.05	1.51
44	0.84	0.92	64.26	2.21	82.59	1.77
45	29.96	3.06	63.40	1.94	82.02	1.79
46	29.78	2.33	59.12	1.41	79.66	1.69
47	1.64	0.98	48.05	0.64	70.69	1.86
48					66.12	1.27
53			52.81	1.38	76.93	2.14
54	18.49	1.32	64.02	3.87	83.34	2.74
55	30.08	2.70	63.85	4.17	82.90	3.18
56	29.71	2.30	63.89	3.45	83.25	2.77
57	26.32	1.77	63.73	2.08	78.47	2.34
58					70.76	2.10
63			52.21	3.38	79.66	2.48
64			62.19	6.24	82.43	4.61
65					81.04	6.56
66			62.30	5.58	81.05	4.49
67	26.98	5.58	63.23	4.95	82.32	4.56
68					68.14	1.67
73					77.28	1.67
74					79.09	7.23
77			56.87	8.34	81.15	6.80
78					82.31	5.15
88					75.14	6.28
89					79.29	1.59

DEPTH AVG.

I=0

1			40.93	37.15		
2	26.82	5.63	47.47	5.87	46.08	39.55
3	15.87	6.43	44.61	5.50	67.08	3.14
4	28.79	2.65	60.23	1.81	51.74	1.74
5	29.30	2.42	63.18	3.64	81.04	2.76
6	26.98	5.58	60.96	5.23	79.35	4.52
7			56.87	8.34	80.49	5.71
8					75.14	4.15
9						
PLANE AVG.	28.77	2.96	59.34	3.61	66.15	4.33

TEST NO. 162

INJECTOR: EDM-LOL

GRID NO	PLANE NO. 1		PLANE NO. 2		PLANE NO. 3	
	EVF	MRL	EVF	MRL	EVF	MRL
15			36.26	37.94	36.26	0
23					34.36	0.57
24			40.05	7.89	67.13	2.94
25	14.46	10.64	0	∞	0	∞
26	23.39	1.89	45.58	15.76	47.54	55.51
33			31.32	1.07	33.19	0.53
34			54.70	4.42	75.42	2.10
35	13.39	11.81	49.98	8.35	69.66	3.76
36	0	∞	23.72	0	66.39	2.59
37			24.53	0.52	64.16	3.73
38					37.10	0.62
43			25.21	0.62	45.90	1.32
44	2.72	0.92	54.80	2.01	75.40	1.49
45	23.27	2.99	55.01	1.79	75.33	1.52
46	23.72	2.27	52.51	1.29	73.50	1.32
47	5.26	0.98	43.17	0.64	65.27	1.68
48					60.92	1.10
53			49.24	1.45	72.67	1.44
54	18.49	1.30	54.30	3.53	75.72	2.36
55	23.57	2.64	54.11	3.75	74.66	2.58
56	23.72	2.25	54.73	3.14	75.36	2.34
57	22.82	1.72	55.17	1.89	72.79	2.00
58					66.81	2.12
63			48.05	3.58	73.56	2.33
64			52.48	5.73	74.15	3.93
65					72.93	5.56
66			53.14	5.11	72.63	3.85
67	20.47	5.49	53.99	4.24	74.94	3.99
68					61.91	1.67
73					71.09	3.77
74					70.59	6.22
77			46.58	7.63	72.79	5.77
78					74.91	4.33
88					65.53	5.54
89					72.03	1.37

DEPTH AVG.

I=0

1			26.26	37.94		
2	22.00	5.60	38.35	5.51	46.21	17.72
3	11.38	6.43	39.77	4.98	61.45	2.79
4	22.78	2.59	52.72	1.66	70.98	1.45
5	23.44	2.36	54.13	3.31	73.98	2.31
6	20.47	5.49	52.47	4.76	71.74	3.91
7			46.58	7.63	72.93	4.92
8					65.53	3.65
9						
PLANE AVG.	22.87	2.91	51.64	3.33	70.71	3.10

TEST NO.	164	INJECTOR	EDM-LOL			
GRID NO	PLANE NO. 1		PLANE NO. 2		PLANE NO. 3	
	EVF	MRL	EVF	MRL	EVF	MRL
15			30.28	35.07	30.28	0
23					20.58	0.42
24			39.09	8.36	64.36	3.33
25	14.02	10.73	0	∞	6.64	64.50
26	19.64	1.96	41.02	17.06	48.31	59.18
33			13.89	1.20	19.40	0.38
34			49.79	4.56	70.71	2.43
35	13.02	11.89	46.09	9.14	66.34	4.41
36	0	∞	20.32	0	60.84	2.90
37			19.81	0.53	59.94	4.19
38					31.67	0.65
43			17.52	0.80	28.17	1.49
44	0.90	0.92	49.71	2.24	70.60	1.83
45	20.26	3.09	49.40	1.99	70.28	1.85
46	20.32	2.35	46.55	1.43	68.11	1.57
47	1.35	0.98	37.46	0.68	59.33	1.66
48					54.36	1.05
53			42.30	1.60	66.16	1.86
54	14.15	1.33	49.41	3.93	71.11	2.84
55	20.39	2.72	49.27	4.20	70.48	3.23
56	20.30	2.32	49.51	3.51	70.91	2.86
57	18.86	1.78	49.60	2.12	67.47	2.43
58					57.28	2.00
63			41.72	3.92	67.86	2.79
64			48.00	6.33	70.01	4.76
65					68.99	6.71
66			48.28	5.67	68.83	4.75
67	18.00	5.62	48.97	4.77	70.25	4.77
68					56.32	2.14
73					65.74	4.43
74					67.25	7.43
77			43.87	8.65	68.83	6.84
78					70.24	5.16
88					63.01	6.92
89					67.32	1.52

DEPTH AVG.

I=0

1			30.28	35.07		
2	18.77	5.67	36.68	5.91	38.81	41.67
3	11.06	6.47	33.61	5.36	55.75	3.19
4	9.36	1.99	47.04	1.85	65.16	1.68
5	20.25	2.44	48.96	3.70	68.94	2.82
6	18.40	5.62	47.39	5.29	67.19	4.75
7			43.87	8.65	68.47	5.85
8					63.01	4.47
9						
PLANE AVG.	14.28	2.64	46.10	3.62	65.29	4.47

TEST NO. 165 INJECTOR: EDM-LOL

GRID NO.	PLANE NO. 1		PLANE NO. 2		PLANE NO. 3	
	EVF	MRL	EVF	MRL	EVF	MRL
15			13.57	23.55	13.57	0
23					60.05	0.55
24			81.10	16.35	95.15	11.56
25	46.03	13.99	0	∞	14.58	55.25
26	12.86	2.08	56.43	23.33	70.18	89.44
33			56.49	2.07	59.80	0.48
34			69.87	10.79	70.26	6.79
35	44.44	15.24	80.50	17.98	94.56	14.40
36	0	∞	34.58		86.91	4.55
37			33.66	0.60	87.13	9.15
38					50.31	0.78
43			35.09	1.09	42.71	1.49
44	14.31	0.94	80.66	4.40	92.91	5.31
45	46.78	4.09	71.15	2.08	92.51	3.91
46	34.58	2.81	61.07	2.06	83.23	4.49
47	14.61	1.01	11.81	0.60	61.11	2.95
48					72.29	1.34
53			42.70	1.06	79.10	5.64
54	16.32	1.41	80.80	7.88	94.55	8.22
55	41.70	3.45	80.78	9.40	95.96	11.69
56	34.04	2.77	76.43	6.43	95.59	11.07
57	6.03	1.84	70.67	3.47	84.10	4.78
58					69.54	2.10
63			61.79	4.54	96.55	13.01
64			79.48	12.22	95.67	17.93
65					95.16	25.37
66			75.44	10.14	94.78	16.41
67	52.44	7.89	76.40	9.88	92.11	10.59
68					93.60	10.68
73					93.48	12.83
74					94.24	23.56
77			84.13	25.89	94.62	23.55
78					92.13	11.90
88					94.85	29.60
89					90.54	3.79

DEPTH AVG.

I=0

1			13.57	23.55		
2	18.01	7.10	69.86	9.62	72.26	49.40
3	37.76	8.30	57.76	11.04	76.97	8.19
4	39.01	3.39	66.01	2.50	80.55	3.98
5	34.99	2.97	76.10	7.43	90.65	9.12
6	52.44	7.89	74.44	9.79	94.36	16.44
7			84.13	25.89	93.21	16.90
8					94.85	17.90
9						
PLANE AVG.	36.98	3.75	68.19	6.30	85.08	10.73

TEST NO 168

INJECTOR· EDM-LOL

GRID NO	PLANE NO. 1		PLANE NO. 2		PLANE NO. 3	
	EVF	MRL	EVF	MRL	EVF	MRL
15			4.83	22 69	4.83	0
23					57.63	0.73
24			81.92	22.15	94.96	18.10
25	47.29	16.02	0	∞	11.15	61.86
26	1.34	2.05	55.87	27.46	71.94	115.12
33			54.78	2.17	57.47	0.64
34			47.56	6.56	49.18	4 15
35	46.25	17.48	73.41	19.74	93.46	20.71
36	0	∞	6.52	0	80.19	5.24
37			30.14	0.64	88.18	13.65
38					46.22	0.87
43			31.44	1.19	33.63	1.51
44	12.47	0.98	68 07	4.37	86.02	5 39
45	34.61	4.05	45.08	2.34	85.07	4.72
46	6.52	2.52	41.43	1 96	69.11	3.44
47	12.73	1.05	36.07	0.89	57.95	1.93
48					56.97	1 03
53			26 26	1.80	64.52	3.96
54	14.05	1.47	71.65	8.27	89 71	8.32
55	28.30	3 37	71.56	9 45	94.26	19 08
56	6.15	2.49	66.56	6.81	93.32	13.96
57	0.59	1.85	52.01	3.27	73.98	4.94
58					60.59	2.41
63			58.75	6.44	95.65	23 87
64			71.06	13.09	94.13	24 68
65					93.51	33.62
66			67.51	11.18	93.74	24.85
67	50.36	8.80	67.92	9.30	85.23	10.51
68					73.19	5.00
73					92.94	21.17
74					92.92	33.23
77			83.60	35.60	93.26	32.03
78					85.17	10 55
88					94.91	50 41
89					86.01	4 14

DEPTH AVG.

I=0

1			4.83	22 69		
2	8 48	7.95	70.32	12.25	70.82	61.15
3	39.30	9 51	41.80	10 56	69.61	10.41
4	18.68	3.23	47.34	2 61	71.10	3.71
5	14 19	2 79	65.38	7.68	85.59	12.17
6	50.36	8.80	67.01	10.37	88 49	20.91
7			83.60	35.68	89.58	21 81
8					94.91	29 42
9						
PLANE AVG.	10.07	3.72	52 53	6.59	77.92	13.49

TEST NO. 169

INJECTOR: EDM-LOL

GRID NO	PLANE NO. 1		PLANE NO. 2		PLANE NO. 3	
	EVF	MRL	EVF	MRL	EVF	MRL
15			3.25	26.74	3.25	0
23			73.55	18.80	49.74	0.83
24			0	∞	90.57	13.04
25	38.22	15.46	48.93	27.35	14.88	71.22
26	2.17	2.20			65.55	112.67
33			48.68	2.05	51.49	0.73
34		45.43	6.87	45.86	45.86	4.35
35	37.35	16.94	68.39	19.19	88.68	15.53
36	0	∞	10.40		72.83	4.96
37			26.28	0.67	82.22	11.69
38					41.40	0.91
43			27.42	1.25	29.44	1.53
44	10.34	1.03	65.00	4.47	83.20	5.24
45	31.80	5.22	45.58	2.52	82.42	4.61
46	10.40	2.75	39.81	2.09	67.87	3.66
47	10.55	1.11	31.81	0.91	55.04	2.04
48					54.19	1.10
53			28.02	1.91	60.47	3.99
54	11.66	1.55	66.86	8.08	86.03	7.94
55	26.89	3.57	66.79	9.39	89.49	12.66
56	9.89	2.71	60.36	6.63	88.41	10.42
57	0.93	1.99	50.17	3.47	70.33	5.06
58					48.44	2.35
63			51.70	6.30	87.36	10.21
64			66.09	12.79	89.30	17.63
65					88.67	25.27
66			60.44	10.69	88.27	17.51
67	41.18	8.41	60.93	9.03	81.52	10.93
68					67.09	4.88
73					87.10	15.21
74					87.85	25.14
77			75.52	27.65	87.86	23.45
78					81.49	11.27
88					90.50	35.42
89					80.83	3.70

DEPTH AVG

I=0

1			3.25	26.74		
2	7.77	7.86	62.87	11.15	64.78	62.97
3	31.74	9.20	39.85	10.46	64.32	8.55
4	19.50	3.43	46.25	2.74	68.82	3.76
5	15.71	3.00	60.86	7.58	80.65	9.19
6	41.18	8.41	60.43	10.06	83.32	15.75
7			75.52	27.65	84.90	17.49
8					90.50	20.98
9						
PLANE AVG.	17.97	3.88	50.16	6.52	74.07	11.23

TEST NO. 171 INJECTOR: EDM-LOL

GRID NO	PLANE NO 1		PLANE NO 2		PLANE NO 3	
	EVF	MRL	EVF	MRL	EVF	MRL
15			35.66	30.01	35.66	0
23					34.15	0.49
24			56.72	9.84	78.78	4.70
25	24.32	11.17	0	∞	14.34	60.50
26	21.59	2.04	47.77	19.57	58.11	70.22
33			32.51	1.35	33.49	0.46
34			58.76	7.99	59.02	5.03
35	23.19	12.31	61.21	11.25	80.46	6.26
36	0	∞	26.23		72.49	3.40
37			23.17	0.55	71.90	5.45
38					37.24	0.68
43			15.19	0.99	36.16	1.18
44	8.69	0.89	62.82	2.81	80.59	2.64
45	29.85	3.31	58.15	2.26	78.52	2.47
46	26.23	2.48	51.61	1.67	68.35	2.44
47	8.92	0.96	38.70	0.69	63.13	1.83
48					57.02	1.09
53			44.76	1.57	63.82	3.86
54	1.88	1.32	63.19	4.94	82.28	3.96
55	28.77	2.91	63.12	5.55	83.21	5.21
56	26.01	2.46	60.75	4.35	82.53	4.24
57	18.76	1.84	58.39	2.58	72.81	3.18
58					58.05	1.98
63			45.80	3.88	78.03	3.63
64			61.87	7.86	82.81	7.04
65					82.08	10.20
66			59.64	6.97	80.93	6.82
67	29.17	5.99	60.43	6.43	79.81	6.23
68					63.84	2.51
73					76.64	5.60
74					80.59	10.57
77			60.91	11.80	81.06	9.87
78					79.84	6.97
88					79.18	10.74
89					77.03	2.05

DEPTH AVG.

I=0

1			35.66	30.01		
2	22.01	5.88	50.66	6.87	51.92	43.79
3	19.70	6.71	43.91	7.28	62.10	4.54
4	27.12	2.85	54.84	2.16	69.59	2.30
5	25.84	2.59	60.81	4.70	78.15	4.17
6	29.17	5.99	58.15	6.58	78.09	6.75
7			60.19	11.80	79.46	8.06
8					79.18	6.80
9						
PLANE AVG.	26.37	3.15	55.41	4.41	72.46	5.79

TEST NO 178

INJECTOR: PAT

GRID NO	PLANE NO. 1		PLANE NO. 2		PLANE NO. 3	
	EVF	MRL	EVF	MRL	EVF	MRL
25			0	0	0	0
26			0	0	0	0
34					50.74	2.40
35	0	0	0	0	31.20	1.77
36	0	0	0	0	20.94	1.35
37			0.69	1.60	40.94	1.79
43				55.99		49.94
44	0	∞	53.34	∞	95.63	10.44
45	53.34	6.17	84.27	5.00	95.52	8.70
46	39.73	3.12	79.66	6.46	95.55	8.52
47	0	∞	39.73	0	40.17	3.01
48			0	∞	39.73	∞
53	0	∞	0	∞	64.63	∞
54	0	∞	64.63	67.36	90.46	6.75
55	33.18	2.62	67.98	2.94	90.61	6.08
56	30.77	2.47	67.09	3.03	90.99	6.29
57	0	∞	3.077		75.30	3.78
58			0	∞	74.31	57.41
65	11.19	0.44	51.30	2.99	76.46	1.13
66	53.41	6.56	74.14	1.01	79.55	1.02

DEPTH AVG.

1=0

1

2

3

4

5

6

7

8

9

PLANE AVG

1	0	0	0.06	0.16	33.94	1.84
2	47.65	4.78	73.17	4.59	85.95	9.13
3	32.16	2.20	60.12	8.15	87.62	7.29
4	27.82	2.89	68.15	1.87	78.18	1.07
5						
6						
7						
8						
9						
PLANE AVG	34.11	3.44	58.02	4.87	77.71	7.55

TEST NO 179/184

INJECTOR: PAT

GRID NO	PLANE NO 1		PLANE NO 2		PLANE NO 3	
	EVF	MRL	EVF	MRL	EVF	MRL
25			0	0	0	0
26			0	0	0	0
34					3.28	1.76
35	0	0	0	0	0.95	1.49
36	0	0	0	0	0.18	1.11
37			25.51	1.71	71.76	1.98
43					52.08	∞
44	0	∞	52.08	∞	96.20	6.97
45	52.08	5.55	85.50	4.01	96.30	5.98
46	48.78	3.13	83.95	5.70	96.07	5.69
47	0	∞	83.75	8.32	94.86	6.01
48			0	∞	83.75	∞
53	0	∞	0	∞	68.42	∞
54	0	∞	68.42	81.66	91.05	11.94
55	44.73	2.69	80.36	2.97	94.90	5.28
56	42.92	2.55	79.56	3.05	44.96	5.37
57	0	∞	80.60	7.66	94.20	6.21
58			0	∞	80.60	∞
65	12.05	0.45	54.88	2.83	79.44	0.98
66	51.81	5.88	73.25	0.84	79.36	0.83

DEPTH AVG.

I=0

1

2

3

4

5

6

7

8

9

PLANE AVG.

40.28

3.27

68.86

5.81

81.56

5.14

TEST NO 182

INJECTOR: PAT

GRID NO.	PLANE NO 1		PLANE NO 2		PLANE NO 3	
	EVF	MRL	EVF	MRL	EVF	MRL
25			0	0	0	0
26			0	0	0	0
34					35.58	2.98
35	0	0	0	0	34.13	2.50
36	0	0	0	0	14.36	1.67
37			0.34	1.69	18.67	1.81
43					79.35	64.28
44	0	∞	64.52	51.08	79.85	6.00
45	28.72	5.41	60.27	3.71	79.58	5.07
46	22.34	3.00	56.35	5.24	79.46	4.93
47	0	∞	22.34	0	22.65	2.47
48			0	∞	64.56	39.41
53	0	∞	0	∞	44.67	∞
54	0	∞	44.67	44.60	71.53	5.85
55	18.88	2.59	46.92	2.71	72.25	4.51
56	17.57	2.46	46.11	2.80	72.56	4.58
57	0	∞	17.57	0	17.73	2.78
58			0	∞	17.57	∞
65	6.27	0.46	33.47	2.98	57.32	1.06
66	28.74	5.75	49.88	0.85	57.12	0.86

DEPTH AVG.

I=0

1						
2			0	0	0	0
3	0	0	0.03	0.17	27.76	2.39
4	26.05	4.27	51.10	5.91	70.14	7.39
5	18.33	2.17	40.67	6.13	61.75	4.07
6	15.12	2.58	45.58	1.78	57.21	0.95
7						
8						
9						
PLANE AVG.	18.95	3.17	40.17	5.31	60.41	5.66

TEST NO 187 INJECTOR: PAT

GRID NO	PLANE NO 1		PLANE NO 2		PLANE NO 3	
	EVF	MRL	EVF	MRL	EVF	MRL
25			0	0	0	0
26			0	0	0	0
34					49.77	2.59
35	0	0	0	0	47.90	2.16
36	0	0	0	0	22.78	1.42
37			2.23	1.70	55.83	2.06
43					51.20	47.77
44	0	∞	48.49	∞	94.40	9.15
45	48.49	6.07	81.59	4.74	94.28	7.70
46	39.31	3.24	78.05	6.42	94.32	7.54
47	0	∞	39.31	0	52.43	3.15
48			0	∞	39.31	∞
53	0	∞	0	∞	68.07	∞
54	0	∞	68.07	78.89	89.69	7.47
55	33.82	2.75	68.46	3.09	89.96	6.06
56	31.83	2.60	67.80	3.19	90.23	6.21
57	0	∞	31.83		76.47	4.03
58			0	∞	31.83	∞
65	10.70	0.46	50.64	3.13	75.89	1.19
66	38.40	6.44	70.44	0.98	76.59	0.99

DEPTH AVG.

I=0

1			0	0	0	0
2			0.20	0.17	42.99	2.11
3	0	0	0.20	0.17	42.99	2.11
4	44.65	4.75	71.35	4.49	86.85	8.24
5	32.98	2.30	60.88	9.40	86.95	5.49
6	25.55	2.86	62.25	1.92	76.28	1.08
7						
8						
9						
PLANE AVG	33.13	3.47	57.02	5.07	78.99	6.54

TEST NO 190 INJECTOR. PAT

GRID NO	PLANE NO. 1		PLANE NO. 2		PLANE NO. 3	
	EVF	MRL	EVF	MRL	EVF	MRL
25			0	0	0	0
26			0	0	0	0
34					43.83	2.58
35	0	0	0	0	25.75	1.96
36	0	0	0	0	17.64	1.44
37			0.45	1.60	23.75	1.71
43					89.60	91.58
44	0	∞	78.47	77.13	90.44	7.37
45	41.53	5.52	74.62	4.07	90.22	6.20
46	32.17	2.98	70.63	5.62	90.12	5.96
47	0	∞	32.17	0	32.51	2.68
48			0	∞	77.41	56.25
53	0	∞	0	∞	56.58	∞
54	0	∞	56.58	55.51	83.70	6.41
55	27.15	2.54	60.01	2.76	84.02	5.01
56	25.25	2.40	59.03	2.84	89.38	5.13
57	0	∞	25.25	0	25.43	2.91
58			0	∞	25.25	∞
65	9.01	0.44	43.61	2.92	68.84	1.07
66	41.57	5.87	63.67	0.88	70.19	0.89

DEPTH AVG.

I-0

1						
2			0	0	0	0
3	0	0	0.04	0.16	27.35	1.99
4	13.46	1.13	64.51	7.33	80.66	9.51
5	26.35	2.13	52.59	6.94	72.81	4.50
6	21.84	2.62	58.41	1.76	69.59	0.97
7						
8						
9						
PLANE AVG.	18.45	1.60	51.00	6.43	69.60	6.93

TEST NO 193

INJECTOR

PAT

GRID NO	PLANE NO. 1		PLANE NO. 2		PLANE NO. 3	
	EVF	MRL	EVF	MRL	EVF	MRL
25			0	0	0	0
26			0	0	0	0
34					55.38	2.74
35	0	0	0	0	32.83	1.90
36	0	0	8.78	0.59	91.11	5.10
37			0.15	1.63	19.63	1.73
43					98.85	662.16
44	0	0	95.88	394.88	98.56	34.08
45	66.08	8.76	91.14	9.56	98.43	27.07
46	26.42	3.04	82.43	9.12	98.72	33.57
47	0	∞	26.42	0	26.74	2.52
48			0	∞	26.42	∞
53	0	∞	0	∞	57.61	∞
54	0	∞	57.61	57.22	92.03	7.69
55	8.43	2.39	60.81	3.10	91.87	9.20
56	5.05	2.25	62.04	3.30	92.82	10.15
57	0	∞	5.05	0	74.88	3.88
58			0	∞	76.36	63.33
65	13.52	0.46	54.54	3.43	79.84	1.47
66	67.36	9.58	84.06	1.69	87.87	1.77

DEPTH AVG.

I=0

1

2

3

4

5

6

7

8

9

PLANE AVG.

0 0 0 0

50.54 2.76

86.33 44.18

88.77 9.96

84.32 1.63

24.68 4.18 57.87 18.29 80.48 28.09

TEST NO	194	INJECTOR	PAT			
GRID NO	PLANE NO. 1		PLANE NO. 2		PLANE NO. 3	
	EVF	MRL	EVF	MRL	EVF	MRL
25			0	0	0	0
26			0	0	0	0
34					51.74	3.08
35	0	0	0	0	30.74	2.17
36	0	0	8.02	0.62	87.48	4.38
37			0.16	1.75	27.90	1.94
43					96.50	279.04
44	0	∞	91.01	199.00	96.67	20.35
45	56.90	7.92	86.59	7.86	96.56	16.92
46	35.58	3.52	79.07	8.77	96.61	17.43
47	0	∞	35.58	0	35.87	3.08
48			0	∞	35.58	∞
53	0	∞	0	∞	53.66	∞
54	0	∞	53.66	56.67	89.71	9.12
55	13.68	2.64	60.08	3.36	89.77	8.89
56	8.17	2.45	59.74	3.50	90.40	9.42
57	0	∞	8.17	0	72.28	4.13
58			0	∞	67.84	50.79
65	11.76	0.49	51.41	3.63	76.88	1.52
66	57.45	8.49	77.30	1.45	82.24	1.52

DEPTH AVG.

I=0

1			0	0	0	0
2			0	0	0	0
3	0	0	4.55	0.45	48.93	2.84
4	47.98	5.99	73.33	15.56	86.25	22.90
5	11.36	2.19	44.82	7.55	86.36	9.39
6	29.76	3.70	70.51	2.41	79.87	1.52
7						
8						
9						
PLANE AVG.	25.49	4.07	55.66	12.12	79.38	16.03

TEST NO 197

INJECTOR PAT

GRID NO	PLANE NO 1		PLANE NO 2		PLANE NO 3	
	EVF	MRL	EVF	MRL	EVF	MRL
25			0	0	0	0
26			0	0	0	0
34					90.14	4.42
35	0	0	37.09	1.17	90.03	3.71
36	0	0	0	0	23.98	1.40
37			21.92	1.82	65.32	2.16
43					46.72	45.66
44	0	∞	44.32	∞	93.15	7.28
45	44.32	5.80	78.84	4.14	93.11	6.18
46	40.70	3.27	77.34	5.89	93.01	5.91
47	0	∞	40.70	0	79.51	3.51
48			0	∞	40.70	∞
53	0	∞	0	∞	38.42	38.36
54	0	∞	36.79	∞	71.56	∞
55	36.79	2.81	71.56	3.05	90.47	5.48
56	35.21	2.67	71.06	3.16	90.61	5.59
57	0	∞	35.21		80.00	4.06
58			0	∞	35.21	∞
65	10.15	0.47	49.97	3.09	75.09	1.11
66	44.08	6.15	66.45	0.89	73.01	0.88

DEPTH AVG.

I=0

1

2

3

4

5

6

7

8

9

PLANE AVG

	0	0	14.75	0.72	70.84	3.27
4	42.81	4.59	70.25	4.05	90.32	6.89
5	36.12	2.35	63.66	2.01	85.77	6.15
6	23.52	2.75	62.13	1.86	73.93	0.99
7						
8						
9						
PLANE AVG	33.60	3.42	58.75	3.25	83.71	6.11

F. NOMENCLATURE

C_R	Chamber Contraction Ratio
H_V	Heat of Vaporization, J/kg
L_c	Length of Straight Chamber Section, cm
K_J	Constant Containing Drop Size and Velocity
K_p	Constant Containing Propellant Properties
L_{gen}	Generalized Length, cm
L_N	Length of Converging Chamber Section, cm
M	Molecular Weight
P_c	Chamber Pressure, kPa
r_m	Mass-Median Droplet Radius, μm
r_m , uncor	Uncorrected Mass-Median Droplet Radius, μm , Figure 27
S	Converging Nozzle Shape Factor $(1 + 1/\sqrt{C_R} + 1/C_R)/3$
T	Propellant Temperature, °K
T_c	Propellant Critical Temperature, °K
T_r	Reduced Temperature, T/T_c
V_α	Propellant Injection Velocity, m/s Spray Fan Half Angle, degree
μ	Dynamic viscosity, kg/m-sec
ρ	Density, kg/m ³
σ	Surface Tension, N/m

End of Document